Seton Hall University Dissertations and Theses (ETDs)

2009

Determination of Partition and Activity Coefficients Using Headspace- Gas Chromatography

Gregory Paul Bullock
Seton Hall University

Follow this and additional works at: http://scholarship.shu.edu/dissertations

Part of the Chemistry Commons

Determination of Partition and Activity Coefficients Using Headspace-Gas Chromatography

By:

Gregory Paul Bullock

Dissertation submitted to the Department of Chemistry and Biochemistry of Seton Hall University in partial fulfillment of the requirements for the degree of
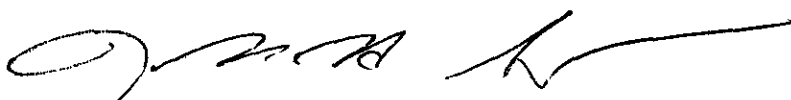
DOCTOR OF PHILOSOPHY
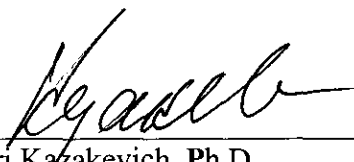
in

Chemistry

May 11, 2009

We certify that we have read this dissertation and that in our opinion it is sufficient in scientific scope and quality as a dissertation for the degree of Doctor of Philosophy.
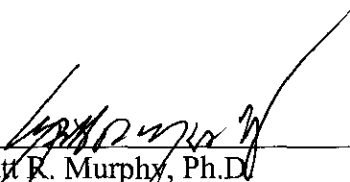
APPROVED:

Nicholas H. Snow, Ph.D.
Research Mentor
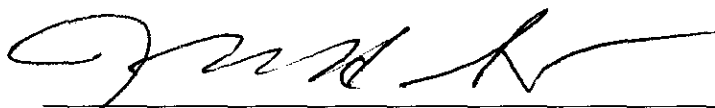
Yuri Kazakevich, Ph.D.
Member of Dissertation Committee

Wyatt R. Murphy, Ph.D.
Member of Dissertation Committee

Nicholas H. Snow, Ph.D.
Chair, Department of Chemistry and Biochemistry

DEDICATION

This work is dedicated to:

My parents:

Edward and Michele Bullock

My grandparents:

Roland and Carmella Bullock

and

Salvatore and Norma Napoli

My sister:

Alison Bullock

Thank you for your unending inspiration, encouragement, and patience.

ACKNOWLEDGEMENTS

Mentor and Graduate School Chemistry Professor:

Dr. Nicholas H. Snow

Graduate School Chemistry Professors:

Dr. Yuri Kazakevich, Dr. Wyatt R. Murphy, Dr. Joseph T. Maloy, and Dr. Alexander Fadeev

Undergraduate Chemistry Professors:

Dr. Louis J. Rivela, Dr. Robert J. McCallum, and Dr. Daniel E. Pierce

High School Chemistry Teacher:

Mr. Richard Hodges

The Seton Hall Chromatography Group

including Alex Giaquinto and Rafael Acosta

Thank you for your guidance, inspiration, and support.

TABLE OF CONTENTS

ABSTRACT

"Headspace" is a term defined as vapor that forms above or around a liquid or solid sample in a closed container. Headspace extraction is a sampling technique in which the headspace of a sample is extracted to be analyzed. Headspace extraction originated in 1939 for use in determining alcohol in body fluids. In the 1950s, it was used to monitor freshness of foods in closed containers as well as to make physicochemical measurements of aqueous solutions. In 1958, it was first used with gas chromatography, and in 1967, the first automated headspace-gas chromatograph was introduced for commercial use. Since its beginning, it has become a mainstream sampling technique.

Static headspace extraction is a form of headspace extraction in which a sample is brought to equilibrium at a given temperature and a single aliquot of the headspace is extracted with the intention of being analyzed. It is common for headspace extractions to be analyzed on gas chromatographs, and there are headspace-gas chromatographs that are commercially available. Before samples are extracted, they are heated and brought to equilibrium at a given temperature.

This study was initiated to verify that the temperature inside a headspace vial was in agreement with the temperature read-out of the instrument. This was performed mainly using a chromatographic method, according to an equation derived, relating the peak area of an analyte to temperature and concentration of the headspace inside a vial. From that study, two other studies were performed to supplement and add perspective to the temperature study, since temperature and chromatography (peak area) are

mathematically related to physicochemical properties. The partition and activity coefficients were the physicochemical properties studied.

The partition coefficient is a constant that reflects the ratio of the concentration of a sample in the liquid or solid phase with the concentration of the headspace, at equilibrium. The activity coefficient is a correction value associated to the concentration of a solute in a solvent. The partition coefficient is also mathematically related to the activity coefficient.

These studies were conducted using two similar static HS-GC instruments: a pressure-balanced system, and a non-pressurized system. The pressure-balanced system pressurizes the sample in order to move the headspace sample to the GC inlet. The non-pressurized system withdraws an aliquot of the headspace with a microsyringe and directly injects it into the GC inlet. In addition to the studies of temperature, partition coefficients, and activity coefficient, there was an underlying study in which the precision of the two static-headspace extraction systems were compared.

The air-water partition coefficients of methyl ethyl ketone, cyclohexane, benzene, and toluene were determined by the vapor phase calibration (VPC) method and phase ratio variation (PRV) method, and were compared to values in the literature. The activity coefficients for a mixture of benzene/toluene was determined at various mole ratios using the total vaporization technique (TVT).

The results from determining the partition and activity coefficients had high experimental uncertainties associated with the determined values. The partition coefficients determined by the PRV method were more accurate and precise than the partition coefficients of the same analytes determined by the VPC method. The activity coefficient for the benzene/toluene mixture was determined to be near 1.00, and within

one order of magnitude of the expected value of 1.00 (with a few exceptions). The results from the pressure-balanced system were more accurate and precise than the results from the non-pressurized system.

There was a high degree of uncertainty determined in the temperature study. Since a high degree of uncertainty was determined in the physicochemical properties studies, and since those properties are mathematically related to the temperature inside the vial, it was concluded that those uncertainties degrade the precision and accuracy of the results of the temperature study. Additionally, there are sources of systematic error and uncertainties from the instruments and preparation devices used, such as syringes, pipettes, and sample vials. These sources of error contribute to the uncertainties determined with the results of the partition coefficients, activity coefficient, and the temperature inside the vial.

1. INTRODUCTION

1.1 Introduction to Headspace Extraction

The definition of headspace is the vapor above a liquid and/or solid phase sample (sometimes called the "sample phase"). Headspace-gas chromatography is the separation technique in which an all-vapor aliquot is taken and injected with the intention of being separated and analyzed by a gas chromatograph. Headspace vapors can occur spontaneously, as in the case of volatile organic compounds (VOCs), or can be induced by, for example, heating the sample; it can also be completely volatilized, in which no non-vapor phase sample is present. Any vapor emitted from an organic chemical such as toluene, benzene, and trichloroethene in a solvent such as water is a result of being a volatile organic compound [1]. Volatile organic compounds are often analyzed and detected in environmental water samples with headspace extraction. There are a few forms of headspace-gas chromatography, including static headspace extraction, dynamic headspace extraction, multiple headspace extraction (MHE), and solid phase micro-extraction (SPME). Static headspace extraction was used exclusively in this research.

1.2 Origin of Headspace-Gas Chromatography

Although headspace extraction is often thought of and directly associated with gas chromatography, some of its earliest applications were not used with GC [2]. In 1939, an aerometric-permanganate analysis was used to rapidly determine alcohol in water and

body fluids including blood and urine. The method is a combination of static and dynamic sampling of the headspace above the liquid sample through a sulfuric acid-permanganate reagent, which allowed for the alcohol content to be quantitatively determined by a method of titration with dichromate [3]. In this and a later paper in 1950 by the same author, air-water partition coefficients of alcohol were also determined and compared to values published by other authors in the temperature range of 0°C to 40°C [4-14]. They used the partition coefficients to calculate the concentration of alcohol in the original sample, based on the amount present in the gas phase.

Use of headspace sampling was documented in the late 1950s for work performed in the early 1950s (due to political reasons) in Hungary for making various physicochemical measurements of aqueous solutions. The group, led by Schulek at the University of Budapest, presented a paper in Vienna and published papers on using all-glass apparatus to investigate the changes in the tension of aqueous alcohol and phenol solutions containing various non-volatile constituents, by measuring the concentrations of analytes in the headspace by classical analytical techniques [2, 14-21].

The first use of headspace sampling combined with gas chromatography was to monitor hydrogen content in the water of high pressure power stations and was published in 1958 but the authors claimed to have used an operational system for more than a year by the time of publication [22, 2]. Trace amounts of hydrogen at the parts per billion level were analyzed from the aliquots of the equilibrium gas using a thermal-conductivity detector on a gas chromatograph.

The first time the term "headspace" was used and adapted was in 1960 in a paper by Stahl [23]. Prior to that there was no specific English language expression for the

2

term. Previous expressions for it were "aerometric" by Harger, "dampfraumanalyse" and "dampfphase," which, translated from German to English directly translate into "vapor space analytical procedure" and "vapor phase" and are still used in German [3, 2].

As the use of GC was on the rise in the late 1950s, it started being used with headspace extraction for food science studies to study volatiles related to foods. Another of the earliest uses of headspace extraction and analysis with GC was to study the degree of rancidity of potato chips when an aliquot of the headspace was taken from the bag and analyzed [2]. Ettre monitored differences between bags stored properly and improperly, at room temperature and warmer than room temperature. This was soon similarly studied and published by Stahl. To perform this analysis, the bag was pierced with a hypodermic needle which withdrew 0.5 to 1 mL of the gas that was injected into the GC, with the intention of determining gases, such as oxygen, in the headspace by a polarographic oxygen sensor coupled with a direct readout [23, 24].

Beckman Corporation created a device that could be used with Stahl's work that could puncture a container and draw the headspace gas into a small closed volume that could then be evacuated directly to a polarographic oxygen sensor or to a syringe through a rubber septum on the side, leading to a GC [24, 25]. Figure 1 is a photograph of the "Beckman Head Space Sampler" [2]. It can be seen that a sample is placed into the air-tight glass container and let set to equilibrium at room temperature. When a sample is ready to be extracted, an air-tight syringe (at room temperature) enters an air-tight valve at the top right. A sample is drawn and transferred to an analytical instrument, such as a gas chromatograph.
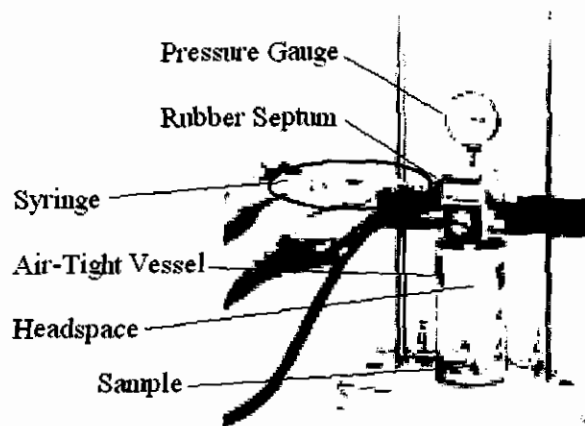
Figure 1 – An original photo of a "Beckman Head Space Sampler." In the photo, a gas (headspace) sample is being withdrawn by a syringe in order to inject into an analytical instrument [2].

Figure 2 is a photograph of a can-piercing apparatus and assembly for sampling the headspace of an aluminum can of food. It can be seen that the plunger handle on the left is pulled down until the needle pierces the can. When the syringe valve is closed and the gauge valve is opened, the pressure gauge gives a reading of the pressure in the can. When the syringe valve is opened, a sample of the headspace can be drawn through the silicon tubing into the gas-tight syringe [26].

Figure 3 is a diagram of a Budenberg true vacuum (pressure) gauge, which is an example of a can-piercing apparatus used for sampling the headspace of aluminum cans of food [27]. The gauge face is shown on the right. Shown on the left is the inside of the gauge, which is located behind the gauge face. Located near the bottom is the Schrader valve, which is a spring-loaded valve encased in a small, hollow metal cylindrical tube, with a flat end on the inside (of the gauge), which, creates a seal when flush with the cylindrical valve case, or, when pushed (towards the inside of the gauge), allows air to exit through to the other end. (Schrader valves are the valves commonly known on bicycle and car tires through which air can be added or released.)

To measure the air pressure in a can of food with the Budenberg True Vacuum Gauge, a can is pierced with the puncturing needle, which allows air to flow up into the air reservoir of the pressure gauge. The rubber ferrule creates an air-seal and prevents air leaks. The air in the reservoir exerts pressure on the valve spring, which gives the pressure reading on the gauge face. Once the pressure of a sample has been taken, the air in the reservoir is released out the Schrader valve by pushing the button and opening the valve cap.
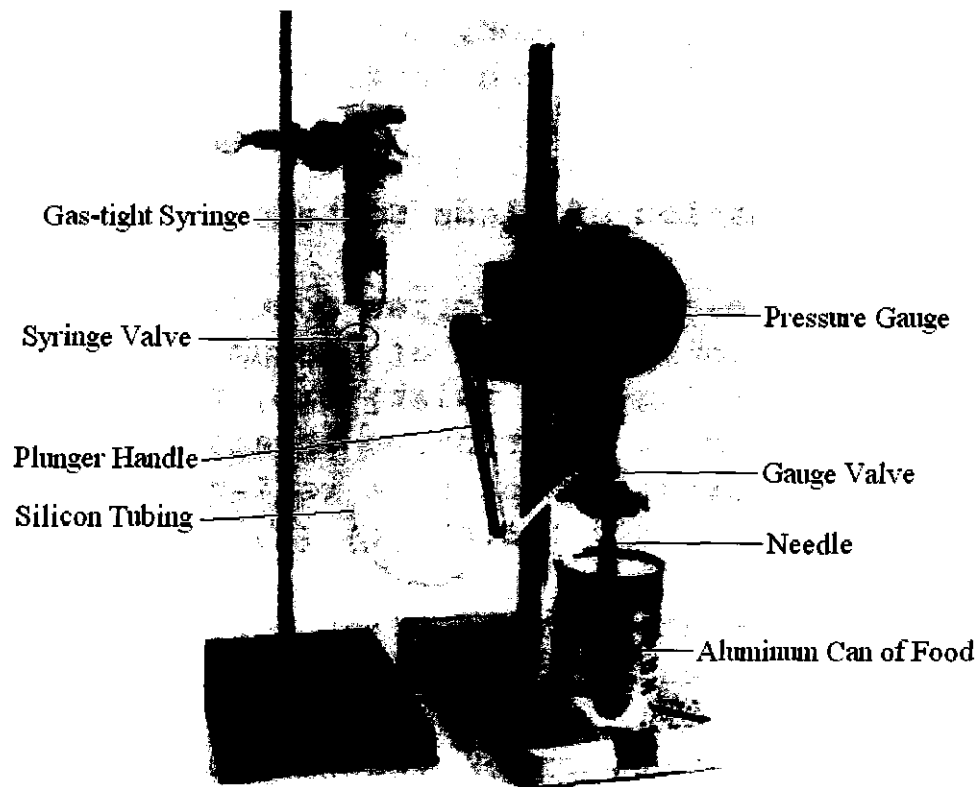
Figure 2 – Can-piercing apparatus assembly for collection and analysis of headspace gas from an aluminum can of food [26].
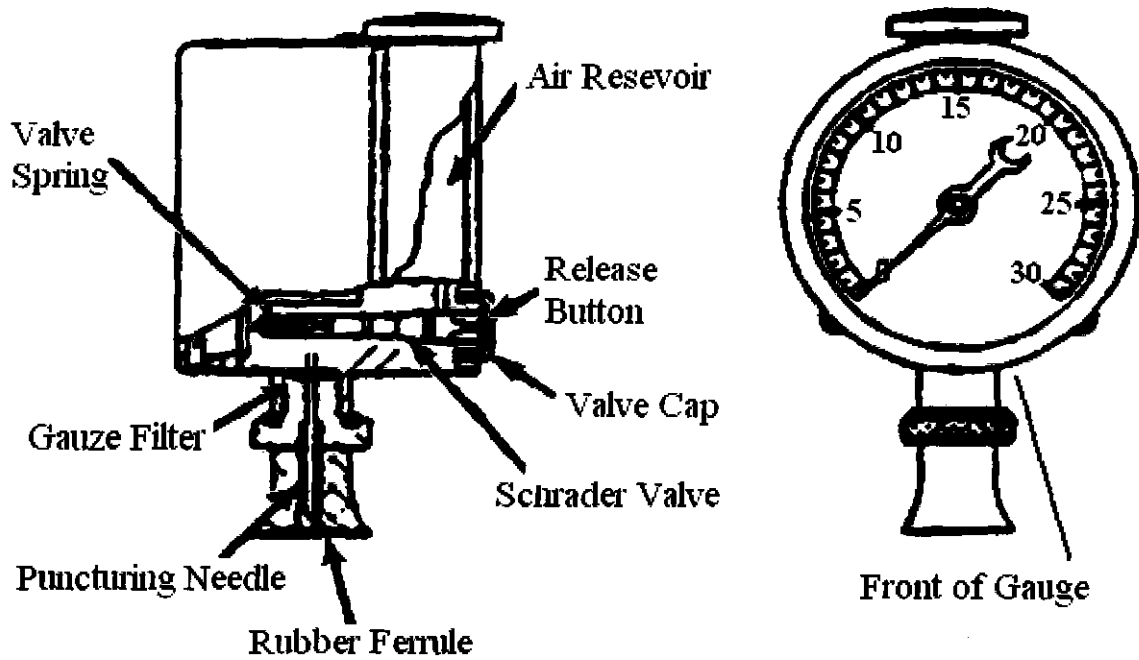
Figure 3 – "Budenberg True Vacuum Gauge." The left side shows the details behind the gauge readout face shown on the right [27].

Figure 4 is a close up diagram of the needle segment of a can vacuum gauge [27]. The sharp needle-edge tip is pressed through the top of a can until the side opening port is exposed to the headspace of the contents of the can. The sealing device gasket keeps the inside of the needle segment sealed from exposing the headspace and pressure out to the atmosphere. The vapor in the headspace travels through the side opening port in the needle up to an air reservoir where the pressure generated on a spring valve produces a pressure on the face of the pressure gauge.

Toward the end of the 1950s, the introduction of flame ionization detectors and argon ionization detectors accelerated the use of headspace extraction with gas chromatography to investigate volatile organic compounds, because these detectors were more sensitive than thermal-conductivity detectors used in previous years [2, 28]. These detectors could detect trace quantities of volatile compounds and at the time were being used to investigate a range of samples of fruits, vegetables, peppermint oil, honey and coffee [29-35]. These were mainly qualitative studies intended on identifying a vast variety of compounds. For example, Dorrscheidt and Friedrich distinguished different origins of honey samples based on the presence of 31 volatile compounds such as benzaldehyde, benzenacetaldehyde, dimethyl sulphide, pentanenitrile, benzylnitrile, isobutane, octanoic acid, nonanoic acid, furfural, linalool, and nonanal [28, 34]. Although thermal-conductivity detectors are more sensitive to and used to analyze permanent gases such as oxygen and carbon dioxide, it is less sensitive overall compared to a flame ionization detector for detecting hydrocarbons. For that reason along with the high incidence of samples containing hydrocarbons, the flame ionization detector has translated into wide contemporary use in modern gas chromatographic systems.

Pressure Gauge

Sharp-edged
Needle

Side Opening Port

Sealing
Device
Gasket
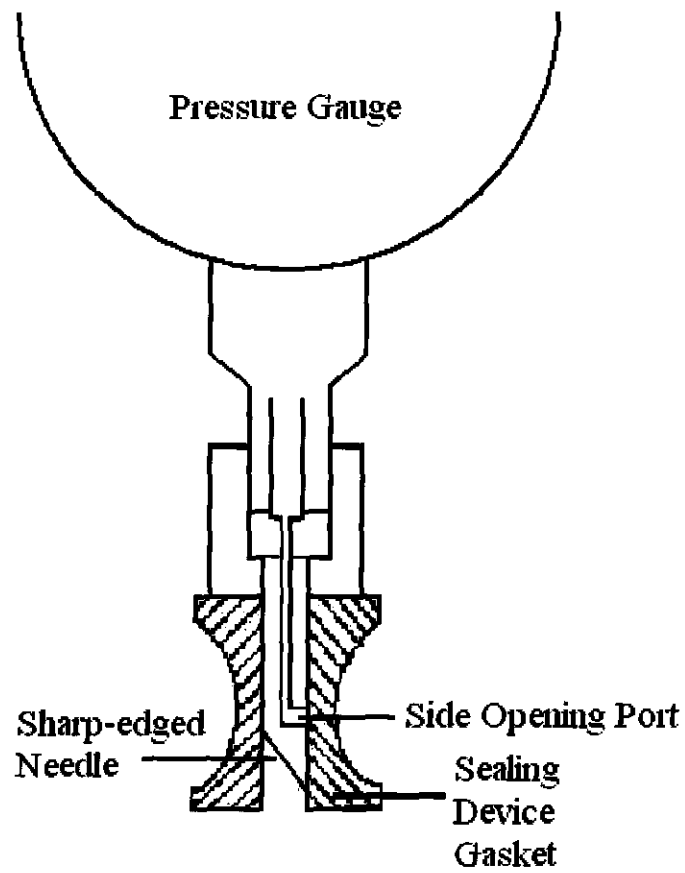
Figure 4 - A close-up of a can vacuum gauge [27].

1.3 Automated Systems

In 1964, static headspace analysis was advanced for work centered on determining the ethanol levels in blood, this time using a semi-automatic system [36-37]. The use of a syringe to manually transfer samples led to some pressure, temperature, and volume related difficulties, such as loss or condensation of sample. These difficulties hampered the ability to make quantitative measurements.

As scientists around the world were looking for faster techniques to analyze volatile organic compounds, such as ethanol, in blood, the idea for developing an automated system was proposed. In 1967 from a cooperated effort between G. Machata and Bodenseewerk Perkin-Elmer & Co., the first automated headspace-gas chromatography instrument was introduced, which (an original production unit) can be seen in Figure 5 [2]. This photo shows that the vial carousel is located on the top of the cube-shaped heater. The vials are heated to a specific temperature for a sufficient time that the contents inside the vial reach equilibrium. Then, the sampler extracts an aliquot of the headspace which is directly injected into the gas chromatograph, located behind and to the right of the heater. The resulting peaks are drawn on the paper in the analog recorder, located to the left of and attached to the GC.

Figure 6 is a schematic diagram of a contemporary automated system [38]. It shows that the sample vials are in the carousel, which moves the vial of interest into the position of the air-pressurized cylinder, which pushes the vial from below into the heater above. When the vial has heated and thermostatted for the desired time, the syringe (which can also be heated) pierces the septum of the vial, and withdraws a sample with
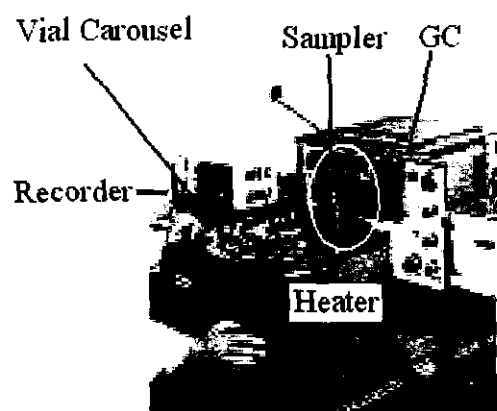
Figure 5 – The production unit of the Model F-40 Headspace Analyzer, the first automated headspace-gas chromatograph [2].
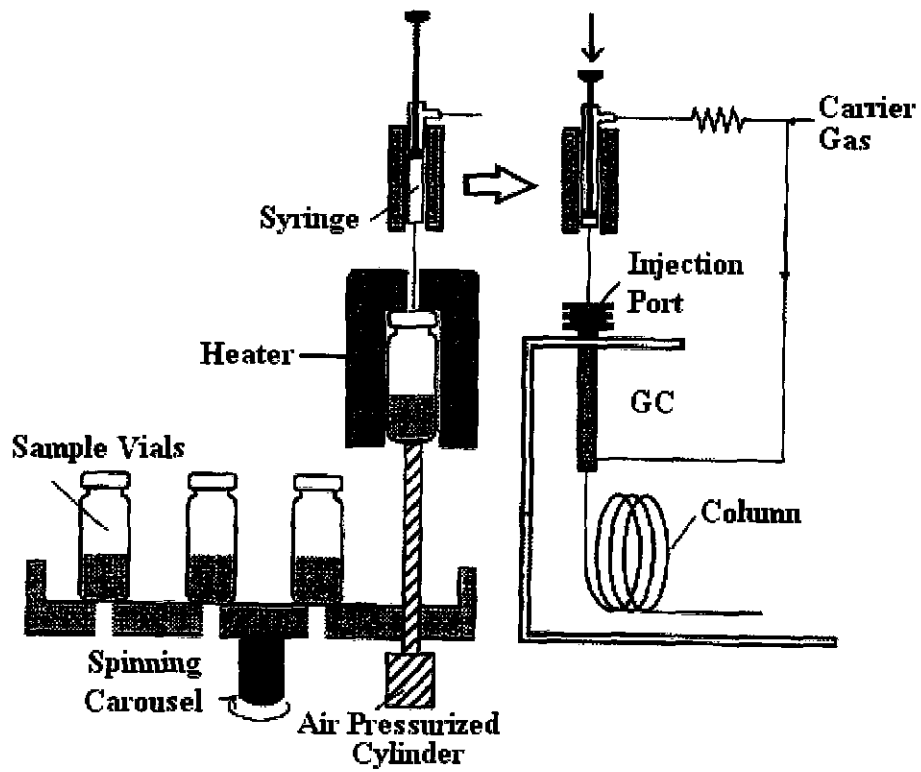
Figure 6 – Diagram of automated HS-GC system [38].

the automated plunger. The syringe carrying the sample is then automatically transferred into the injection position where the plunger pushes the sample into the GC inlet.

In order to resolve the initial problem of sampling the headspace of closed sample vials with precise control and reproducibility, it was decided to pressurize the closed and thermostatted sample vial with an inert gas, such as helium gas, allowing the headspace gas to expand for a controlled time into the gas chromatographic column. This technique allowed for the volume of the sample aliquot to be accurately and precisely controlled by controlling the pressure and time, and came to be known as "balanced-pressure sampling." This is explained in more detail along with a diagram in section 1.6 on "static headspace extraction."

The desire to improve the technique of headspace sampling not only gave rise to improving headspace-gas chromatography analysis but also to mobile, handheld devices that are battery powered and could be brought to a scene to accurately determine the blood alcohol level of a person (driver) from their breath. These are referred to as "breath measurement devices" and include models such as the Breathalyzer, the Intoxylizer, the Alcotest, IntoXimeters, the Alcomonitor, the Alco-Sensor, the Alcolmeter, and the Alco-Analyzer [39].

1.4 Breathalyzer Chemistry

The first reported use of testing a person's breath for alcohol content was in 1927 by Dr. Gorsky, a Police Surgeon from England, who testified in a court case [40]. Prior to 1953, Robert Frank Borkenstein collaborated with Dr. Harger of Indiana School of

Medicine to develop the "drunkometer." In 1953, the independent creator of the

breathalyzer (smaller and easier to use than the drunkometer) was R. F. Borkenstein who

was an Indiana State Police captain and professor at Indiana University at Bloomington.

His device measured the blood alcohol level of the breath sample of a subject by

chemical oxidation and photometry, to determine the concentration of alcohol, according

to the following chemical reaction [41].

$$3H_5C_2OH + 2K_2Cr_2O_7 + 8H_2SO_4 \xrightarrow{AgNO_3} H_3COOH + 2Cr_2(SO_4)_3 + 2K_2SO_4 + 11H_2O \qquad [42]$$

In that chemical reaction, ethanol is mixed with potassium dichromate, sulfuric

acid, and silver nitrate as a catalyst to produce acetic acid, chromic sulfate, potassium

sulfate, and water. This reaction takes place when ethanol comes into contact

with the other reactants because the ethanol causes the dichromate ion to be reduced to

chromium ion and the ethanol is oxidized to acetic acid. The dichromate ion exists in the

form of potassium dichromate, which has a yellowish color. When the dichromate ion is

reduced, the yellowish color fades (depending on the amount of ethanol present) and the

resulting color can be photometrically analyzed, based on the difference of transmittance

of light through the cell. Since two cells are used, a referece (blank) cell and a test cell,

the difference of light tranmitted through gives a reading of how much ethanol was

present in the test cell and the person of the breath it came from [41].

Figure 7 is a picture of the Alcohawk Precision Breathalyzer digital alcohol

detector breath measurement device [43]. For a breathalyzer to determine the blood

alcohol concentration of a person, the subject must blow a steady breath of air from the

deep lungs for 5 seconds into the mouthpiece no sooner than 20 minutes after drinking,

eating, or smoking, in an environment that is between a temperature range of 10-40°C

Breath
Exhaust

Removable
Mouthpiece

Blood
Alcohol
Content
LED
Display

Power
Button

12 Volt DC
Adapter Port
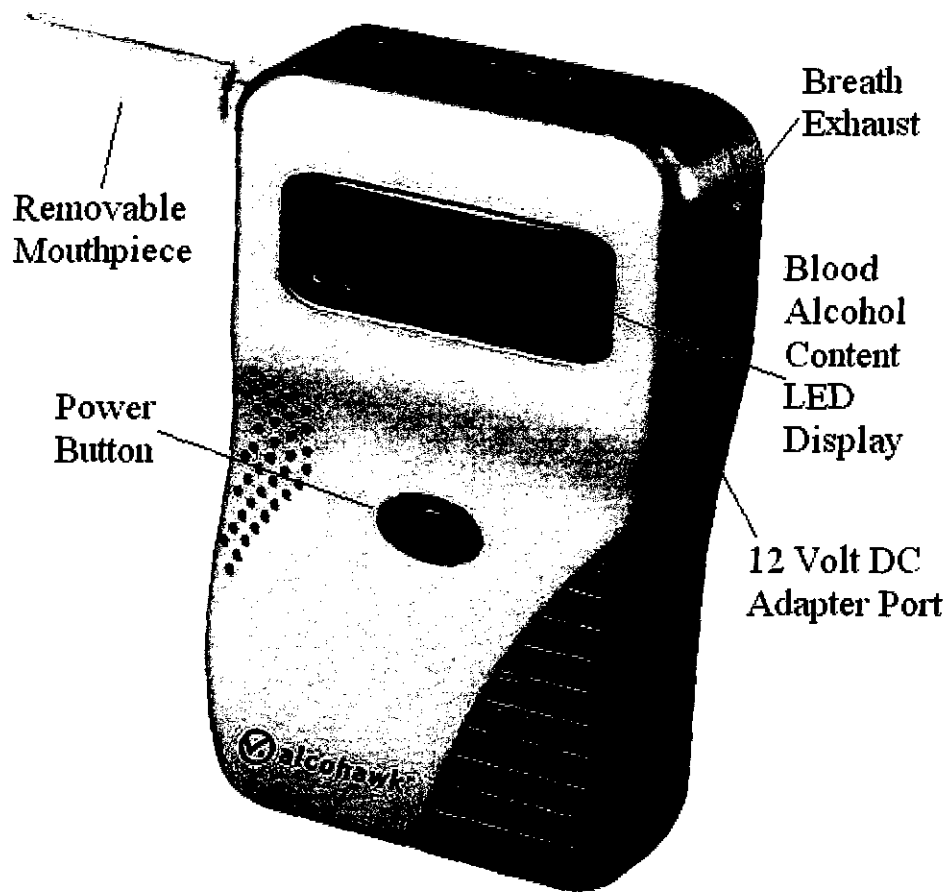
Figure 7 – Alcohawk Precision Breathalyzer digital alcohol detector [43].

and does not have strong winds or the presence of people consuming alcohol [44]. The aliquot of breath is analyzed differently depending on the model of the device.

One type contains a vial with a mixture of sulfuric acid, potassium dichromate, silver nitrate, and water that the breath sample is bubbled through. The resulting product ends up in a vial-like cell and, depending on how the breath sample reacts with those chemicals, will be a certain color, which is compared to an unreacted mixture in the photocell system. An electric current is produced based on how the colors of the 2 cells compare [42].

A second type, such as the Intoxilyzer, uses infrared spectroscopy to identify molecules based on how they absorb IR light. The light passed through each filter is detected by a photocell, and then converted to an electric pulse, which finally is relayed to the microprocessor, which interprets the pulses and calculates the blood alcohol concentration [42].

A third type, such as the Alcohawk or the Alcosensor III or IV, has a fuel cell and sensitive semi-conductor sensor. The fuel cell has a porous acid-electrolyte substance in the middle of two platinum electrodes. The platinum oxidizes the alcohol in the breath sample which produces acetic acid, protons, and electrons that flow through a wire connected to an electrical-current meter and to the platinum electrode on the other side. The electrical current is proportional to the amount of alcohol oxidized [42].

1.5 Balanced-Pressure Headspace Sampling

Balanced-pressure sampling is a three step process. First, the closed vial is thermostatted until the contents reach equilibration, which takes the longest time of the three steps. Next, the vial is pressurized with carrier gas which generally occurs for about 2 minutes. Finally, the sample is introduced to the GC which takes a matter of milliseconds. One of the advantages to automated sampling is that vials can undergo preparation, particularly equilibration, while other samples are thermostatting or being analyzed in the GC, which can save time.

The first automated and integrated headspace GC system based on these principles was the model F-40, and was introduced in early 1967 at the International Exhibition-Congress on Chemical Engineering (ACHEMA) in Frankfurt am Main, Germany [45-46]. The system could thermostat a maximum of 30 sample vials in a carousel to a precise temperature and rotate the vials into the position to be sampled next, by the instrument. Over time, improvements to the instrument, along with external manipulations such as use of different standards, columns, and conditions, have reduced sampling time down to a matter of a few minutes [2], and replaced the classical Widmark method [47-51].

The Widmark method, also commonly known as "isothermal distillation," was named after E. M. R. Widmark, a professor at the University of Lund, Sweden, who created the first frequently used procedure in the early 1920s to determine alcohol in blood. This method was carried out by placing a sample of blood in the bottom of a customized Erlenmeyer flask, which held an open container containing a bichromate

solution suspended in the vapor phase above the blood sample. During the time the closed flask thermostatted at 60°C for 1 hour, the low-boiling compounds present in the blood vaporized and reacted with the bichromate solution, causing the Cr^{IV} to reduce to Cr^{III}. The amount of volatile organic compounds was calculated from the titration of the remaining bichromate, allowing the determination of acetone [50] and ethanol [51]. Since the technique was not specific enough, an additional independent, enzymatic method using alcohol dehydrogenase was developed by Bonichsen and Theorell [52] which was expensive and called for unstable reagents.

Figure 8 is a timeline of important historical developments of headspace sampling and analysis. It can be seen that alcohol testing had a significant impact on the demand for and innovation behind headspace samplers. Tests for alcohol in blood and breath began in the early 1920s and spanned through the 1950s with significant improvements by Widmark, Gorsky, Harger, and Borkenstein. By the early 1960s, headspace sampling was being used for a more diverse range of media to monitor the gas contents of water power stations and foods, in addition to alcohol testing. Then in 1967, automatic headspace samplers with gas chromatographs were introduced, which was a significant corner stone in the ease of use and diversity of applications of headspace-gas chromatography.

1920 — "Widmark Method" for determining alcohol in blood [50, 51]

1927 — First breath test for alcohol by Dr. Gorsky [40]

1939 — Headspace sampling used to determine alcohol in body fluids by Harger, et. al. [3]

1950 — Air-water partition coefficient of alcohol determined using headspace sampling by Harger, et. al. [4]

1953 — Breathalyzer invented by Dr. Borkenstein [41]

— Headspace sampling used for physicochemical measurements of aqueous solutions by Schulek, et. al. [14-21]

1958 — Headspace sampling first used with gas chromatography to monitor hydrogen content in water of power stations [22]

— Headspace extraction used with GC and polarographic oxygen sensor to analyze rancidity of potato chips in bag [2]

— Introduction of FID and Argon detector [2, 28]

1960 — "Beckman Head Space Sampler" used for monitoring oxygen content in food cans and containers [24, 25]

1964 — Static HS analysis advanced for determining ethanol in blood [36, 37]

1967 — Model F-40, first automated HS-GC instrument by Machata and Bodenseewerk Perkin-Elmer & Co. [2]

Figure 8 – A timeline of important developments in the history of headspace

sampling and analysis.

1.6 Static Headspace Extraction

In static headspace extraction (HSE)-gas chromatography, displayed in the diagram in Figure 9, first a closed vessel (here, a crimped or screw-capped vial) is inserted into a heater where it is heated until thermal equilibrium of the vial contents is reached. Then, a single aliquot of the headspace is removed and injected into a gas chromatographic column, travelling with analytes to the detector where the results are revealed in the form of peaks displayed on an output device [38].

Thermostatting is the process of heating the vial for a set time at a constant temperature, with the intention of bringing the vial and its contents to equilibrium at a given temperature. Equilibrium is considered to be established when the concentration of the vapor in the headspace and the concentration of the liquid sample phase stop changing.

Once the contents of the vial have reached equilibrium, an aliquot of the headspace is taken from the vial and injected into the GC. There are generally 2 types of headspace sampling systems: a pressure-balanced system and a non-pressurized system. In a "pressure-balanced" or balanced-pressure system, shown in Figure 10, the vial is brought to equilibrium, the needle pierces the septum, enters the vial, and pressurizes the vial with carrier gas (helium) for a fixed time (usually about 2 minutes). During pressurization, the pressure inside the vial must be brought equal to the carrier gas inlet pressure of the column. Then, once the contents of the vial (headspace) are opened and released into the column gas flow, it flows forward into the carrier gas flow, into the transfer line, and finally into the column [38].
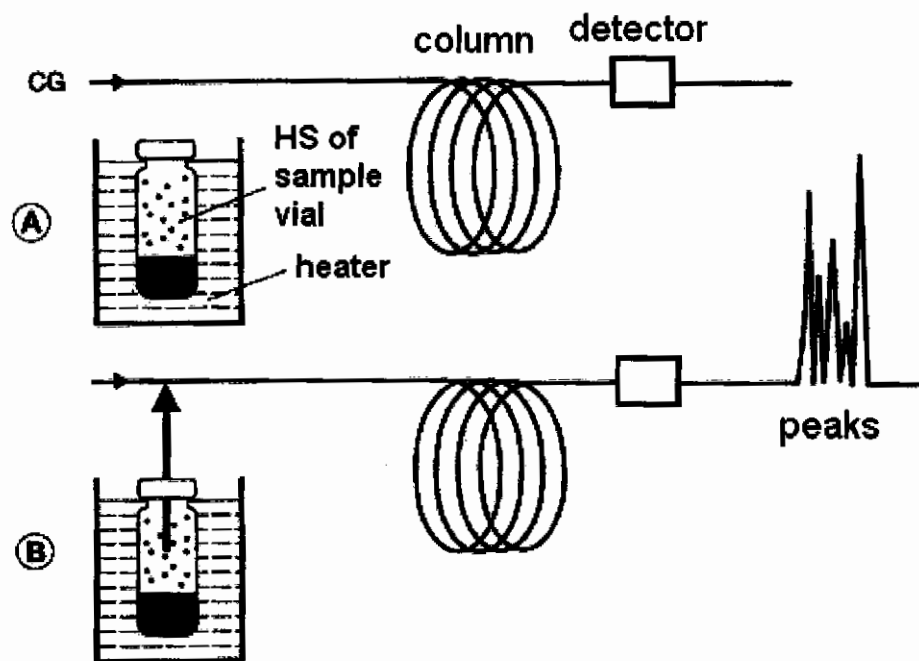
Figure 9 – A schematic of a static headspace-gas chromatograph. Section A displays the process of heating the vial (usually until equilibration is attained), and is closed from the GC column. Section B displays injection of an aliquot of the headspace into the GC, resulting in data as peaks from the detector [38].

sampling needle

open
solenoid
valve 1

needle valve

needle shaft

heated transfer line

open
solenoid
valve 2

carrier
gas

closed
solenoid
valve 1

closed
solenoid
valve 2

Equilbrium/
Standby

Pressurization
of Sample

Sample Extraction,
Transfer, Injection
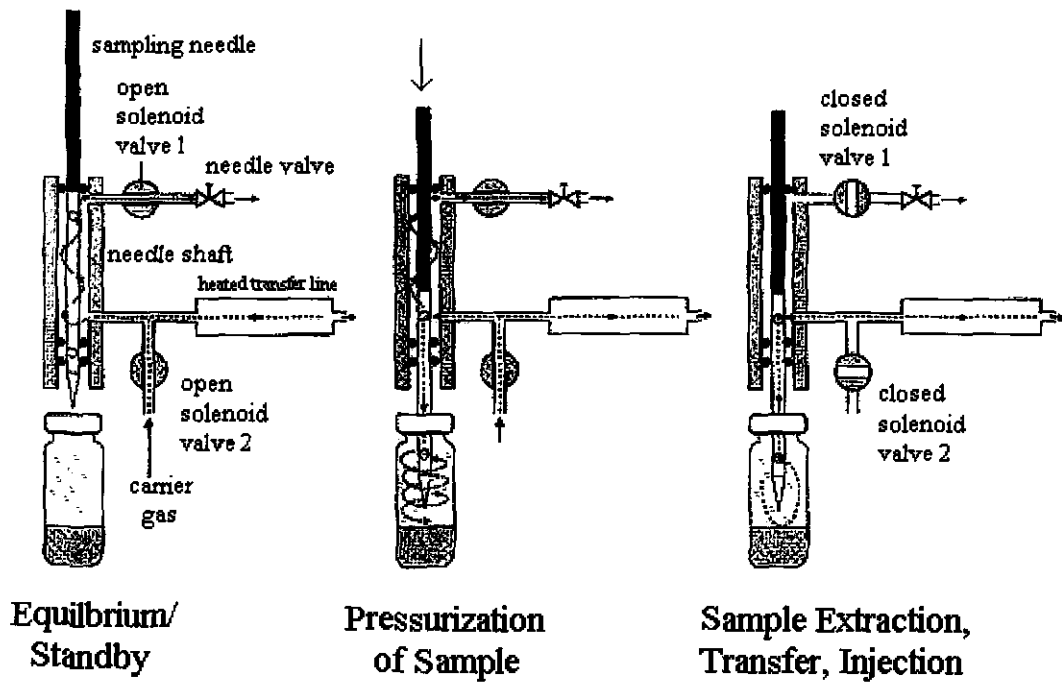
Figure 10 – A diagram of a balanced-pressure headspace sampling setup [38].

The other headspace sampler is a "non-pressurized" system, in which the vial is thermostatted and brought to equilibrium, and a gas tight syringe pierces the septum, enters the vial, and withdraws an aliquot of headspace out, which is then directly injected into a GC column. Once the analytes reach the detector, the resulting signal produced is transduced into peaks, which are displayed via the data acquisition program.

HS-GC is similar to traditional GC in the sense that the sample is in the vapor phase in the column and through the detector. The main difference though is that the sample injected into the GC inlet from headspace sampling is completely vapor (going in) whereas a sample in a traditional GC is usually in the liquid phase when it enters the GC inlet, before vaporizing in the column within the GC oven. Because of this, the concentration of components in a liquid sample would be proportionately reflected as vaporized sample as peak response from the GC, but this is not necessarily the case with HS-GC.

The concentration of components of the vapor sample to be injected and analyzed in a GC may deviate from the concentration of components in the liquid sample, because the vapor sample is a result of certain components vaporized from the liquid phase-sample. This is true because of the differing tendencies of each individual chemical component to vaporize with respect to partitioning due to the temperature inside the vial as well as the activity of each component with the matrix and other components. (For example, a non-polar analyte dissolved in a more polar solvent may have more of an affinity to the headspace than a non-polar analyte dissolved in a less polar solvent.) Due to these variations, headspace samples must be carefully calibrated with their GC peak

responses to account for differences between the concentration of analytes in the liquid phase and the concentration of analytes in the headspace, reflected as GC peak responses.

1.7 Dynamic Headspace Extraction

In dynamic headspace extraction, liquid samples are continuously extracted and transferred to the gas chromatographic column by a carrier gas, such as helium. It is used when gas is extracted from substances having unknown or particularly large partition coefficients (favoring the solution phase) because a large increase in the ratio of the volume of the vapor phase to volume of the liquid phases is used. An example of this is the analysis of oxygenated compounds such as ethanol, 1-propanol, 1-butanol, and dioxane in aqueous solutions of which K is greater than 10^3 [53]. The example mentioned of the first HS-GC publication on the monitored hydrogen content in water of high pressure power stations [22] is an example of dynamic HS-GC. In this method, volatile constituents are separated from the sample matrix by either a continuous flow of an inert gas over the liquid or solid sample or by the purge and trap (P&T) technique. A system like this passes large quantities of up to 100 liters of air or inert gas through a a few milliliters liquid sample in the form of a continuous flow of small bubbles. The vapor is analyzed prior to and after the purging process of the sample or could be analyzed by direct analysis of the gas flow passed through the investigated solution [53].

1.7.1 Purge and Trap

The purpose of using purge and trap is to completely separate (or purge) the volatile components of interest from the sample matrix with the intention of performing quantitative analyses on the final concentrated headspace extract (that was originally concentrated in the headspace during the purge process), which must then be collected in a trap (such as a cold trap). During purging, an inert gas is bubbled through a liquid sample and the analytes are collected (trapped) in an adsorbent trap.

For example, for using a purge and trap system to determine volatile organic compounds in water, a syringe is used to transfer a controlled volume of sample from a sample container into a glass purge chamber, where it is heated to a desired temperature to increase the vapor pressure of compounds of interest. An inert purge gas such as N_2 or He is introduced as tiny bubbles through the bottom of a purge chamber, which contains the sample. Smaller bubble sizes, made possible by a fritted disperser, will ensure better gas-water (or solvent/matrix) contact, allowing more analyte to be dissolved in the purge gas, which in turn will be collected. The purge gas then passes through a cooled trap, with dimensions of about 4 mm internal diameter and a length of 25 cm, packed with Tenax or a multisorbent trap. Upon completion of the purging, the trap is heated rapidly to between 200°C and 350°C, backflushed with carrier gas, and the sample is transferred to the GC [54]

Figure 11 displays the components of the P&T technique. In section A, the sample is purged and volatile compounds are removed and collected from the sparging vessel of an adsorption trap with multisorbent packing. In section B, the sample desorbs

from the adsorption trap from backflushing of the heated trap, then is refocused in a cryo-trap and transferred into the capillary column [38, 53].

The trap consists of a cartridge packed with an adsorbent that releases the trapped analytes by thermal desorption into a flow of carrier gas which transfers it to the column; it can also be a cold trap. However, the charged adsorbent may also be desorbed by a small quantity of liquid solvent such as that used by Grob in the closed-loop stripping procedure [55-57]

An adsorption trap with a sufficient capacity is required to avoid breakthrough during the purge time because of the high flow rate necessary to complete an exhaustive extraction from the sample in a shorter, rather than extensively longer time. A trap such as this has similar dimensions to a short packed GC column and it permits comparable flow rates of around 20-40 mL/min for both adsorption and desorption [38]. An example of a popular porous polymer is Tenax, but due to its weak nature as an adsorpant, precautions must be made to handle it carefully in order to avoid breakthrough of the more volatile compounds. There are numerous publications containing data of these volatile compounds at temperatures ranging from $-10^{\circ}C$ to $170^{\circ}C$ (some of which are referenced in this respective source) [58].

Fewer precautions are essential in the case of a trap filled with several adsorbents in series with increasing adsorptivity because an adsorption gradient is formed causing the most volatile compounds to be absorbed last at the end of a line of multi-sorbent packing. The trapped compounds are thermally desorbed and back-flushed onto a capillary GC column or are often also trapped with the intention of being refocused (re-trapped) in a cryo-trap.
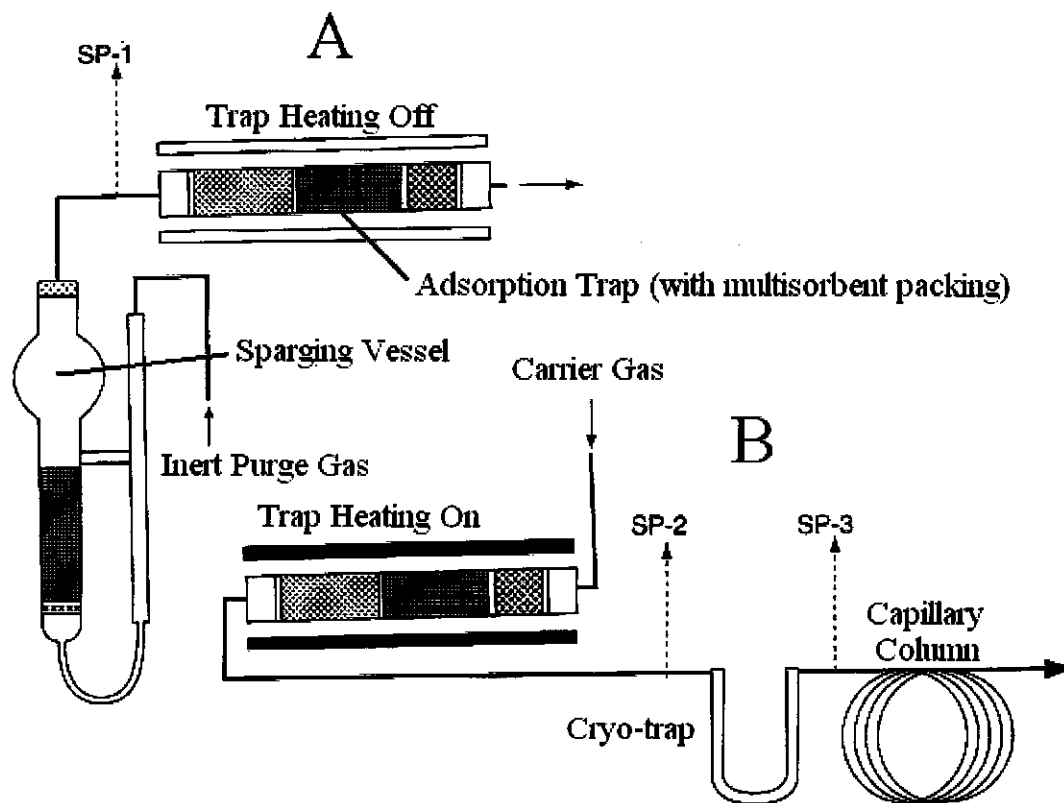
Figure 11 - Dynamic HS-GC "Purge and Trap" Setup [38].

A major drawback to a strong adsorbent is artifact generation caused by labile compounds, such as limonene, which is a terpene, in fruit drinks, often encountered in flavor analysis. Safe solvent extraction such as liquid desorption of headspace volatiles trapped on activated carbon open tubular traps is preferable in this case to prevent artifact generation, being an alternative to traditional thermal desorption [59]. Artifacts are formed by the energy released during adsorption and thermal stress during thermal desorption. However, for rapid desorption from strong sorbents, high temperatures are often needed. This can lead to the release of artificial decomposition products which make spurious peaks in the chromatogram in the case of Tenax and other porous polymer sorbents [60].

Figure 12 is a sample chromatogram from a study in which residual solvents in a water-soluble active pharmaceutical ingredient were determined using purge-and-trap gas extraction with gas chromatography [61]. Another purpose of the study was to compare the sensitivity of the purge-and-trap technique to the sensitivity of static headspace-gas chromatography. The purge-and-trap apparatus consisted of a SOLATek 72 Autosampler, a Velocity XPT Sample Concentrator, high purity nitrogen as the purge gas, and Tenax/silica gel/charcoal as the trap adsorbent. Chromatogram A is a blank run and chromatogram B is from the sample, which is shown to contain 1,1-dichloroethane,1,2-dichloroethane, and benzene. The results show that the purge-and-trap technique is suitable for determining residual solvents of the ICH Class 1 group. They also show that the purge-and-trap technique is more sensitive than using static headspace-gas chromatography for the same group of residual solvents [61].
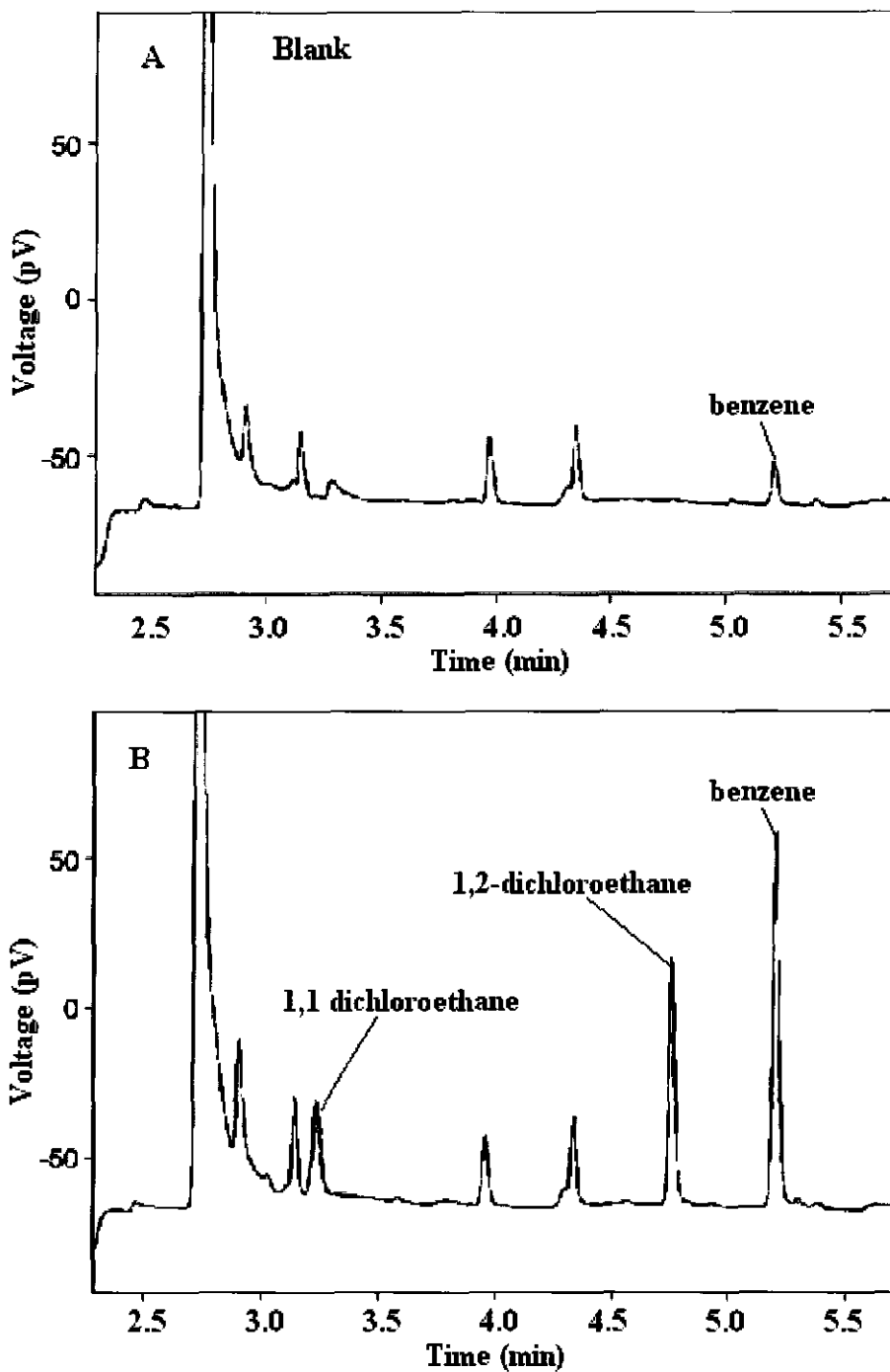
Figure 12 – Chromatograms of a residual solvent in an API study in which purge-and-trap extraction is used with gas chromatography. Chromatogram A is a blank and chromatogram B is a sample [61].

There are 3 noteworthy problems associated with thermal desorption from such a trap: water, flow, and time. The problem from water is that the diluted gas extract will contain water vapor along with the analytes of interest, which are usually trapped by adsorption on a hydrophobic adsorbent such as Tenax, Carbotrap, Carbopack, Carboxen, etc. When excess water passes through a trap that is at a temperature lower than the sparging container and is cooled, water can condense and be trapped [62-64]. This can be prevented either by water-removal techniques or desiccants [65]. The problem associated with the flow is the capillary columns in which desorption occurs are not usually compatible with flow rates greater than a few mL/min, while flow rates from the P&T extractor exceed this, up to about 20mL/min in adsorption tubes, which have similar dimensions to a short packed GC column. This can be adjusted by applying a capillary inlet splitter, but this is at the sacrifice of reduced sensitivity and waste of headspace gas [66, 67]. The time problem comes from the desorption step because it takes too long for the sample to be introduced into a capillary column. This can be dealt with by using a two step focusing procedure which includes adsorption/desorption with a cryo-trap, or a one step trap utilizing one or the other [38].

1.7.2 Static HS-GC Compared to Purge and Trap

The differences between static HS-GC and P&T center on sensitivity. P&T is about 10 times more sensitive compared to static HS-GC, and can strip virtually all analyte out of a sample. This was proven by an example in which a sample was analyzed separately using static HS-GC and HS-GC with P&T, and the results were compared. A

20 mL vial was filled with 10 mL of a liquid sample containing 100 µg of a volatile

analyte, and then equilibrated. The concentration of the volatile organic compound in the

vapor phase is 5 µg/mL, under the assumption that half of it is present in the headspace.

It is expected that 2 mL of the headspace will be sampled when using static HS-GC, and

transferred with a split ratio of 1:20, which would make the corresponding volume

injected into the capillary column 100 µL and the amount of analyte injected to be 0.5 µg.

Since P&T will successfully strip of the entire 100 µg amount of analyte, 5 µg will enter

the column, at the same split ratio of 1:20, and 5 µg is ten times greater than 0.5 µg [38].

The opposite is true, however, when cryo-trapping is applied. An example of this

was shown in an experiment in which samples of methyl-*tert*-butyl ether in water were

analyzed using both static HS-GC and P&T with a cryo-trap. The results showed that the

limit of detection was 50 µg/L by static HS-GC and 2 µg/L by the P&T procedure [68],

making the static HS-GC with cryo-trap technique 25 times more sensitive.

1.8 Multiple Headspace Extraction

In multiple headspace extraction (MHE), successive aliquots are taken from the

same vial's headspace, and it is considered dynamic gas extraction carried out stepwise.

The advantage to this method is the ability to extract virtually the whole amount of

analyte from a sample matrix by removing the analytes in parts until there is no analyte

left in the original sample to extract [38]. This technique and associated mathematical

model and theory originated from McAuliffe, Suzuki et. al, and others [69-76].

Figure 13 shows a MHE analysis in which an aqueous solution sample containing chloroform, 1,1,1-trichloroethane, carbon tetrachloride, trichloroethylene, and tetrachloroethylene is analyzed 3 times consecutively from the same vial [77]. It can be seen that the size of the peaks decrease from the first to the second to the third analysis, respectively. As suggested before, and supported by equation 1, it may be assumed that in order to determine the total amount of analyte present in a sample, the number of analysis must be many, until the analyte of interest is completely exhausted and analyzed. The same outcome can be achieved however by carrying out a limited number of extractions and extrapolating the peak area data.

Figure 14 is a plot of peak response versus extraction number for the MHE analysis of methyl methacrylate from a study to determine monomer solubility in water. The transition point, indicated by subscript t, is the point or extraction number at which the peak response indicates that the headspace is no longer becoming saturated, which indicates that the analytes of interest in the liquid sample are nearing exhaustion. The transition point occurs at the sixth extraction where A_t is the associated peak response at the transition point, A_{t+1} is the GC peak response at the first extraction after the transition point t and A_{t+2} is the second extraction after the transition point. It can be seen that the slope of the peak area of methyl methacrylate remains constant until the transition point, and then decreases for every consecutive extraction [78].
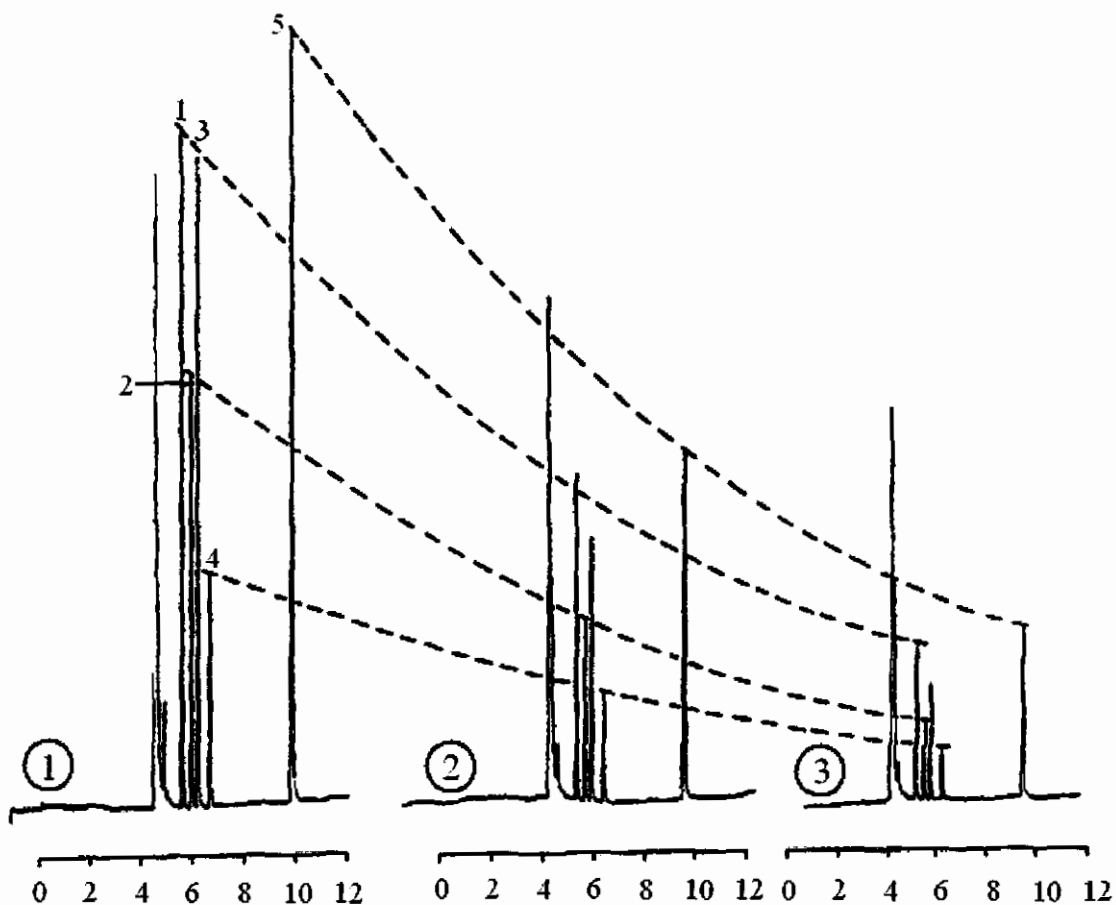
Figure 13 – A demonstration of the decrease of peak areas of volatile halogenated hydrocarbons in an aqueous solution of three consecutive multiple headspace analyses. Corresponding peaks (initial concentration): 1 – chloroform (25 µg/L); 2 – 1,1,1-trichloroethane (5 µg/L); 3 – carbon tetrachloride (.5 µg/L); 4 – trichloroethylene (4 µg/L); 5 – tetrachloroethylene (2 µg/L) [38, 77].
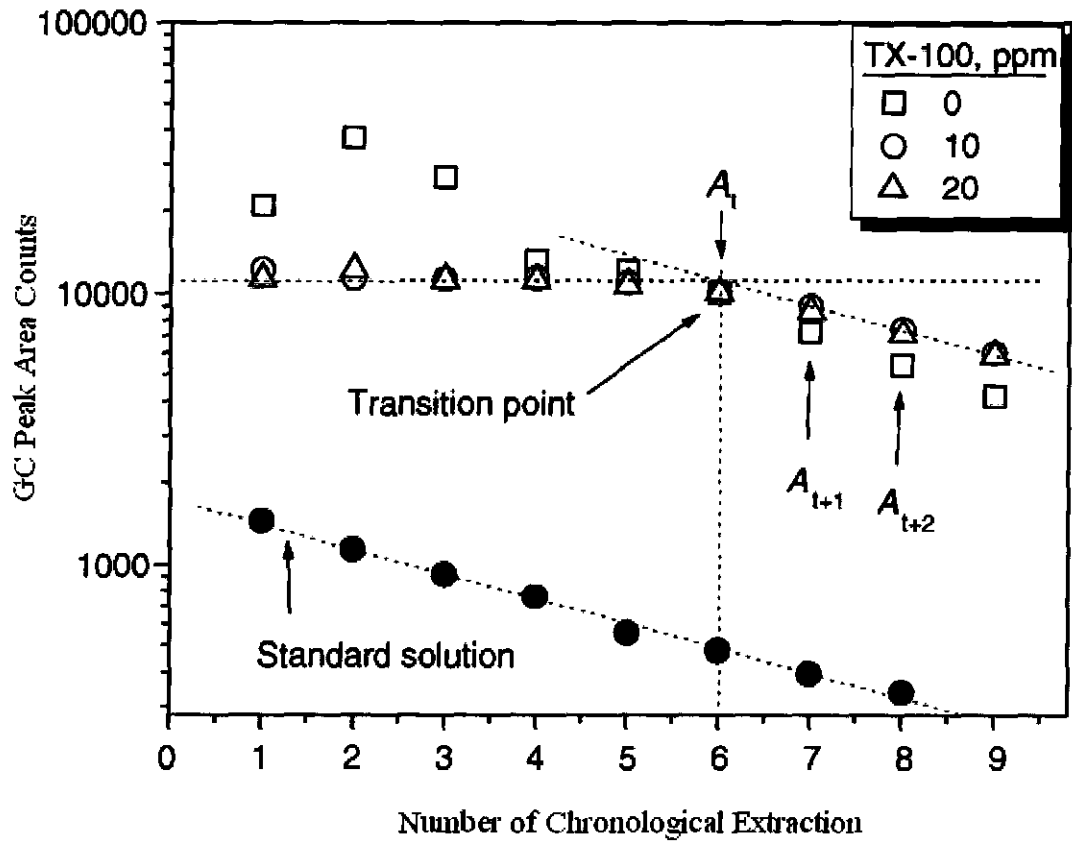
Figure 14 – A profile of a MHE process of the vapor content of methyl methacrylate with respect to each consecutive extraction [78].

1.9 Solid Phase Micro-Extraction (SPME)

Solid phase micro-extraction (SPME) was developed in the early 1990s by Dr. Pawliszyn et. al. The purpose of using SPME with HS-GC instead of HS-GC alone is so a fiber can discriminate and sample specific analytes of interest that may be in the headspace or liquid sample, according to the absorption properties of the surface of the fiber. Additional selectivity is a result of different solubilities of volatile compounds in the fiber coating [79]. In one of its earliest published uses in 1992 by Hawthorne, et. al., SPME was used in a study to determine the amount of caffeine in beverages using fused-silica fibers [80]. Also in 1992 by Potter, et. al, SPME was used with gas chromatography-ion trap mass spectrometry in an experiment to detect substituted benzenes in water at the pg/mL level [81].

SPME is a technique that can be applied to HS-GC in a multiple step process [81-85]. First, a sample vial is prepared the same way as in other static HS-GC techniques. A fiber with a fused-silica coated film of an immobilized stationary phase is attached to the plunger of a GC syringe, modified to hold the coated fiber and move up and down through the needle. As sampling of the vial begins, the syringe needle pierces the septa, enters the vial, and the fiber comes out of the tip of the needle and becomes exposed to the contents of the vial. Depending on the method, a fiber may come into contact with either the headspace gas or the liquid sample.

Once the analyte is absorbed into the fiber, the fiber pulls back up into the needle, the syringe comes out of the vial, and transfers to the inlet, similar to a normal HS-GC system. Once the syringe is inserted into the hot GC inlet, the compound dissolved on

the fiber are released by thermal desorption and transferred to the GC column in the flow of carrier gas.

Figure 15 shows a diagram of an SPME syringe, the absorption process, and injection into a GC. In picture A, the plunger pushes the SPME fiber through the protective fiber sheath so that the tip of the SPME fiber is exposed to the sample of interest. In picture B, the fiber is exposed to the headspace and volatile molecules absorb into the SPME fiber. The SPME fiber is then retracted up into the fiber sheath while the needle is moved to the GC inlet port. In picture C, the plunger pushes the SPME fiber back down through the fiber sheath so the fiber is exposed to the inside of the inlet of the GC, where the sample on the fiber is desorbed and analyzed.

When SPME is used, there is a three-phase system and there are two equilibrium systems. There are two equilibrium systems because of the presence of the liquid sample phase, the headspace (vapor phase), and the fiber, which is a solid phase. The first equilibrium system is between the liquid phase and the vapor phase and the other equilibrium phase is between the vapor phase and the fiber. Equilibrium is attained when the concentrations at each phase stop changing [78].

1.9.2 HS-GC Compared to HS-SPME

The sensitivities of HS-GC and HS-SPME vary with respect to one another, and depend on a number of properties such as volatility, polarity, solubility of the analytes and the solvents, and film thickness and polarity of the SPME fiber coating. For reasons related to these parameters, analytes with higher volatility may be derivatized to have a
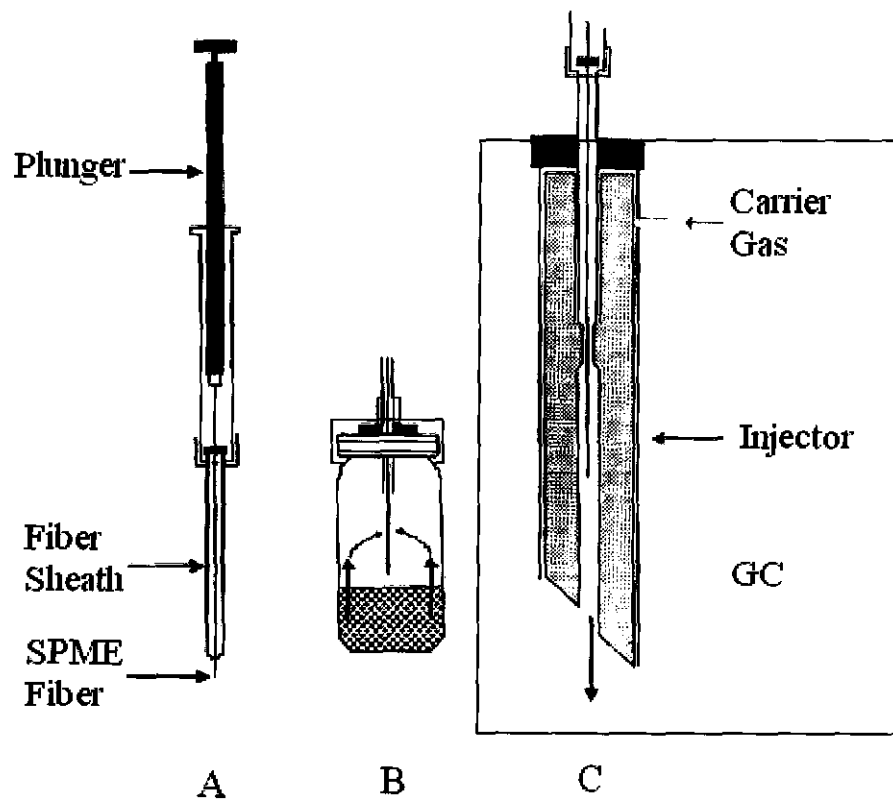
Figure 15 – Diagram of an SPME Fiber [38].

lower volatility for analysis using HS-SPME, whereas the opposite may be the case for analysis using static HS-GC, in which a low-volatility analyte would be derivatized to have a higher volatility.

An experiment is described as an example in which 2 mL of a dilute aqueous solution containing 5 ppm (μg/mL) of benzene is in a 10 mL vial at 25°C in order to compare the sensitivity when analyzed by static HS-GC and HS-SPME. The concentration in the headspace is 60 μg/mL. When analyzed with static HS-GC with a standard open-tubular column having a 0.32 mm I.D., 1.5 mL/min carrier gas inlet flow, and sampling time of 2 seconds, making the sampled amount 30 ng, it is about 6 times more sensitive than when sampled by SPME with a 7 μm fiber, which samples 5.05 ng of benzene. When the same analyte is sampled by SPME with a 30 μm fiber, it absorbs 23.7 ng of benzene, which is more than 4 times as sensitive as the 7 μm fiber, but still less sensitive than when sampled by HS-GC [38].

1.10 HS-GC Compared to GC

Headspace-gas chromatography differs from traditional gas chromatography and there are advantages to using headspace-gas chromatography. The differences and advantages revolve around sample preparation, sample extraction, and sample injection being attributed to the fact that only the vapor phase is used. First, sample preparation for traditional GC involves preparing a solution that not only contains the proper concentrations of analytes, but an injectable sample matrix as well. For instance, in an environmental study to determine volatile organic compounds in soil, the analytes of

interest would have to be extracted and filtered from the soil sample. For studies to determine the ethanol content of blood or urine, a sample would have to be manipulated to be suitable for injection into the GC column. If these same soil or blood samples were studied with a headspace-gas chromatograph, the sample could be put in a vial, set to equilibrate, and the VOCs or ethanol detected on the GC.

In a case where an analyte of interest is dissolved in a solvent that yields a signal by the detector, this becomes a problem in traditional GC, either because the solvent peak would be too big in comparison to a trace amount of analyte, or because in order for enough of the analyte to be detected, a large sample would have to be injected, that could saturate the column. A perfect example is studying the vinyl chloride monomer (VCM) content in wastewater [86]. The volatile analytes of interest will be present in the vapor phase of a vial containing a sample, while the sample matrix remains in the solution (other than the amount that also vaporizes) and is not injected. Furthermore, for studies of samples containing solid materials, such as determining residual solvents in packaging materials, solid samples can be placed in the vial, and the analytes will vaporize into the headspace to be extracted and analyzed [87].

1.11 Temperature in Headspace Extraction

Temperature is an important property that is related to many aspects of headspace extraction. Temperature affects the partitioning and interactions of the solutes and solvent and ultimately how much analyte will be present in the headspace for analysis. The temperature inside the vial affects the time it takes for the partitioned components to

reach equilibrium within a vial, before sample extraction occurs. The exact temperature inside the vial during extraction is unknown because the temperature sensor of an automated headspace gas chromatograph is located on the heating block; it is difficult for that sensor to be inside the vial without disrupting equilibrium in the currently existing commercial systems.

Temperature is also directly related mathematically to several important physical properties. The partition coefficients, activity coefficients, and vapor pressure are all functions of temperature (and partition coefficients are also indirectly proportional to activity coefficients). Temperature also has an affect on chromatographic results expressed in the form of peak area, with respect to the sample. Since partition coefficients and activity coefficients are essentially determined from peak areas, and because of the relationship of the partition coefficient to the activity coefficient, temperature can affect the determined values of partition coefficients and activity coefficients [53].

1.12 Physicochemical Properties

Physicochemical properties are values of certain measurements that are thermodynamically and physically related to phases and concentrations of a chemical system. Some physicochemical properties are partition coefficients (which are the inverse of Henry's law constants), activity coefficient, and selectivity. These properties can be determined using various methods of HS-GC; however other instruments and techniques have been used to determine them in the past (discussed in sections 1.12.1 and

1.12.2). Physicochemical properties are numeric values that reflect the measurable behavior of analytes in multi-component chemical mixtures, such as (chemical) interactions with other chemicals, and reactions to outside (physical) stimulus such as temperature. Using these physicochemical properties in conjunction with chemical systems can improve analysis on certain samples by using the chemical-specific information to manipulate optimal pathways for samples to be most efficiently analyzed by HS-GC.

When a sample is prepared and set to reach equilibrium for HS analysis, reproducibility of the detected response is reliant on the consistent behavior of the chemicals inside the vial. The equilibrium of the contents in a vial can be monitored by determining the concentrations of the phases present. The number of phases can range from 1 to 3. The vial will have 1 phase present if it contains only vapor or a solid that is completely non volatile. A vial usually contains 2 phases, which are the liquid sample phase and the vapor phase. A vial can also have 2 phases when a volatile solid sample is present inside, such as naphthalene for example. A vial can also have a maximum of 3 phases when it contains a solid phase, a liquid phase, and a vapor phase.

Partition coefficients and activity coefficients are defined and discussed in more detail in sections 1.13.1 and 1.13.2, respectively. Henry's law constants are dimensionless numerical values reflecting the ratio of the concentration of a component in the headspace to the concentration of a component in the liquid phase under ideal gas and ideal liquid behavior. Henry's law constants vary with temperature and pressure and can be considered the inverse of partition coefficients for the same component when the activity coefficient of the liquid is zero [88]. Selectivity is a separation measurement of

the relative capacity analytes are retained with respect to other analytes, related to chemical interactions between solutes and the liquid phase, and adsorption to surfaces (in gas chromatograph columns), in separation chemistry [89].

1.12.1 Physicochemical Properties – Partition Coefficient

The partition coefficient is an equilibrium constant, K, which expresses the quotient of the concentrations of liquid (as products) and vapor (as reactants). For example, for the simple chemical equation of benzene in the gas phase at equilibrium with benzene in the liquid phase,
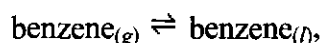
$$benzene_{(g)} \rightleftharpoons benzene_{(l)},$$

the equilibrium constant would be written

$$K = \frac{[benzene_{(l)}]}{[benzene_{(g)}]}.$$

The higher the value of the partition coefficient is above 1, the more the analyte favors the liquid sample phase. The lower the value of the partition coefficient is below 1, the more the analyte favors the headspace (vapor phase). The information published on partition coefficients for compounds analyzed by headspace-gas chromatography is growing.

Prior to determining partition coefficients using headspace-gas chromatography methods, they were measured using other methods, dating back to the early 1950s [3,4]. A table of air-water partition coefficients was published by Ioffe and Vitenburg [53]. These coefficients were measured at lower temperatures, ranging from 0°C to 30°C, some by static HS-GC, some by dynamic HS-GC, and the solutes include hydrocarbons,

oxygen compounds, and sulfurous compounds [53, 90-96]. Some more recent alternative techniques are gas chromatography (GC) and gas liquid chromatography (GLC) [97, 98].

1.12.2 Physicochemical Properties – Activity Coefficient

The activity coefficient, γ, reflects the deviation of the concentration of a solute in a non-ideal liquid from the concentration of a solute in ideal liquid conditions. These deviations can be due to intermolecular forces and interactions between particles of the solute with particles of the solvent or other solute particles. For this reason, the activity coefficient is considered a correction factor to the concentration (including mole fraction) of the solute. The activity coefficient is further defined (mathematically) in section 2.6. A solution is said to be "ideal" when the activity coefficient is 1. When the activity coefficient is not 1, a solution is non-ideal [99]. Examples of ideal binary mixtures include hexane/heptane, ethanol/isopropanol, benzene/toluene, p-xylene/m-xylene. Examples of non-ideal mixtures with activity coefficients greater than 1 are ethanol/water, ethanol/acetonitrile, and heptane/toluene, ether/ethanol, ethanol/heptane, benzene/aniline, and toluene/phenol [100].

An ideal solution is a solution containing more than one compound in which no interaction occurs between molecules. A real solution is a mixture of more than one compound of which the molecules interact due to intermolecular forces such as London-type, dipolar interactions, hydrogen bonding, and specific interactions. These interactions can be between like or unlike adjacent molecules in a liquid mixture and of comparable magnitude (ideal systems) or dissimilar (non-ideal systems). A real solution

may be made of two or more liquids or one or more solutes dissolved in one or more liquids [100]. (Some applications involving the use of activity coefficients are discussed in section 1.12.2.)

Although there is information published on activity coefficients, there is a moderately large amount of information published on "infinite dilution activity coefficients", $\gamma\infty$ (also known as "limiting activity coefficients") [101, 102]. Infinite dilution activity coefficients characterize the behavior of single solutes on a molecular level, in which the solute molecule is expected to be completely surrounded by solvent. There are only solute-solvent interactions, and an infinitesimal amount of solute-solute interactions, due to the ratio of solute to solvent being extremely low [101]. For a binary system, infinite dilution activity coefficients are activity coefficients of component i in which the mole fraction of solute approaches the limit of zero and the mole fraction of the solvent approaches the limit of unity [102]. There are so few solute to solvent interactions due to the solute to solvent arrangement (very few solute particles : many solvent particles), the level of non-ideality is taken to such an extreme limit that the infinite solution state is considered to be an ideal state of solution.

The concentration region of infinite dilution is extremely narrow, meaning that at any higher concentration it will be just a dilute (and finite) concentration, and any concentration lower will be zero. Because of that difficult to define and produce range of concentration, it (that particular concentration in the infinite dilution range) cannot be evaluated theoretically or determined experimentally. Some systems, however, can be defined by a finite concentration, such as ethanol in hexadecane, in which the extension of the dilute region may be approximately 10^{-2} mole fraction, for a mixture of similar

hydrocarbons [101]. The true infinite dilution region may be smaller than 10^{-4} mole fraction for solutions of highly associated species, or even as low as 10^{-7} [103]. It is suggested that it is easier to model by using statistical mechanical theories or computer simulation methods as it provides useful information in the testing of possible applicability of a simulation method or theoretical model [104, 105].

It is referred to as a "preparatory period" for infinite dilution activity coefficients up to 1955 because up to this point, it was impossible to directly make accurate measurements of infinite dilution activity coefficients. Up to this time, the concept of activity coefficients at infinite dilution and theoretical and experimental studies were conducted [106-110]. In 1955, four equations for obtaining infinite dilution activity coefficients in binary systems from vapor-liquid equilibrium (VLE) under various experimental conditions were derived and carried out by Gautreaux and Coates, setting the theoretical foundation for the direct determination of infinite dilution activity coefficients using the ebulliometric method [111-117].

Gas-liquid chromatography (GLC) techniques were also used to measure infinite dilution activity coefficients at the time [118-119]. Of the variations of GLC, conventional GLC was limited to volatile solutes in nonvolatile or slightly volatile solvent, while the attention was paid to non-steady-state GLC [120]. The headspace GLC was used mainly for vapor-liquid equilibrium measurements and rarely for measurements of infinite dilution activity coefficients [121]. A period of more progressive development began in 1977 when a new technique of gas stripping was proposed [122]. Measuring infinite dilution activity coefficients of low volatile solutes was achieved in 1990 by the liquid analysis gas-stripping method [123], which has been

45

supported by experimental results to be efficient [124], particularly for large measurements [125].

In 1981, the expressions deduced by Gautreaux and Coates [126] were further modified by the proposed differential ebulliometric method by introducing a non-ideality correction for the vapor phase [101, 127]; improvements in the ebulliometer design were made in years to follow [128]. In 1986, the differential static method was proposed for measuring infinite dilution activity coefficients, which is said to complement the differential ebulliometric technique [94]. It was during this year that the non-steady state gas-liquid chromatography, headspace gas-liquid chromatography, and stationary phase gas-liquid chromatography techniques were improved [129-134]. Of these, the SGLC method was most widely used due to its fast speed, reliability, and simplicity. Liquid-liquid chromatography, especially high-performance liquid chromatography [135, 136], were used to measure infinite dilution activity coefficients, but were not as accurate as GLC methods, and thus were used less frequently [96].

Beginning in 1991, new techniques were proposed and emerging that dealt with compounds of various volatilities (vapor pressures), and methods from the past such as NSGLC, HGLC, and HPLC were being used to measure activity coefficients at infinite dilution more than ever. A low volatility is considered to be less than 1 and a large volatility is considered greater than 1000. Activity coefficients of a dilute solution with a relative volatility of between 1 and 70 were measured by the Raleigh distillation methods [137]. A modified version of the liquid-analysis gas-stripping method was used to measure systems with low volatile solutes [138]. In 1993, a further developed gas stripping method was used to measure systems of large relative volatility up to 10^5 [139]

and the dew point method was proposed for very low relative volatility systems measurements [140]. The relative stationary gas-liquid chromatographic method was used to measure infinite dilution activity coefficients of halogenated hydrocarbons and other organic pollutants in water [141-142], and the differential static method was applied to a variety of systems, including water systems [106].

1.13 General Applications of HS-GC

Headspace extraction with gas chromatography (HS-GC) as a combination of sampling technique and instrumentation has proven to be useful and relevant to a wide range of applications, increasing with time, since its beginning. Even though HS-GC is still used in the applications it was originally created for, the number of applications is still growing. The range of applications HS-GC is used for is extremely large, used in a diverse range of fields and industries, including environmental, food science, flavors and fragrances, pharmaceutical, biological, petrochemical, polymer science, and biomedical analysis. HS-GC is used in regulatory methods along with theoretical and experimental physicochemical properties related to such applications.

Studies were done to compare volatile compounds from Tunisian and Sicilian monovarietal virgin olive oils and to measure volatile sulfur compounds in heat-shocked and pasteurized milk cheese [143, 144]. Headspace solid phase microextraction is used to study the impact of feeding and rearing systems of Iberian pigs on volatile profile and sensory characteristics of dry-cured loin and to determine the methanol content in biodiesel [145, 146]. Static headspace-gas chromatography is used for (semi)-volatile

drugs in pharmaceuticals for topical use, and purge-and-trap is used to measure residual solvents in drug substances [105, 106]. HS-GC is used to make official measurements in various laboratories around the world in countries such as Germany, and Japan, and the Environmental Protection Agency (EPA), the Food and Drug Administration (FDA), and the American Society for Testing and Materials (ASTM) in the United States [38].

1.13.1 Regulatory Methods

In the United States, a number of methods utilizing static and purge and trap dynamic HS-GC have been published by the Environmental Protection Agency. The vinyl chloride monomer (VCM) content in wastewater and poly(vinyl chloride) (PVC) resin, slurry, wet cake, and latex samples are determined using the static HS-GC method [147-148]. It is also used to screen for volatile analytes in soil and sediments and to screen and quantitatively analyze volatile organic compounds (VOCs) [149-151].

There are a number of official static HS-GC methods accepted by the FDA for the analysis of vinyl chloride monomer in corn oil and food-simulating solvents [152], vinegar and oils [153], and PVC food packaging [154]. The use of static HS-GC for the analysis of organic volatile impurities (OVIs) has been proposed by the U.S. Pharmacopeia [155].

There are a number of static HS-GC methods used in polymer analysis used by the ASTM [156-161]. One is the standard method for determining residual solvents in flexible packaging materials such as cellophane polyethylene films, which recognized the need to establish proper equilibration settings [156]. Other methods include the

headspace analysis of volatiles in polymer samples such as vinyl chloride monomer [157-160], acetonitrile [161, 162], and flammable residues from debris samples by dynamic headspace concentration [163] and HS-SPME [164].

Figure 16 displays the chromatogram of the headspace-SPME analysis of a 100 ng/mL standard solution from a study of determining residual solvents in pharmaceutical products by headspace-GC and GC-MS-SPME. In the study, techniques and fibers were compared. Headspace SPME results were compared to gastight SPME, which is the same as normal SPME except that it withdrawals 200 μL of headspace gas into the needle of the SPME device along with the fiber, and injects both into the inlet of the GC. The headspace SPME results were more precise and the gastight SPME was more sensitive and had lower detection limits. Three fibers with different polymer films were compared and the film that was determined to be the best was the polydimethylsiloxane/divinyl-benzene coated fiber, having the best sensitivity and ability to extract compounds of different volatility and polarity [165].

1.13.2 HS-GC Applications Involving Physicochemical Properties

There are many applications of partition coefficients using headspace-gas chromatography in fields including environmental studies and biomedicine. Studying the phase partitioning can lead to understanding and controlling the release of hazardous compounds into the atmosphere due the solubility and adsorptivity of those compounds in water and soil. The partitioning of noxious compounds between blood and air in the lungs is important for measuring the biological
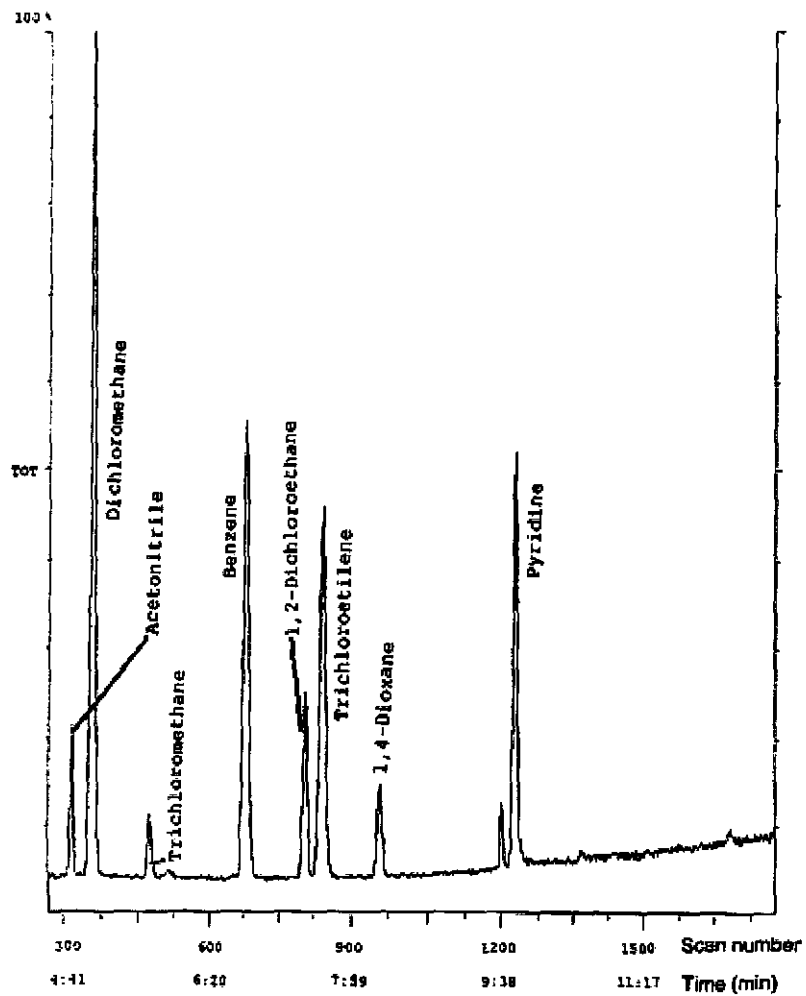
Figure 16 – A chromatogram of the headspace-SPME analysis of a 100 ng/mL

standard solution [165].

exposure index (BEI) and the biological tolerance (BAT) values for working materials [166].

Partition coefficients are also used for characterizing solvents which are related to retention behavior in chromatographic separations. Rohrschneider discussed the theory of solubility parameters, solvent polarity, polarity data, and solvent strength [167, 168] previously discussed by Hildebrand [99], Reichardt [169], and Snyder [170]. Partition coefficients are useful for understanding solvent properties for volatile solvents that cannot be investigated as stationary phases. Rohrschneider measured partition coefficients of six reference compounds in 80 different solvents of different polarities.

In other recent publications, there are applications of partition coefficients outside of drug and environmental related fields. For instance, in food science, the partition coefficients of aroma compounds were studied. In 2000, Friel, et. al. used an empirical model to predict the headspace concentration of 40 volatile compounds dissolved in aqueous sucrose solutions using headspace analysis by atmospheric pressure chemical ionization-mass spectroscopy [171]. In 2003, Jouquand, et. al. determined the partition coefficients of aroma compounds, such as ketones, hexanal, t-2-hexanal, ethyl butanoate, and 1-hexanol, in polysaccharide solutions by static headspace gas chromatography using the phase ratio variation method [172]. In a more recent publication by the same author, the influence of chemical composition on aroma retention is discussed [173].

Applications of infinite dilution activity coefficients cover a wide range of fields, from industrial to environmental. They are used and extrapolated to predict phase behavior of a mixture over the entire range of concentration. As a dilute property, it can be used to directly and accurately determine the equilibrium composition of a dilute

mixture, useful in industrial processes such as specialty chemical separation, high-purity extraction, and azeotropic distillation. The infinite dilution activity coefficient data is used to predict environmental properties such as n-octanol/water partition coefficients and water solubility [174, 175].

1.14 Experiments in this Research

In this research, the relationship between temperature, partition coefficients, and activity coefficients are explored, both theoretically and experimentally. The affect that a static headspace extraction system has on the actual temperature of a sample during the extraction process is explored from a chromatographic perspective. In other words, how efficiently the instrument heats a sample vial, and how accurately the system reports the expected measured temperature from within the system, is compared to the actual temperature inside a sample vial. Two similar static headspace-gas chromatographs are compared by the data produced by each from identical experiments to determine physicochemical properties such as the partition coefficient and activity coefficient.

In the temperature study, the temperature of the inside of a sample vial was measured by a thermocouple and by a chromatographic method in which the temperature is mathematically related to the gas chromatographic peak responses of the headspace of a binary mixture. The two binary mixtures studied were naphthalene with dodecane and benzene with toluene. Internal standards of methyl ethyl ketone, benzene, and toluene were studied by analyzing the gas chromatographic peak responses of individual pure components with respect to temperature, volume of the sample, and volume of the vial.

The air-water partition coefficients of methyl ethyl keytone, benzene, toluene, and

cyclohexane were experimentally determined by the vapor phase calibration (VPC)

method and the phase ratio variation (PRV) method. The activity coefficient of benzene

in toluene was experimentally determined by analyzing the gas chromatographic peak

responses from pure components and mixtures of the two components, at various sample

volumes.

2. THEORY

2.1 Headspace-Gas Chromatography

In headspace-gas chromatography, the headspace sample to be extracted is first brought to equilibrium with the components in a closed container, which in many cases is a vial. There can be up to 3 phases in a vial when solid, liquid, and vapor are present. The volumes of liquid and vapor in a vial can be expressed mathematically. The Greek letter β is a variable used to represent the ratio of the volume of the gas phase (headspace) to the volume of the liquid (or sample) phase. This is known as the phase ratio, and is represented by Equation 1 [176].

$$\beta = \frac{V_G}{V_S} \qquad (1)$$

The variable V_G represents the volume of the gas phase or headspace and V_S represents the volume of the liquid (or sample) phase. The concept of the phase ratio is shown in the diagram in Figure 17. The diagram shows a small liquid sample layer at the bottom of the vial and tiny dots in the headspace that represent vaporized molecules of the original sample after equilibrium has been reached in the vial. The volume of the vial can be expressed mathematically in terms of the volume of the headspace and the volume of the sample phase, as in Equation 2 [38].

$$V_v = V_G + V_S \qquad (2)$$

Equations 3, 4, and 5 are concentration equations. Equation 3 represents the initial sample concentration, C_o, in which W_o is the initial amount of analyte and V_S is the volume of the sample.

Gas (vapor) Phase

(Headspace, V_G)

$$\frac{V_G}{V_S} = \text{Phase Ratio} = \beta$$
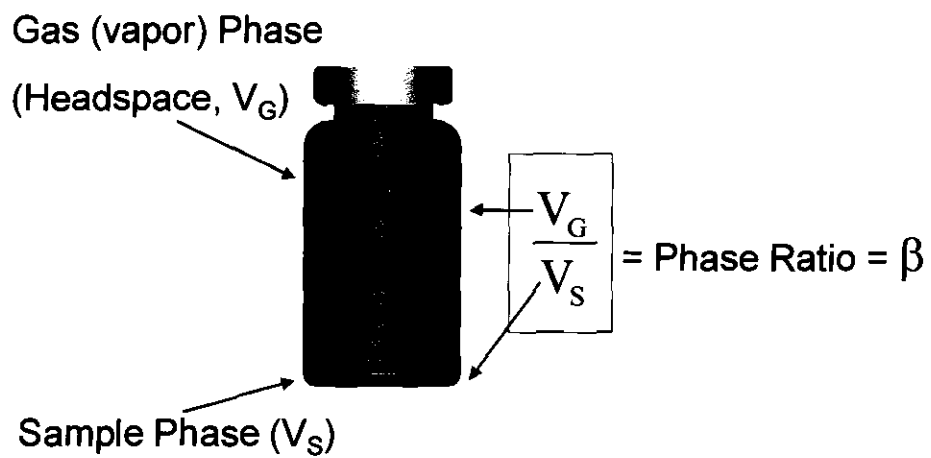
Sample Phase (V_S)

Figure 17 – Diagram of a sample vial and the phases as they relate to the phase ratio.

$$C_o = \frac{W_o}{V_s} \qquad (3)$$

Equation 4 represents the concentration of the sample phase (the analyte in the liquid phase), C_S, in the vial after the vial has been brought to equilibrium, W_S is the amount of non-vapor sample at equilibrium, and V_S is the volume of the non-vapor sample at equilibrium.

$$C_s = \frac{W_s}{V_s} \qquad (4)$$

It is assumed that the loss of volume to the headspace from the initial sample to the sample at equilibrium is negligible. Equation 5 represents the concentration of the headspace, C_G, in the vial after the vial has been brought to equilibrium, W_G is the amount of analyte in the headspace at equilibrium, and V_G is the volume of the headspace at equilibrium.

$$C_G = \frac{W_G}{V_G} \qquad (5)$$

Equation 6 is the mass balance Equation and shows that the initial amount of analyte is the sum of the amount of analyte in the sample phase and the amount of analyte in the headspace [38].

$$W_o = W_S + W_G \qquad (6)$$

When Equation 4 is divided by Equation 5, the result is a ratio of the concentration of the (liquid) sample phase to the concentration of the headspace. The variable K, the partition coefficient, is substituted as a constant for that ratio, shown in Equation 7 [53, 72, 166].

$$K = \frac{C_S}{C_G} \qquad (7)$$

The partition coefficient is also sometimes known as the distribution coefficient because it is a constant value reflecting how a sample is distributed into the liquid and vapor phase. According to Equation 8, the concentration of the headspace, C_G, is proportional to the initial concentration of the liquid sample, C_o [38].

$$C_G = \frac{C_o}{K + \beta} \qquad (8)$$

Since the resulting gas chromatographic peak area, A, is proportional to C_G, then A is also proportional to C_o, and is expressed by Equation 9.

$$A \propto C_G = \frac{C_o}{K + \beta} \qquad (9)$$

Equation 9 is a "headspace sensitivity" expression which shows that the obtained peak area is dependent on a combined effect of the quantity $(K + \beta)$ [38]. Therefore there are three variables that can affect the headspace sensitivity: temperature, volume, and sample matrix. Temperature variation while keeping volume (and phase ratio) and sample matrix constant can influence the partition coefficient of different compounds. For example, increasing the temperature of a sample of benzene in water can cause the partition coefficient to decrease, raising the sensitivity of the sample. If the temperature (and partition coefficient) and sample matrix remains constant but the volume is varied, the phase ratio will vary. For example, if the volume of a sample is increased, the phase ratio will decrease and the sensitivity will increase. If the temperature and volume (and phase ratio) are kept constant, but the sample matrix is varied, the activity coefficient, γ, and the partition coefficient, K, will vary [38].

2.2 Multiple Headspace Extraction (MHE)

In multiple headspace extraction (MHE), successive aliquots are taken from the

headspace of the same vial, and it is considered dynamic gas extraction carried out

stepwise. The objective to this method is to extract virtually the entire amount of analyte

from a sample matrix by removing the analytes in parts until there is no analyte left in the

original sample to extract [38]. Equation 10 shows mathematically how each individual

peak area found step-wise are added to get the sum of the all the peak areas, A_{1-i}.

$$\sum_{i=1}^{i \to \infty} A_i = A_1 + A_2 + ... + A_i \qquad (10)$$

Equation 11 shows that the sum of the peak areas is directly proportional to the total

amount of analyte present in the original sample, W_o.

$$W_o \propto \sum_{i=1}^{i \to \infty} A_i \qquad (11)$$

Examples of the individual peak areas taken from multiple extractions from the same

sample can be seen in Figures 13 and 14. Figure 13 on page 32 shows that peaks from

the same chemical from the same sample are resolved at the same retention time. Figure

14 on page 33 shows a different perspective of peak areas taken step-wise on a graph in

which the peak area counts are graphed with respect to the number of chronological

extraction. Both figures indicate that the peak areas resulting from multiple extractions

of the same vial eventually decrease as the number of extractions taken and analyzed

increases.

2.3 Solid Phase Micro-Extraction

Solid Phase Micro-Extraction (SPME) is a technique that can be applied to HS-GC, in a multiple step process [78-81]. In SPME there is a three-phase system and there are two equilibrium systems: equilibrium between the liquid sample and the headspace, and equilibrium between the headspace and the fiber. Since each phase has a concentration of the analyte from the original sample, the total amount of analyte can be shown mathematically in Equation 12, in which C stands for concentration, V stands for volume, the subscript o stands for initial, the subscript S stands for liquid sample, the subscript G stands for gas phase or headspace, and the subscript F stands for fiber.

$$C_o \cdot V_S = C_S \cdot V_S + C_G \cdot V_G + C_F \cdot V_F \qquad (12)$$

The partition coefficients of each phase are represented by Equations 13 and 14

$$K_{G/S} = \frac{C_G}{C_S} \qquad (13)$$

$$K_{F/G} = \frac{C_F}{C_G} \qquad (14)$$

in which $K_{G/S}$ stands for the partition coefficient between the headspace and the liquid sample phase and $K_{F/G}$ stands for the partition coefficient between the fiber and the headspace. Due to the fact that the amount of analyte, W_F, absorbed in the fiber can be determined by Equation 15,

$$W_F = C_F \cdot V_F \qquad (15)$$

Equation 16 can be derived using the relationships in Equations 6-9 to determine the amount of analyte absorbed by the fiber and ultimately the sensitivity of the GC response.

In order to complete a calculation using Equation 16, $K_{G/S}$ and $K_{F/G}$ must be known at the temperature the vial is heated at.

$$W_F = \frac{C_o \cdot V_S \cdot V_F \cdot K_{F/G} \cdot K_{G/S}}{K_{F/G} \cdot K_{G/S} \cdot V_F + K_{G/S} \cdot V_G + V_S} \qquad (16)\ [60]$$

2.4 Temperature Inside the Vial

2.4.1 Instrument Construction

The construction of the pressure-balanced headspace auto-sampler is relevant to the results of a method to determine the temperature inside a sample vial using a thermocouple. Figure 18 shows a photo of the outside of the heater of the pressure-balanced auto-sampler on the left and a diagram of the vial positions inside the heater shown on the digital interface screen of the same auto-sampler on the right. On the left, a circle is drawn to indicate the small opening on the top of the heater in which a thermocouple wire could be inserted. Although it may not appear obvious from the photo, this small hole is located below a piece of the metal structure that holds the syringe apparatus in place. The small hole is located above the "LOAD" position of the vial carousel in the heater, as can be seen in the vial carousel diagram on the right. When a vial is moved from the sample tray up and into the heater, it is placed into the LOAD position of the carousel. As a vial is prepared to be (heated and) brought to equilibrium and sampled, it is rotated counterclockwise into one of the positions to be heated. Once the vial is ready to be sampled, it is rotated into the "INJECT" position. A vial will not

Measuring Vial Temperature
Thermocouple Method

Insert
thermocouple
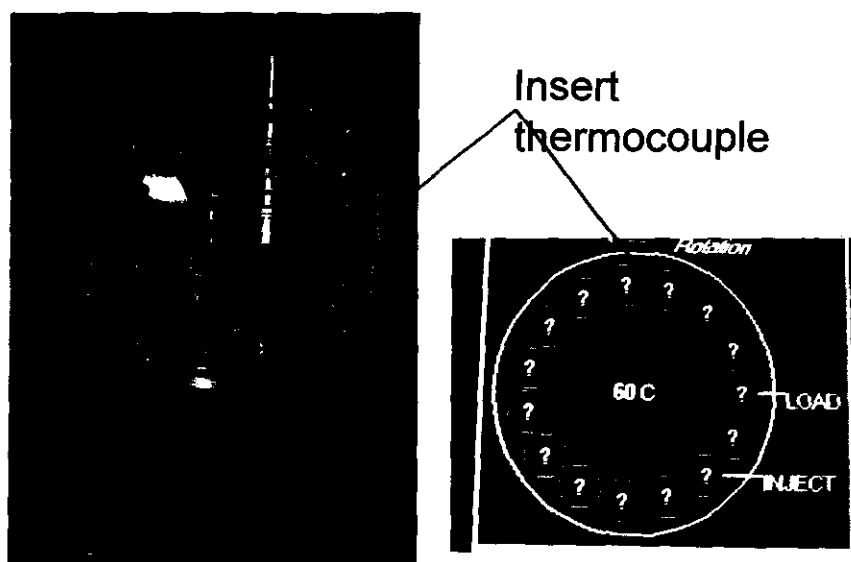
Figure 18 – A picture of the vial heater inside the pressure-balanced auto-sampler and the associated diagram of the vial positions inside the heater.

begin the heating and equilibrium process while it is in the LOAD position of the vial carousel.

The heater in the non-pressurized headspace auto-sampler is a compartment with six vial slots and a spring-loaded door on top that keeps it closed. A robotic arm moves the vials from the sample tray into the heater. When the vials have reached equilibrium, the robotic arm moves the syringe to the vial in the heater where it extracts the sample and injects it into the injection port of the gas chromatograph.

2.4.2 Chromatographic Method

In this work, the temperature inside the vial was to be determined using a chromatographic method in which actual data from a sample analysis under analytical conditions was used. It was hypothesized that the ratio of individual peak areas of the two respective components would change over a temperature range. This hypothesis was supported by the resulting chromatograms of a mixture of constant concentration of naphthalene and dodecane shown in Figure 19. It can be seen that at 44°C, the peak of dodecane on the left is higher than the peak of naphthalene on the right. Then, as the temperature increases to 72°C in 4 degree steps, the height of dodecane decreases relative to the height of the peak of naphthalene. This is an indicator that the relative peak areas of dodecane and naphthalene in the chromatograms in Figure 19 change with respect to temperature as well.

A calibration curve was to be constructed from a mathematical relationship between the ratio of resulting peak areas of two components and the temperature inside
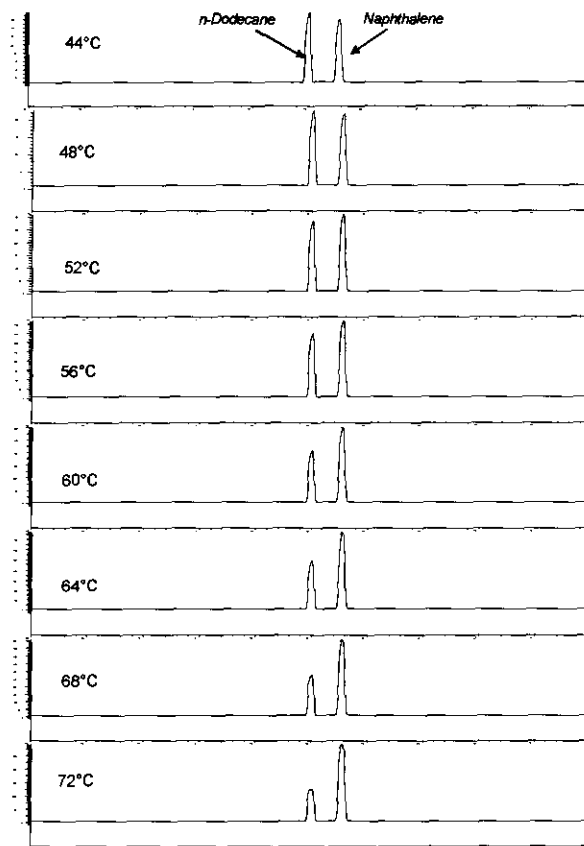
Figure 19 – Chromatograms of naphthalene and dodecane over the temperature range of 44°C to 72°C.

the vial. To relate these variables and measurements, Equation 17 was derived from a simplified form of the Clausius-Clapeyron Equation (full derivation explained in

$$\ln\left(\frac{A_{ref}}{A_i}\right) = \frac{(q_i - q_{ref})}{T} + (b_{ref} - b_i)\ln\left[(RF)\left(\frac{M_{ref}}{M_i}\right)\right] \qquad (17)$$

section 4.2.1). The data used were to be the resulting gas chromatographic peak areas of selected components in the vial and the temperatures in which they were heated (and brought to equilibrium) to. When a plot is produced from peak area data, the relative peak area ratio of two components is plotted vs. $1/T$.

2.5 (Gas-Liquid) Partition Coefficients

When an analyte is in the presence of (for instance, dissolved in) a solvent, it exists in both phases: partially in the liquid phase, and partially in the vapor phase. This phenomenon is known as partitioning. The partition coefficient (K) is the ratio of the concentration of the analyte in the sample phase (C_S) to the concentration of the analyte in the gas phase (C_G) at equilibrium, and is shown in Equation 7 and Figure 20:

$$K = \frac{C_S}{C_G} \qquad (7)$$

The gas-liquid partition coefficients vary from compound to compound, and are dependent on many different factors, especially temperature and activity coefficient. Two methods to determine the partition coefficient of an analyte in a binary-mixture system in a headspace vial at constant temperature using HS-GC are vapor phase calibration (VPC) and phase ratio variation (PRV).
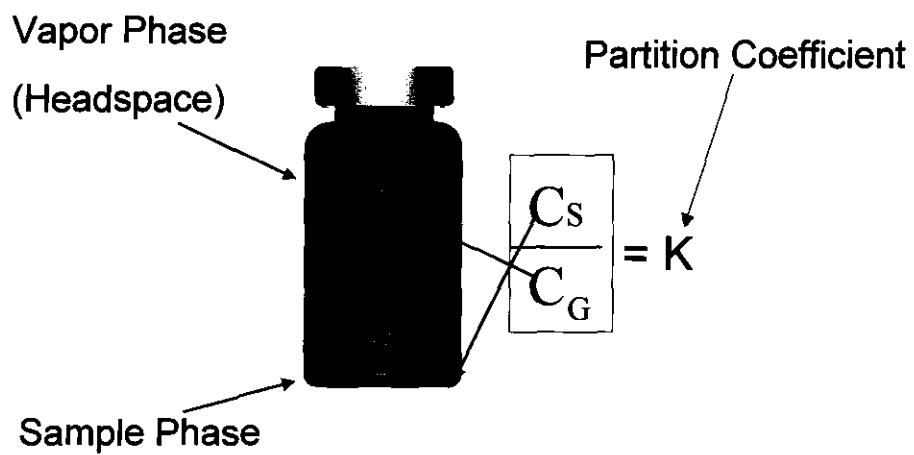
Figure 20 – Diagram of a sample vial and the phases as they relate to the partition coefficient.

2.5.1 Vapor Phase Calibration (VPC)

Vapor phase calibration was developed in 1992 by Kolb, et. al. [166]. In the VPC method, there are two sets of vials. In one set, (known as) the "calibration" set, a known volume of analyte that is expected to totally vaporize under the set conditions of the vial is added to the vials; this is known as the total vaporization technique (TVT) [38]. The TVT is used in order to create a vapor-phase only system, which allows the sample to be used as a calibration standard. The same volume of analyte as added to the first set is also added to the second set of vials, which contains a liquid phase as well. (The complete method for this is explained in the experimental section.) Since the volume of the vial (Vv), the volume of liquid solvent (sample) added (Vs), the volume of vapor (a.k.a. headspace, a.k.a. gas) phase ($V_G = Vv - Vs$), the resulting peak area of the calibration vials (A_C), and the peak area of the sample vials (A_G) are known, those respective values can be substituted into Equation 18 and K can be solved for [166].

$$K = \frac{A_C V_v - A_G V_G}{A_G V_s} \qquad (18)$$

Equation 27 is derived, beginning from the equation for the partition coefficient, Equation 7, which is shown in Equation 19 to equal the amount of analyte in the liquid sample phase, m_S, over the volume of the liquid sample phase, V_S, times the volume of the gas phase, V_G, over the amount of analyte in the gas phase, m_G. The fraction m_S/V_S equals C_S and the fraction V_G/m_G equals $1/C_G$.

$$K = \frac{C_S}{C_G} = \frac{m_S}{V_s} \frac{V_G}{m_G} \qquad (19)$$

Equation 20 shows that m_S is equal to the difference of the original amount of analyte, m^o, and m_G.

$$m_S = m^o - m_G \qquad (20)$$

In Equation 21, $C_G{}^C$ is the concentration of the gas phase in the vial for the "calibration" set of vials in VPC, and is shown to equal the fraction of the original amount of analyte over the volume of the vial. (It should be known that m^o must be small enough so it completely vaporizes at the temperature the vial is set to equilibrate at, such as about 4 μL at 75°C in a 20 mL vial, otherwise the conditions are not correct for use as "calibration" samples. This is discussed in more detail in the experimental section.) The concentration of the gas phase for calibration vials is also equal to the calibration factor, f_c, times the chromatographic peak response for calibration samples, A_c.

$$C_G{}^C = \frac{m^o}{V_v} = f_c A_c \qquad (21)$$

Equation 22 is a rearrangement of Equation 20 in which the original amount of analyte is solved for by multiplying both sides of Equation 21 by V_v.

$$m^o = f_c A_c V_v \qquad (22)$$

Equation 23 is then written in similar terms of Equation 21, except this is for the "sample" set of vials, showing the concentration of the gas phase of a sample equal to the product of the calibration factor and the peak response of the sample

$$C_G = \frac{m_G}{V_G} = f_c A_s \qquad (23)$$

Equation 24 is written in similar terms as Equation 22, except this is for the amount of analyte present in the gas phase for a sample and is equal to the product of the calibration factor, the peak response of the sample, and the volume of the gas phase.

$$m_G = f_c A_S V_G \qquad (24)$$

Equation 25 is Equation 20 written with $A_c V_v$ substituted for m^o, $A_S V_G$ substituted for m_G, and the calibration factor factored out.

$$m_S = f_c (A_c V_v - A_S V_G) \qquad (25)$$

Equation 19 is written with substitutions for m_S and m_G from Equations 25 and 24, respetively, as shown in Equation 26.

$$K = \frac{m_S}{V_S} \frac{V_G}{m_G} = \frac{f_c (A_c V_v \ A_S V_G) V_G}{f_c A_S V_G V_S} \qquad (26)$$

Finally, the common factors of f_c and V_G are eliminated to yield Equation 18.

$$K = \frac{A_c V_v - A_G V_G}{A_G V_S} \qquad (18)$$

2.5.2 Phase Ratio Variation (PRV)

Phase ratio variation was developed in 1993 by Ettre et. al. [176]. In the phase ratio variation (PRV) method, known, varied volumes of a solution of constant concentration are added to the vials. Since the volumes are varied, β, the phase ratio, is also varied, by default, according to Equation 1.

The phase ratio variation (PRV) method is based on a linear relationship between the phase ratio, β, of a vial and the reciprocal peak area of the respective sample solution. When different volume aliquots of a solution of constant concentration are added to a vial and analyzed, the resulting areas of the peak response of the volatile analyte will also be different. If the reciprocal of both sides of Equation 27 is taken,

$$A \propto C_G = \frac{C_o}{K + \beta} \qquad (27)$$

Equation 28 is the result, with the right side of the Equation written in expanded form.

$$\frac{1}{A} \propto \frac{1}{C_G} = \frac{K}{C_o} + \frac{1}{C_o}\beta \qquad (28)$$

The proportionality symbol between A and C_G is eliminated with the use of the proportionality constant, f, according to Equation 29.

$$C_G = \frac{A_G}{f} \qquad (29)$$

When A_G/f is substituted for C_G from Equation 28 and both sides of the Equation are divided by f, the f is moved to the right side and distributed into both denominators to yield Equation 30.

$$\frac{1}{A_G} = \frac{1}{f \cdot C_o}\beta + \frac{K}{f \cdot C_o} \qquad (30)$$

Equation 30 now corresponds to a linear equation in which $1/A_G$ is y, $1/(f \cdot C_o)$ is the slope, $K/(f \cdot C_o)$ is the y-intercept, A_G is the peak area of the headspace, f is the proportionality constant, and C_o is the concentration of the analyte in the original (liquid) sample. The reciprocals of the peak areas are plotted against the phase ratio, according to Equation 30 so that numerical values are produced for the y-intercept and the slope of the line. When the y-intercept value is divided by the value of the slope, K is determined mathematically, according to Equation 31 [176].

$$\frac{\left(\dfrac{K}{f \cdot C_o}\right)}{\left(\dfrac{1}{f \cdot C_o}\right)} = K \qquad (31)$$

69

2.6 Activity Coefficients

The activity coefficient is defined as the ratio of the activity of a component to the mole fraction of that component, as defined in the Equation 32:

$$\gamma_1 = \frac{a_1}{x_1} \qquad (32)$$

in which γ_1 is the activity coefficient of a component, a_1 is the activity of a component and x_1 is the mole fraction of that component. Activity can be considered a correction quantity to the chemical potential at a pressure and/or composition condition to a standard or reference state [177], and is mathematically defined as the ratio of fugacity of a substance in a solution to its fugacity in some arbitrarily chosen standard state (such as a pure liquid), as shown in the Equation 33:

$$a_1 = \frac{f_1}{f_1^o} \qquad (33)$$

Fugacity is defined as the "escaping tendency" of a solute from a solvent.

Activity coefficient can also be considered a "correction factor" to concentration, which modifies it to the "active concentration." This can be expressed in relation to Raoult's law. According to Raoult's law, the vapor pressure (or partial pressure, p_i) of a dissolved solute over its solution is directly proportional to its mole fraction in the solution ($x_{S(i)}$), and is assumed valid for an ideal solution. This is expressed mathematically in the Equation 34:

$$p_i = p_i^o \cdot x_{S(i)} \qquad (34)$$

70

in which p_i^o is the vapor pressure of the pure analyte (for example, when $x_{S(i)}=1$) and acts as the proportionality constant. When a solution is non-ideal (or real), however, this deviation from the ideal nature of Raoult's law is accounted for in Equation 35:

$$p_i = \gamma_i \cdot p_i^o \cdot x_{S(i)} \qquad (35)$$

Dalton's law states that the total pressure of a gas mixture is equal to the sum of the partial pressures of the gases in the mixture. According to Dalton's law, the fraction of the pressure exerted by a gas is equal to the fraction of its total number of moles present in the gas mixture. This is expressed mathematically in Equation 36

$$\frac{p_i}{p_{total}} = \frac{n_i}{n_{total}} = x_{G(i)} \qquad (36)$$

in which n is the number of moles present, $x_{G(i)}$ is the mole fraction of the particular component in the gas mixture, and can be rearranged in terms of p_i in Equation 37.

$$p_i = p_{total} \cdot x_{G(i)} \qquad (37)$$

When p_i is solved for in the equation from Dalton's law and Raoult's law, they show to be mathematically related, as in Equation 38:

$$p_i = p_{total} \cdot x_{G(i)} = \gamma_i \cdot p_i^o \cdot x_{S(i)} \qquad (38)$$

And since Equation 38 can be rearranged to Equation 39,

$$\frac{x_{S(i)}}{x_{G(i)}} = \frac{p_{total}}{\gamma_i p_i^o} \qquad (39)$$

then Equation 39 is equal to Equation 7, shown in Equation 40,

$$\frac{x_{S(i)}}{x_{G(i)}} = \frac{p_{total}}{\gamma_i p_i^o} = \frac{C_{S(i)}}{C_{G(i)}} = K \qquad (40)$$

proving that the partition coefficient is inversely proportional to the vapor pressure and activity coefficient of the analyte. These relationships are relevant in that a large activity coefficient or vapor pressure will result in a decreased partition coefficient, in the overall scheme of liquid-vapor equilibria.

Likewise, the peak area of an analyte is directly proportional to the headspace concentration (according to Equation 9) and the partial vapor pressure of that analyte, as follows in Equation 41:

$$A_i = c_i p_i \qquad (41)$$

in which A_i is the peak area of component i and c_i is the calibration factor component i. It also follows that the peak area of the pure component i, A_i^o, is proportional to its vapor pressure p_i^o (at the same temperature) as shown in Equation 42.

$$A_i^o = c_i p_i^o \qquad (42)$$

Quantitative interpretation of headspace analysis depends on the equilibrium expression, Equation 43, which is derived from Equations 41 and 42.

$$\gamma_i = \frac{A_i}{c_i p_i^o x_i} \qquad (43)$$

To calculate activity coefficients, first, an internal standard must be used, in order to establish A_i^o. To do this, the total vaporization technique (TVT) is implemented. Once this has been done, and since Equation 42 can be substituted into Equation 43, the values can be substituted into Equation 44 to solve for γ.

$$\gamma_i = \frac{A_i}{A_i^o x_i} \qquad (44)$$

The activity coefficient depends on more than the nature of the components involved. It also depends on the mole fractions of all components, the temperature, and pressure has a slight affect as well [100]. The Gibbs-Duhem Equation, Equations 45, 47, and 48 describe the mathematical relationship of the variation of activity coefficients with concentration in a mixture with a defined temperature and/or pressure [99]. Equation 45 is for an isobaric, nonisothermal case, showing that the activity coefficients of a multicomponent system are related through a differential equation which takes into account the change in molar enthalpy of mixing, h^E.

$$\sum_i x_i d(\ln(\gamma_i)) = -\frac{h^E}{RT^2} dT \qquad (45) [99]$$

The molar enthalpy of mixing change results upon the mixing of pure liquids isothermally and isobarically to form a solution and is described by Equation 46,

$$h^E = h - \sum_i x_i h_i^0 \qquad (46) [99]$$

in which h is the molar enthalpy of the mixture and h_i^0 is the standard state molar enthalpy of the mixture of component i. Equation 47 is for an isothermal, nonisobaric case in which v is the molar volume of the mixture and the standard state for component is the system temperature at a fixed composition and a constant pressure that does not change with the composition.

$$\sum_i x_i d(\ln(\gamma_i)) = \frac{v}{RT} dP \qquad (47) [99]$$

Equation 48 is similar to Equation 47, but differs in how the pressure relates to the composition. The standard state here for component i is at the system temperature at a

fixed composition and at the total pressure P of a system, which varies with composition

and is not constant. The variable v^E is the change in volume resulting from the mixing of

$$\sum_i x_i d(\ln(\gamma_i)) = \frac{v^E}{RT} dP \qquad (48)\ [99]$$

pure liquids at the temperature and pressure of the mixture, and can be defined by

Equation 49, in which is the standart state molar volume of component i.

$$v^E = v - \sum_i x_i v_i^0 \qquad (49)\ [114]$$

The infinite dilution activity coefficients can be shown by a mathematic

relationship in Equation 50,

$$\gamma_A^\infty = \gamma_M^\infty + \varepsilon \qquad (50)\ [101]$$

in which $0 \le x_i < x_i + n$ when the equality in Equation 51 occurs,

$$n = \frac{\varepsilon}{\left(\dfrac{\partial \gamma_i}{\partial x_i}\right)_{x_i = 0}} \qquad (51)\ [101]$$

(In Equation 50, the subscript A stands for actual, the subscript M stands for measured, ε

stands for error, and n is an arbitrary number.) This relationship can be used along with a

model of activity coefficients or a direct extrapolation from the finite dilution

measurement to an extreme value of $(\partial \gamma_i / \partial x_i)_{x_i = 0}$, which would define the infinite

dilution region as inversely proportional to $(\partial \gamma_i / \partial x_i)_{x_i = 0}$ [101]; this represents a

macroscopic perspective. The molecular perspective defines the infinite dilution region

for a binary system as no molecule (i) being around a given molecule of the same type (i),

thus no interactions occur with molecules of the same type and the only interactions with

molecules (i) occur with different molecules [101, 99].

2.7 Relationship of Partition Coefficient with Activity Coefficient

According to Equation 40, the partition coefficient is inversely proportional to the

vapor pressure and the activity coefficient and is expressed in Equation 52.

$$K \propto \frac{1}{(p_i^{\,\circ})(\gamma_i)} \qquad (52)$$

This relationship is important because of the relationship between the activity coefficient,

the gas chromatographic peak response, and the partition coefficient. For example, if the

value of the product of the vapor pressure and activity coefficient increases, the partition

coefficient decreases, according to Equation 51. Then, since the partition coefficient is a

concentration based quantity, the concentration of the headspace would increase

according to Equation 7.

$$K = \frac{C_S}{C_G} \qquad (7)$$

Experimentally, this would mean that the analyte favors the liquid phase of a sample.

Furthermore, according to Equation 9, if the partition coefficient increased and the

$$A \propto C_G = \frac{C_o}{K + \beta} \qquad (9)$$

sensitivity of the headspace increases, the gas chromatographic peak response would

decrease proportionally, because it is inversely proportional to headspace sensitivity.

This can be summarized in that a high activity coefficient in a liquid sample decreases

headspace sensitivity by making the analyte favor the liquid phase, and this would be

reflected in a lower gas chromatographic peak response.

3. EXPERIMENTAL

3.1 Static Headspace-Gas Chromatographs

In all headspace analysis related studies, two static headspace-gas chromatographs and attached auto-samplers were used. Extractions and separations on the pressure-balanced system were performed on a headspace-gas chromatograph (Turbomatrix HS-110/ Clarus 500 GC, PerkinElmer, Shelton, CT). Extractions and separations on the non-pressurized system were respectively performed on a headspace auto-sampler system (CombiPAL, LEAP Technologies, Carrboro, NC) attached to a gas chromatograph (GC-5890 series II, Hewlett-Packard, Avondale, PA). Both GC instruments were equipped with flame ionization detectors (FID).

3.2 Temperature Inside the Vial

The origin of this study was to determine the temperature inside a closed and equilibrated headspace sample vial, in order to verify the "actual temperature" displayed on the interface screen of the Perkin-Elmer Turbomatrix 100. The reason for verifying this parameter is due to the fact the temperature sensor set up to detect and report the temperature inside the instrument is placed on the vial heating container and no sensor is inside the vial. Several methods were used to answer the question of "What is the temperature inside the vial?" ranging from traditional/physical measurements to a more theoretical and analytical chromatographic method.

3.2.1 Temperature Inside the Vial - Traditional Methods

3.2.1.1 Thermocouple Method

The intention of this method was to directly insert a thermocouple into a heated

vial in the heater of the pressure-balanced headspace auto-sampler in order to determine

the temperature inside the vial. First, a vial was half-filled with nuts and bolts, small

items of high thermal mass and conductivity, capped without a septum, and inserted into

the headspace auto-sampler. The instrument was programmed to heat the vial to a

designated temperature, such as 60°C, and once the vial heated, a thermocouple was to be

inserted into the vial heater and into the heated vial so a temperature reading could be

taken of the contents of the vial. The intention was for the thermocouple to be inserted

into the auto-sampler heater via the small hole as indicated in the left picture of the

diagram in Figure 17.

The tops of the vials in the heater of the non-pressurized headspace auto-sampler

are accessible by opening the spring-loaded roof of the heater. The vials containing nuts

and bolts were set to heat (and equilibrate) to various temperatures such as 60°C or 70°C.

Unlike the heater and diagnostic settings of the pressure-balanced headspace auto-

sampler, the heater of the non-pressurized headspace auto-sampler could be set to any

temperature (up to 200°C) while the auto-sampler is at rest. Due to this fact and the easy

access of the vials in the heater, a thermocouple was inserted in through the septum of a

sample vial and the temperature of the contents of the sample vial was taken. When a

sample vial was inserted to be heated, a timer was set so the temperature of the vial could be taken at any desired time, such as 20, 30, or 60 minutes.

3.2.1.2 Melting Point Method

A melting point study was performed next using both the pressure-balanced and non-pressurized systems. The melting point of naphthalene was first measured using a MEL-TEMP melting point apparatus. A few pure naphthalene crystals were added into the bottom of a capillary test tube. The capillary test tube was put into the heating cell of the melting point apparatus and a thermocouple (wire) was placed inside the apparatus in a cell adjacent to the capillary test tube in order to make an accurate temperature measurement. The melting point of pure naphthalene was measured to be 80.5°C. Naphthalene crystals are white and flaky. Upon melting, the naphthalene is a clear liquid. Upon recrystallizing, the naphthalene has a smooth, non-flaky, white appearance.

The melting point of pure naphthalene was then applied to the static headspace auto-sampler heaters. To each vial, 1 gram of pure naphthalene crystals was added. The vials were set to run at temperatures ranging from 75°C to 85°C for 65 minutes as a normal headspace analysis, and a separate timer was set for 60 minutes. After 60 minutes of heating, the run was stopped and the vial was taken out of the instrument for immediate visual analysis to determine if the crystals melted or did not melt. If the crystals did not melt, they remain white and flaky in appearance. If the crystals did melt, the naphthalene appears to be a clear liquid or a smooth, white solid if the naphthalene recrystallized.

3.2.2 Temperature Inside the Vial - Chromatographic Method

For all analyses on the headspace-gas chromatographs, all samples were heated and set to equilibrate for 60 minutes with vial shaker on. The temperature of the sampling syringes was 90°C. Run time was 4.0 minutes for all samples. The split injector temperature was 150°C, split 50:1, with a zero dead volume (ZDL) liner, and the flame ionization detector temperature was set to 300°C with the range of 20 and attenuation of 6. The column was a 30m x .32mm x 1.0μm PE-5 and the oven temperature was 200°C, isothermal. The carrier gas for all samples was helium at a pressure of 12.5 psig with a flow rate of 5 mL/min. Air flow for the FID was at 84 psig. All chemicals used were HPLC grade. For each piece of data, a set of three vials were made and the average of the results from each set of 3 samples was used.

On the pressure-balanced headspace auto-sampler, the vials were pressurized for 2 minutes. Withdrawal time of 0.1 min. and an inject time of 0.01 min. was used. The temperature of the untreated "empty fused silica" transfer line was 100°C and the head-pressure was set to 20 psig with PPC (Programmable Pneumatic Control). On the non-pressurized headspace auto-sampler, the fill speed was 500 μL/min., and the pull-time was 10 sec.

For the chromatographic method of determining the temperature inside an equilibrated headspace sample vial, a 2-component sample was used so the resulting chromatographic data (the peak areas) of a headspace analysis could be applied to and substituted into Equation 26. In order to perform this headspace analysis, 2 suitable chemicals were to be chosen, combined at a suitable constant concentration, and added to

the vial in the most practical and reproducible form of sample preparation. A suitable sample volume which would yield the best reproducibility was also sought.

The chemicals originally selected were naphthalene and dodecane because naphthalene dissolves in dodecane. The following are the various concentrations tested for most reproducible peak areas:

- dodecane saturated with naphthalene

- a concentrated mixture containing 1 g of naphthalene/L of dodecane

- a dilute mixture containing less than 0.5 g of naphthalene/L of dodecane

- a recrystallized sample of dodecane saturated with naphthalene

- a recrystallized sample of dodecane saturated with naphthalene with the addition of 0.1 mL of water

- a saturated sample of naphthalene in dodecane recrystallized onto the walls of a sample vial with the intention of increasing the surface area of the recrystallized mixture.

For each sample mixture, three vials were prepared for each temperature to which the vials would be heated and equilibrated. The vials were equilibrated at temperatures of 44°C to 72°C in 4 degree increments, each for 60 minutes. The two components were completely resolved on the gas chromatogram and the resulting peak areas were transferred to an Excel spreadsheet. The standard deviation was taken for each set of three vials to monitor reproducibility among the samples. The peak area data was then plotted on the y-axis against the temperature on the x-axis, producing linear plots as well as best squares fit regression curves. The correlation coefficient for each plot was monitored and the goal was for data to achieve a correlation coefficient of 1.

3.3 Internal Standard Quantification

Internal standards of individual compounds were analyzed in order to create a calibration curve to monitor the headspace concentration (as peak area) is produced with respect to the volume of the compound in a headspace vial and with respect to the temperature of the vial and the headspace auto-sampler. Additionally from this calibration curve, the volume and temperature at which the headspace of the vial is saturated was to be determined.

Aliquots of benzene, toluene, or methyl ethyl ketone were separately transferred into the 20.0 mL (for the non-pressurized auto-sampler) or 22.0 mL (for the pressure-balanced auto-sampler) headspace vials by means of a micro-syringe, micro-pipette, or macro-pipette, depending on the volumes. Vials of the various samples for analysis were prepared to on the pressure-balanced headspace system and the non-pressurized headspace system. The headspace vials were heated at temperatures ranging from 55°C to 75°C for 60 minutes, to ensure equilibration has been established. The vials were sampled and analyzed on the attached gas chromatograph. From the resulting peak area results, graphs were constructed to display the data in which the peak area was plotted on the y-axis against volume of aliquot on the x-axis. Internal standards for toluene, benzene, and MEK were analyzed as a prelude to the partition coefficient and activity coefficient studies, as portions of these studies overlap with this information. Although the partition coefficient of cyclohexane was studied, the internal standard for cyclohexane was not.

3.4 Partition Coefficients

3.4.1 Vapor Phase Calibration (VPC)

The vapor phase calibration (VPC) method is implemented by preparing two sets of vials: "calibration" vials and corresponding "sample" vials [166]. Calibration vials contain only a small, known amount of analyte, which is expected to completely vaporize (and leave no liquid phase). The corresponding set of sample vials contained the same amount of analyte as in the respective calibration vials plus an additional 3.0 mL of water.

For example, the group of calibration vials contained 2.0 μL of MEK in the first group, 3.0 μL in the second group, 4.0 μL in the third group, and 5.0 μL in the fourth group; the corresponding sample vial groups contain 2.0 μL of MEK plus 3.0 mL of water, 3.0 μL of MEK plus 3.0 mL of water, 4.0 μL of MEK plus 3.0 mL of water, and 5.0 μL of MEK plus 3.0 mL of water, respectively. This is shown in Table 1. A group consists of three identically prepared vials for method accuracy. The reason the "sample" vials contained water was to allow the analyte to partition between the water (liquid phase) and the headspace (vapor phase).

Analytes were added to the vials with a micro-syringe and the water was added with a macro-pipette. The syringe and pipette measure to the 0.1 μL or mL, respectively. The technique of using the "calibration" vials in reference to the phase ratio calibration is the total vaporization technique (TVT) [38]. The TVT is used in order to create a vapor-phase only system, which allows the sample to be used as a calibration standard. Since

"Calibration" vial	vol MEK (mL)	vol. water (mL)
1	2.0	0.0
2	3.0	0.0
3	4.0	0.0
4	5.0	0.0
"Sample" vial	vol MEK (mL)	vol. water (mL)
1	2.0	3.0
2	3.0	3.0
3	4.0	3.0
4	5.0	3.0

Table 1 – Example volumes of analyte and water used with the PRV method for determining the partition coefficient of MEK in water.

the volume of the vial (Vv), the volume of liquid sample (Vs), the volume of vapor

(headspace) phase (V$_G$), the resulting peak area of the calibration vials (A$_C$), and the peak

area of the sample vials (A$_G$) were known, those respective numerical values were

substituted into Equation 26 to solve for K:

$$K = \frac{A_C V_V - A_G V_G}{A_G V_S} \qquad (26)$$

3.4.2 Phase Ratio Variation (PRV)

The phase ratio variation (PRV) method is based on a linear relationship between

the phase ratio (β) of a sample in a vial and the reciprocal peak area of the respective

sample solution [176]. In preparation, 3 sets of samples were prepared, all having the

same concentration of 1 μL of analyte per 1 mL of water. The contents of each vial were

prepared separately, as opposed to making a master solution and distributing an aliquot

into each vial, because of the inability of the amount of the non-polar analyte to mix (and

dissolve with) with the polar solvent, water.

The first set of vials contained 1 μL of analyte and 1 mL of water, having a phase

ratio of 21 mL/1 mL (or 21) for the pressure-balanced system and 19 mL/1 mL (or 19)

for the non-pressurized system. The second set of vials contained 2 μL of analyte and 2

mL of water, having a phase ratio of 20 mL/2 mL (or 10) for the pressure-balanced

system and 18 mL/2 mL (or 9) for the non-pressurized system. The third set of vials

contained 3 μL of analyte and 3 mL of water, having a phase ratio of 19 mL/3 mL (or

Vial	vol MEK (mL)	vol. water (mL)	β^*
1	1.0	1.0	11
2	2.0	2.0	5.5
3	3.0	3.0	3.7

Table 2 – Examples of volumes of analyte and water in a vial used with the PRV method to determine the partition coefficient of MEK in water. * The volume of the vial in this example is 22 mL (used in the pressure-balanced system).

6.3) for the pressure-balanced system and 17 mL/3 mL (or 5.7) for the non-pressurized system. This is shown in Table 2. To calculate the K value, the reciprocal peak area is plotted vs. the respective phase ratio and a line with an equation is produced. When the y-intercept value is divided by the value of the slope, according to Equations 28 and 29, K is determined.

3.5 Activity Coefficient and Total Vaporization Technique (TVT)

In the total vaporization technique, a small enough volume is added to the vial so that the entire sample is in the vapor phase at equilibrium, thus eliminating the condensed phase and a multiple-phase system. In preparing to use this technique, an experiment was conducted in order to define what volume completely evaporated at certain temperatures. Once this was discovered, the volumes equal to and below that could be considered acceptable to be used as an internal standard volume.

According to Hachenberg and Schmidt [100], the mixture of benzene and toluene has an activity coefficient of 1 and is considered an ideal solution. For this reason, benzene and toluene were chosen to be used throughout this experiment, sometimes separately and sometimes as a mixture (with defined concentration). The goal was to calculate, replicate, and verify the activity coefficient of the mixture of benzene and toluene.

The respective sample volumes, temperatures, headspace extraction systems, and volume to volume ratios of the following experimental procedures are summarized in Table 3, where applicable. First, separate, pure volumes of benzene, and toluene were

HS system	T (°C)	Volume of pure analyte (± .1 µL)
PB	55	1, 2, 3, 5, 7, 10, 20, 50, 100, 200, 500, 1000, 2000
PB	65	1, 2, 3, 5, 7, 10, 20, 50, 100, 200, 500, 1000, 2000
PB	75	1, 2, 3, 5, 7, 10, 20, 50, 100, 200, 500, 1000, 2000
NP	75	1, 2, 3, 5, 7, 10, 20, 50, 100, 200, 500, 1000, 2000
		Vol/Vol (mL/mL) ratio of benzene:toluene
PB	75	.1:10, 1:15, 1:2, 1:1, 15:1, 10:1
NP	75	.1:10, 1:15, 1:2, 1:1, 15:1, 10:2
		Volumes (mL) of each benzene:toluene solution
PB	75	.02, .05, .1
NP	75	.02, .05, .2

Table 3 – The volumes and volume ratios of the analytes used in the method to determine the activity coefficient of benzene with toluene. The pure analytes were benzene and toluene, analyzed separately, shown in the top of the table. PB is pressure-balanced and NP is non-pressurized.

added to vials in a range of 1 μL to 2 mL, and the resulting peak area counts were plotted vs. volume added to the vial. Toluene and benzene were analyzed at 55°C, 65 °C, and 75°C in the pressure-balanced system and at 75 °C on the non-pressurized system. In a new headspace vial, a volume was injected with a micro-syringe or appropriately sized pipette and the vial was capped. The individual chemicals used were benzene and toluene. The volumes injected into the individual vials are shown in Table 3. All vials were thermostatted for 60 minutes. In the pressure-balanced system, the vials were thermostatted at 3 different temperatures in the pressurized system: 55°C, 65 °C, and 75 °C. In the non-pressurized system, samples were thermostatted at 75 °C only.

The next experiment involved mixtures of benzene and toluene over a range of varied concentrations. The volume/volume ratios made of benzene/toluene and the volumes of those mixtures added to sample vials are shown in Table 3. Each vial was thermostatted at 75°C for 60 minutes. The values of the resulting peak areas from the pure components, the mixtures, and the respective mole fraction of the mixtures were then substituted into Equation 43 to obtain the experimental value of the activity coefficient of benzene in toluene.

4. RESULTS AND DISCUSSION

4.1 Temperature Inside the Vial

4.1.1 Traditional Methods - Thermocouple Method

The intention of this method was to directly insert a thermocouple into a heated sample vial in the heater of the pressure-balanced headspace auto-sampler. This method was unsuccessful on the pressure-balanced system because the vial was not accessible during an analysis in progress under analytical conditions. To be more specific, the construction of the pressure-balanced instrument, as described in the theory section and supplemented by Figure 18, restricted the use and movement of the thermocouple in the auto-sampler. According to the diagram in Figure 18, the temperature of a vial cannot be taken with a thermocouple because a vial does not begin the heating process in the slot of the carousel which would be accessible from the small hole located above it.

Since vial access became a restriction to the method, an attempt to measure the temperature of the surface of the empty heater was made by placing a thermocouple wire directly into the heater until it touched a surface. Although a temperature reading of 33°C was taken during the inactivity of the instrument, the temperature could not be raised to the higher temperatures that a sample would be heated to, and thus this version of the method was unsuccessful. The unsuccessful outcome of the thermocouple method can be summarized by the fact that it did not simulate an actual analysis under analytical conditions.

The heater for the non-pressurized system is different than the pressure-balanced system in that the non-pressurized system heater has a spring-loaded door on top that keeps it closed. When a thermocouple was inserted into a vial in that instrument, the temperature readings agreed with the set and actual temperature reading on the computer interface. For instance, when the temperature was set to 65°C, and the actual temperature was reported as 65°C, the temperature inside the vial was 65°C. Despite this result, a thermocouple was not present in a vial during sample extraction, and thus did not simulate the conditions of an analytical run-in-progress because the contents in the vial are susceptible to slight thermodynamic changes during sample extraction.

4.1.2 Traditional Methods - Melting Point Method

Table 4 shows the temperature each instrument was set to and whether the naphthalene crystals melted or not. The melting point of pure naphthalene is 80.26°C. On the pressure-balanced system, the naphthalene crystals did not melt at a temperature of 84°C or less and did melt at a temperature of 85°C and higher. On the non-pressurized system, the naphthalene crystals did not melt at a temperature of 80°C or lower and did melt at a temperature of 81°C and higher.

Although there were results from this method, the results are considered inconclusive because the sample data were not produced under actual analytical conditions because the analysis was stopped before sample extraction and analysis. This is relevant because the thermodynamic conditions inside the vial are subject to change upon the vial preparation for extraction and analysis.

That being understood, there are still a few reasons the initial results between the pressure-balanced system and the non-pressurized system were different by about 4°C. First, since a thermocouple could not be present inside a vial during heating in the pressure-balanced system, the only reliable thermometer is that belonging to the instrument. Since the temperature sensor is not located inside the sample vial, there could be a few degrees of difference between the location of the sensor and the temperature inside the vial. Second, the temperature inside the vial may slightly change during the pressurization/sample extraction period. Third, there is a chance that the temperature was not properly calibrated. As stated before, the results from the pressure-balanced system is considered inconclusive because it could not be performed completely under actual analytical conditions. Temperature results of the non-pressurized system are assumed to be reliable, though, since a thermocouple could be inserted into a vial during heating. Since results from the pressure-balanced system are inconclusive, it cannot be compared to the results from the non-pressurized system.

Temperature (°C)	Pressure-balanced	Non-pressurized
78	Did Not Melt	Did Not Melt
79	Did Not Melt	Did Not Melt
80	Did Not Melt	Did Not Melt
81	Did Not Melt	Melted
82	Did Not Melt	Melted
83	Did Not Melt	Melted
84	Did Not Melt	Melted
85	Melted	Melted
86	Melted	Melted
87	Melted	Melted

Table 4 – Melting of naphthalene crystals in the pressure-balanced headspace auto-sampler and non-pressurized headspace auto-sampler.

4.1.3 Chromatographic Method

4.1.3.1 Derivation of Equation

In this work, the temperature inside the vial was to be determined using a chromatographic method in which actual data from a sample analysis under analytical conditions was used. The data used were the resulting peak areas of selected components in the vial and the temperatures in which they were heated (and brought to equilibrium) to. A calibration curve was constructed from a mathematical relationship between the ratio of resulting peak areas of two components and the temperature of the vial. To relate these variables and measurements, Equation 17 was derived from a simplified form of the Clausius-Clapeyron Equation, Equation 53,

$$\ln(p) = \frac{q}{T} + b \qquad (53)\ [177]$$

and Equation 54, which relates the peak area of a reference compound to the respective partial pressure. The molecular mass is designated by M and RF is the response factor.

$$p_i = p_{ref}(RF)\left(\frac{A_i}{A_{ref}}\right)\left(\frac{M_{ref}}{M_i}\right) \qquad (54)\ [38]$$

First, the antilog of both sides of Equation 1 was taken as in Equation 55,

$$e^{\ln(p)} = e^{\left(\frac{q}{T}+b\right)} \qquad (55)$$

yielding Equation 56; the variable b is a constant.

$$p = e^{\frac{q}{T}} \cdot e^{b} \qquad (56)$$

The variable q stands for heat and is represented by Equation 57, in which H is enthalpy and R is the gas constant.

$$q = \frac{-\Delta H}{R} \qquad (57)$$

Equation 54 is rearranged when both sides of it are multiplied by $\dfrac{A_{ref}}{A_i \cdot p_i}$, to result in Equation 58.

$$\left(\frac{A_{ref}}{A_i} \right) = \left(\frac{p_{ref}}{p_i} \right) RF \left(\frac{M_{ref}}{M_i} \right) \qquad (58)$$

Next $e^{\frac{q_{ref}}{T}} \cdot e^{b_{ref}}$ and $e^{\frac{q_i}{T}} \cdot e^{b_i}$ from Equation 56 were substituted in for p_{ref} and p_i respectively in Equation 58 to yield Equation 59.

$$\left(\frac{A_{ref}}{A_i} \right) = \left(\frac{e^{b_{ref}} \cdot e^{\frac{q_{ref}}{T}}}{e^{b_i} \cdot e^{\frac{q_i}{T}}} \right) RF \left(\frac{M_{ref}}{M_i} \right) \qquad (59)$$

The natural log was taken of both sides of Equation 59 to yield Equation 60.

$$\ln \left(\frac{A_{ref}}{A_i} \right) = \ln \left[\left(\frac{e^{b_{ref}} \cdot e^{\frac{q_{ref}}{T}}}{e^{b_i} \cdot e^{\frac{q_i}{T}}} \right) RF \left(\frac{M_{ref}}{M_i} \right) \right] \qquad (60)$$

The right side of Equation 60 is rearranged as the natural log is re-written in an expanded form, yielding Equation 61.

$$\ln \left(\frac{A_{ref}}{A_i} \right) = \ln(e^{b_{ref} - b_i}) + \ln \left(e^{\frac{q_{ref} - q_i}{T}} \right) + \ln \left(RF \left(\frac{M_{ref}}{M_i} \right) \right) \qquad (61)$$

When the natural logs are multiplied by the exponentiation of both sides, the equation is reduced to its final form which is Equation 17. Equation 17 shows that the natural log of

the ratio of the peak area of an analyte i to a reference analyte is inversely proportional to the temperature, which is variable.

$$\ln\left(\frac{A_{ref}}{A_i}\right) = \frac{(q_i - q_{ref})}{T} + (b_{ref} - b_i)\ln\left[(RF)\left(\frac{M_{ref}}{M_i}\right)\right] \qquad (17)$$

When the natural log of (A_{ref}/A_i) is plotted vs. $1/T$, a linear curve is produced, which can be used with the equation of the line to determine the temperature present in the vial.

It was hypothesized that the ratio of individual peak areas of the two respective components would change over a temperature range. This hypothesis was supported by the following chromatograms of a mixture of constant concentration of naphthalene and dodecane shown in Figure 19. It can be seen that at 44°C, the peak of dodecane on the left is higher than the peak of naphthalene on the right. Then, as the temperature increases to 72°C in 4 degree steps, the height of dodecane decreases relative to the height of the peak of naphthalene. This is an indicator that the relative peak areas of dodecane and naphthalene in the chromatograms in Figure 19 change with respect to temperature as well. This is relevant to Equation 17 because when a plot is produced from peak area data, the relative peak area ratio of two components is plotted vs. $1/T$.

4.1.3.2 Results of Chromatographic Method

Most of the mixtures used were made of various concentrations of naphthalene and dodecane and the plots from the data of the samples which produced the best data are shown and discussed. The data used for the plots in Figures 21 and 22 came from a sample of 1.50 g of naphthalene saturated in 1.00 mL of dodecane. The first of these plots is Figure 21 from data and the corresponding sample analyzed on the pressure-
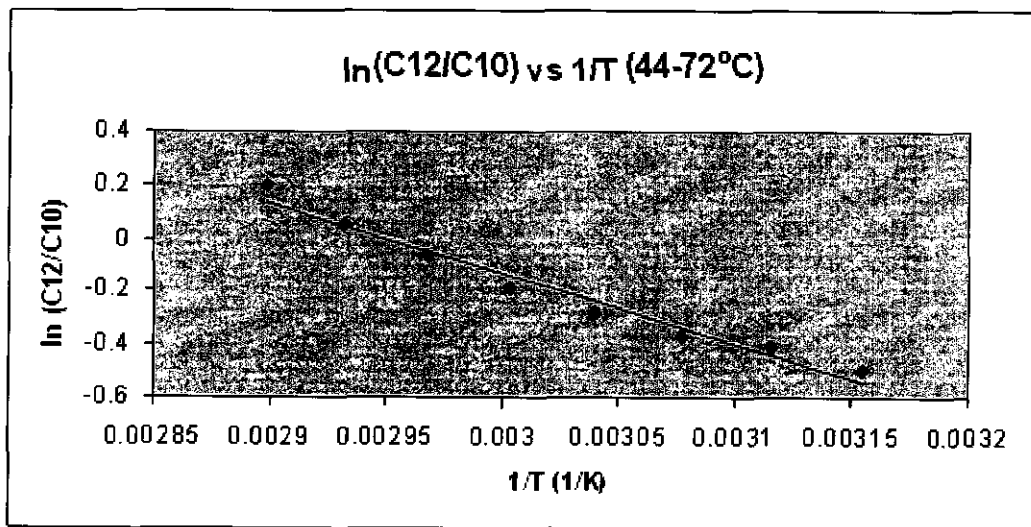
Figure 21 – A plot of ln of the average peak area ratios of dodecane to naphthalene vs. 1/T.

balanced system. It can be seen that the ln of the ratio of dodecane to naphthalene decreases as the inverse of the temperature decreases (or as temperature increases). A linear plot was expected, however, the points show to have a slight curve. This is expected to be due to a systematic error. A trendline was added anyway to check the correlation coefficient. Although the correlation coefficient is 0.97 and the points appear to be slightly curved, the data points have the potential to be more linear. (In the plot titles for Figures 21-23, C12 is used as an abbreviation for dodecane and C10 is used as an abbreviation for naphthalene.)

Figure 22 is a plot of a sample of the same concentration as the sample used in Figure 21, except this was analyzed on the non-pressurized system. Like in Figure 20, the slope of the line produced is negative as the natural log of the ratio of dodecane to naphthalene decreases as the inverse temperature decreases. The resulting correlation coefficient of 0.95 is further below the desired benchmark of 1 than the correlation coefficient from the data in Figure 21.

Figure 23 is from a set of mixtures made in which a slurry of 1.50 g of naphthalene saturated in 1.00 mL of dodecane was melted together in a hot water bath and allowed to recrystallize, forming a solid layer on the bottom of the vial. On top of the recrystallized layer, 0.1 mL of water was added. The recrystallized slurry created a homogenous mixture and more uniform surface area of the analytes (as opposed to loose crystals naphthalene and liquid dodecane, used in the samples from Figures 20 and 21. The addition of water was added in attempt to force more of the non-polar analytes into the headspace, due to the polarity difference between the analytes and water. The data from Figure 23 was analyzed on the pressure-balanced system. It can be noticed that the
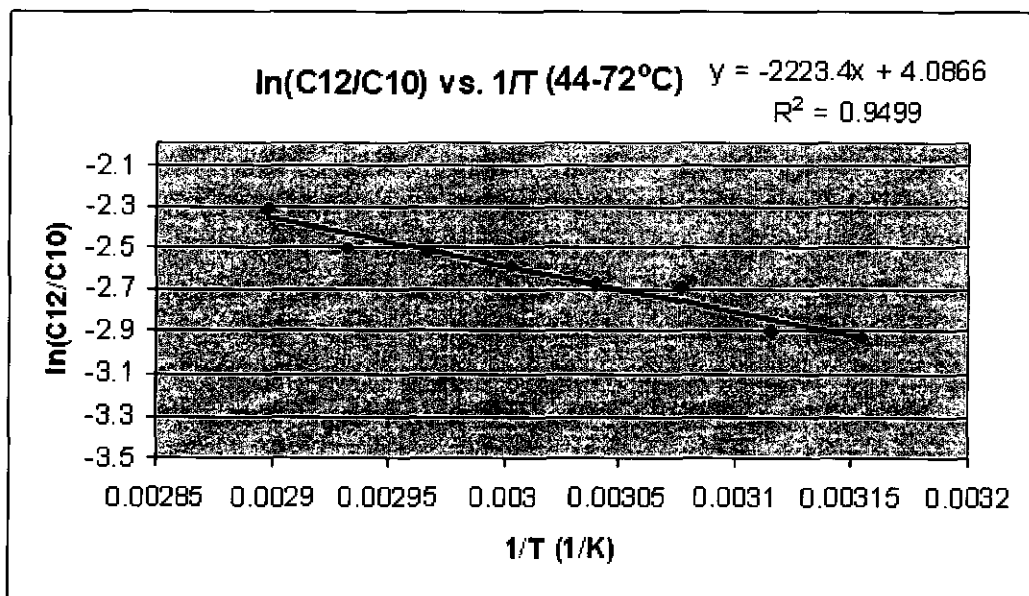
Figure 22 – A plot of the ln of the average peak area ratios of dodecane to naphthalene vs. 1/T from a non-pressurized system.
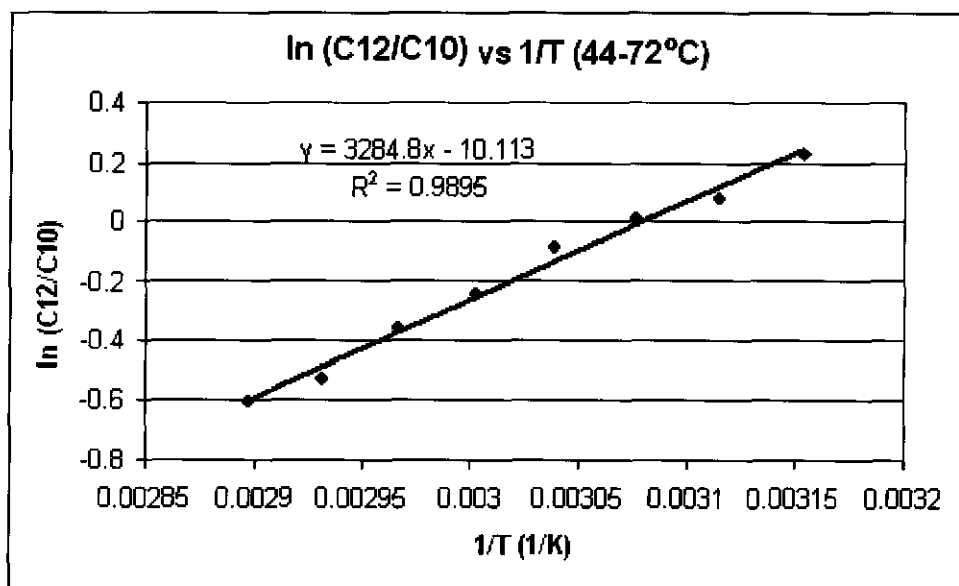
Figure 23 – A plot of the ln of the average peak area ratio of dodecane to naphthalene from a recrystallized slurry of naphthalene saturated dodecane with 0.1 mL of water, analyzed on the pressure-balanced system.

slope of the line is opposite of the other graphs in Figures 20 and 21, and this could be due to the addition of water to the sample, and the fact that the recrystallized solid layer could have had a sealing effect, trapping the analytes in the matrix and preventing them from coming to proper equilibrium with the headspace. If the addition of water changes the chemical process of the dodecane and naphthalene, being that they are hydrophobic, the sign of ΔH may change (from samples not containing water), resulting in a positive slope. Although the correlation coefficient is 0.9895 and is slightly better than previous data, it was not close enough to unity and there were too many variables involved in this sample preparation method.

It was at this point that the sample preparation was investigated to be dramatically changed. Besides the fact that measuring out solid naphthalene and melting and recrystalizing naphthalene-dodecane slurries was tedious and subjected the concentration of the samples to be changed due to evaporation, the extra variables in the samples needed to be reduced. For instance, the water, although it is not detected in the GC, acted as a third component to a 2-component mixture, reduced the correlation coefficient from samples without water, and it was eliminated in future samples.

It was decided to replace naphthalene with a more favorable analyte for a number of reasons. First, the naphthalene is too volatile of a sample to be relied upon for an analytical analysis because the concentration of the analytes during sample preparation could change. Second, weighing the solid naphthalene crystals and transferring them to the sample vial is not as analytically accurate as transferring a liquid with a pipet. Third, the solid naphthalene acted as a third phase of matter, so it was decided to use only liquid solutions in future samples.

Figure 24 is a graph of the peak area ratio of a 1:1 v/v mixture of benzene to toluene. This graph overlaps the data from the pressure-balanced system (diamonds) and the non-pressurized systems (squares). There was 0.1 mL of this solution added to each vial to be analyzed. The benzene-toluene mix was chosen and used because it has an activity coefficient of 1 [100], and because both chemicals are liquid at the temperature range of 44°C to 72°C (.0033 1/K to .0028 1/K, respectively), making a total of two phases, liquid and gas (headspace), in the vial.

The graph in Figure 24 demonstrates three things. First, the data only differs by response factor of the instruments, but still remains proportional. Second, there are segments of linear behavior, but over the whole temperature range, it is not a completely linear profile. Third, it demonstrates that the trends of the graphs are similar from system to system, both increasing and being near parallel between .0030 1/K (60°C) and .0032 1/K (44°C). In that temperature range, the slope of the data from the pressure-balanced system is 2500 and the slope of the data from the non-pressurized system is 2600. In the range of .0029 1/K (72 °C) and .0030 1/K (60 °C), the slope is 2.0 of the pressure-balanced data and the slope of the trendline of the non-pressurized data is 690. The slope of the plots change at 60°C. The amount of (1:1 vol/vol) toluene-benzene mix of 0.1mL in the vial is a volume that borders on being partially vaporized and totally vaporized, depending on the temperature. At 60°C and above, the headspace is saturated with each component, making the slopes between 72-60°C near zero, even if the sample is not completely vaporized.

According to NIST [178], $\Delta H_{v, Benzene}$ = 30.72 kJ/mol @ 80.15°C and $\Delta H_{v, Toluene}$ = 33.18 kJ/mol @ 110.65°C. Being that ΔH is directly proportional to ln(p) and inversely

BenTol PAR vs. 1/T
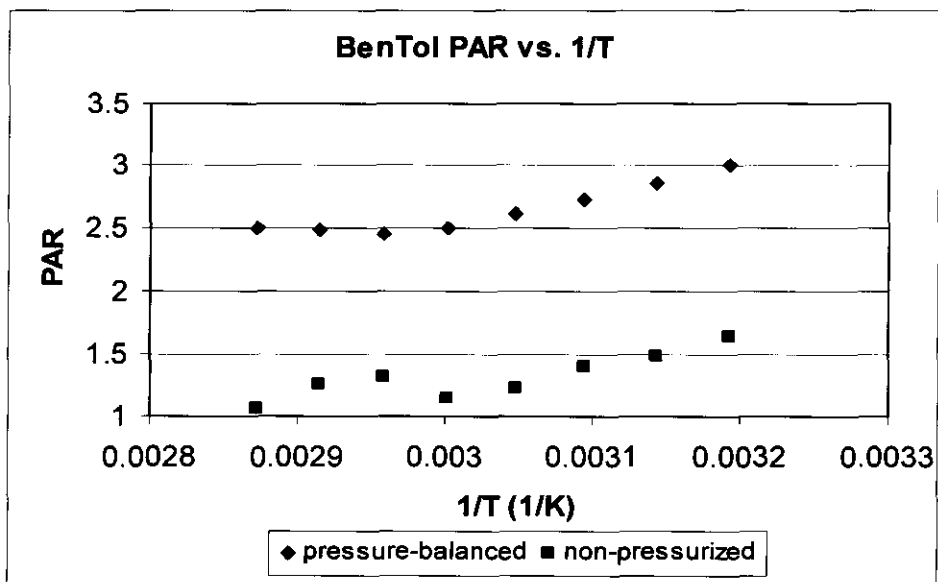
Figure 24 – The peak area ratio of benzene to toluene vs. 1/T, analyzed on the

pressure-balance system (diamonds) and the non-pressurized system (squares).

proportional to T according to Equations 17 and 21, Figure 25 demonstrates this at the temperature range of 60-72°C, in which the vapor pressures of benzene and toluene virtually overlap. Since p_i/p_{ref} is directly proportional to A_i/A_{ref} according to Equation 22, when the pressures are almost equal and change little with respect to temperature, the ratio of the peak area of one compound to the other will not change, which leads to a slope of zero. This can be supported by the internal standard profile of pure toluene at 55, 65, and 75°C, discussed in the next section. This data in Figures 26 and 27 shows that saturation of the headspace occurs when the plot levels off and is sensitive to different temperatures and volumes in the vial.

4.1.4 Discussion of "Temperature Inside the Vial" Methods

The earlier methods for determining the temperature inside the vial proved to be unsuccessful. The methods of inserting a thermocouple into a vial in the auto-sampler heater and inserting a thermocouple into an empty heater were virtually impossible to complete in the physical and pragmatic sense. The melting point method was unsuccessful because it did not reflect the analytical conditions of an actual headspace sample analysis. The chromatographic method using a 2-component chemical mixture showed signs of success in the theoretical sense since Equation 17 provides a suitable

$$\ln\left(\frac{A_{ref}}{A_i}\right) = \frac{(q_i - q_{ref})}{T} + (b_{ref} - b_i)\ln\left[(RF)\left(\frac{M_{ref}}{M_i}\right)\right] \quad (17)$$

and pragmatic relationship between the ratio of peak areas of a 2-component mixture and temperature in the range of 44°C to 72°C for the pressure-balanced and non-pressurized headspace systems because a linear relationship results. The linear behavior is apparent
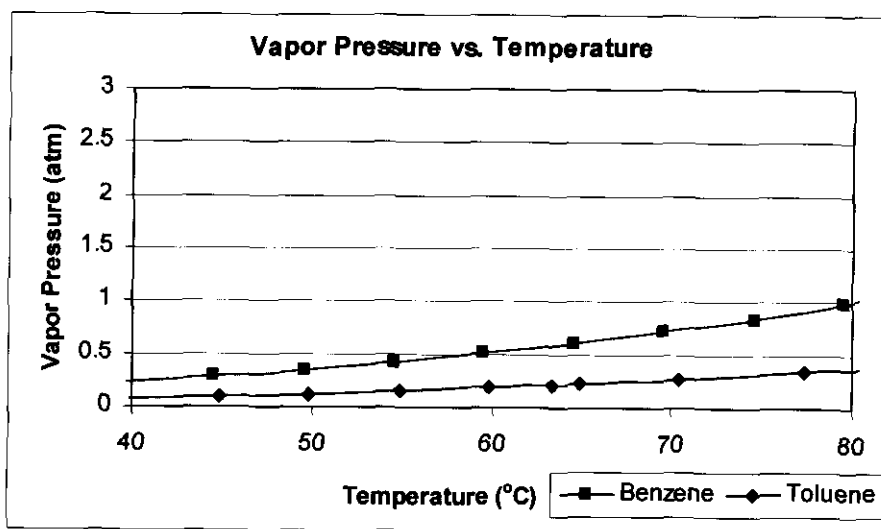
Figure 25 – A plot of the vapor pressure vs. the temperature of benzene and toluene, taken from data from NIST [178].

according to Equation 17, because $\ln\left(\dfrac{A_{ref}}{A_i}\right)$ represents y, $(b_{ref} - b_i)\ln\left[(RF)\left(\dfrac{M_{ref}}{M_i}\right)\right]$

represents the y-intercept b, $(q_i - q_{ref})$ represents the slope m, and $\dfrac{1}{T}$ represents x.

The system of naphthalene and dodecane proved to be unsuitable after a variety of concentrations and sample preparation methods did not yield acceptable analytical results, that being reproducible linear data with an R^2 value close enough to unity. The presence of naphthalene as not only a volatile chemical but a solid caused complications in weighing and transfer accuracy, but more importantly by adding a third phase to the vial in addition to the already present liquid and vapor phases. Due to the consistent liquid nature as well as activity coefficient of 1 at all concentrations, the 2-component mixture of benzene and dodecane proved to be a better choice of chemicals than the naphthalene/dodecane mixture, however, the benzene/toluene system was not perfect either.

4.2 Internal Standards

Early on, studies were performed to determine the gas chromatographic peak response on certain pure chemicals chemicals while keeping experimental variables, such as multiple chemical components and multiple phases, to a minimum. For example, a study was done to determine the maximum volume of each respective aliquot that could be injected into a vial that would completely vaporize at the given temperature (which in this case was 75°C). The results also act as an internal standard calibration as well. This was modeled after a method known as the total vaporization technique (TVT). The TVT

is used in order to create a vapor-phase only system, which allows the sample to be used as a calibration standard [38]. Aliquots of benzene and toluene were separately injected into the headspace vials and heated at 75°C for 60 minutes, to ensure equilibration. The peak area was on the y-axis and plotted against volume of aliquot on the x-axis. It was expected that the peak area would increase with respect to volume until sufficient liquid was added to the vial such that the vapor phase would be saturated. Internal standards for toluene, benzene, and MEK were analyzed; cyclohexane was not.

4.2.1 Internal Standard of Toluene

Figure 26 is an example of what would be expected for a graph used to determine the lowest volume of analyte that would cause a saturated vapor phase. It is clear that the vapor phase is saturated when 20 µL is added an equilibrated at 55°C for toluene. At this volume and above, peak area counts are and remain 410,000.

Figure 27 contains an overlap of the peak areas for toluene found at 55 °C, 65 °C, and 75 °C from the pressure-balanced system, as well as peak areas from the non-pressurized system analyzed at 75 °C. (The data from Figure 26 is in Figure 27.) It can be seen that the peak areas of the pressure-balanced system reach higher saturation points with the increase in temperature. At 55°C, the headspace reached the saturation point at 20 mL with 4.1×10^5 peak area counts, and the saturation points increase by about 1.0×10^5 peak area counts every 10 °C increase. The data from the non-pressurized system does not clearly show the volume at which the headspace becomes saturated because the line made by the data appears be begin leveling off, though, around 1.45×10^6 peak area
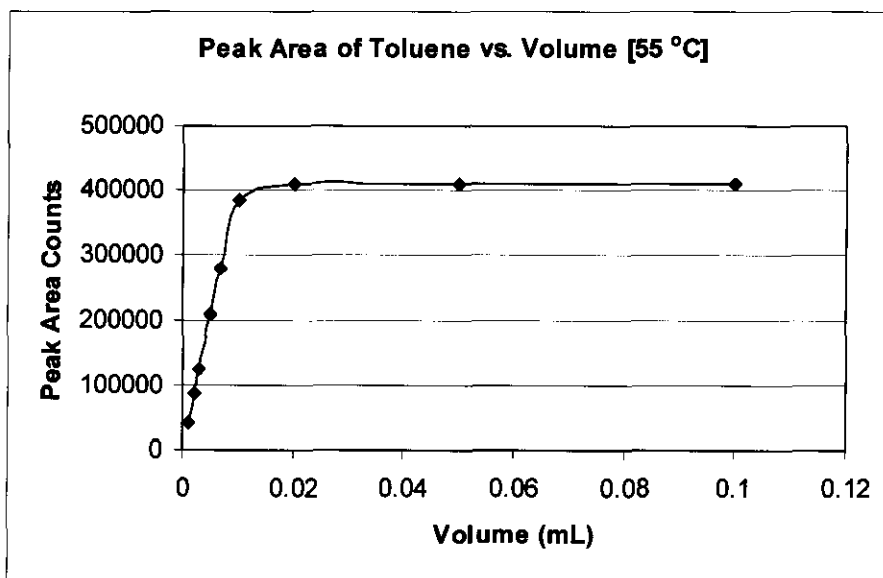
Figure 26 – A graph of the peak area counts of volumes of toluene vs. the corresponding volumes of a range from 0.0 to 0.1 mL at 55°C in the pressure-balanced system.
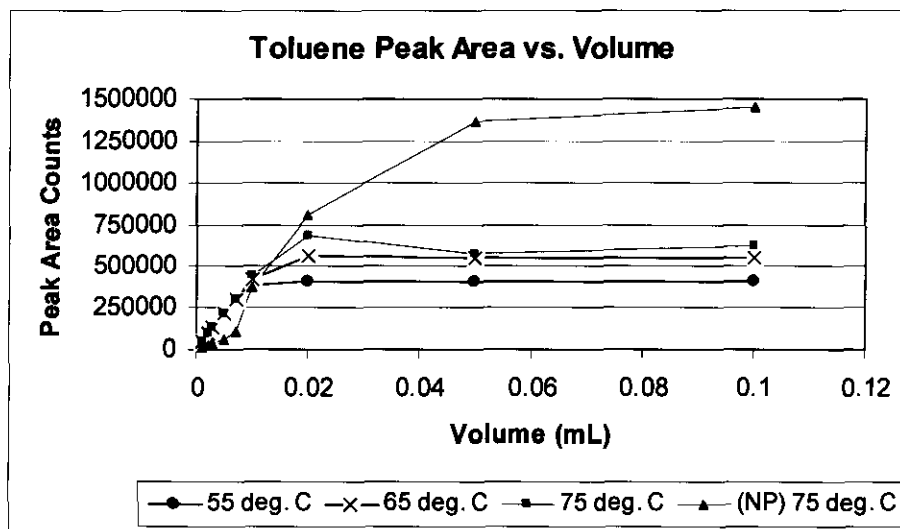
Figure 27 – Plots of the peak area counts of toluene vs. volume of toluene in the vial. The plots are overlapped on this graph, including data from the pressure-balanced system at 55°C, 65°C, 75°C, and 75°C on the non-pressurized (NP) system.

counts at a volume greater than 0.1 mL.

Figure 28 is from data from a second trial of peak areas of pure toluene vs. volume at 75 °C and includes data from both the pressure-balanced and non-pressurized systems. The difference between data from the first trial and the second trial is that in the second trial, volumes for data points were found at each respective μL of toluene up to 18 μL, so the changes in the line can be monitored more closely. For the pressure-balanced data, the peak area of toluene steadily increases with volume up until 15 μL, and after that, the increasing trend is broken. This shows that when a sample of equal or less than 15 μL is injected into the vial and heated to 75°C for 60 minutes, the sample will always be completely vaporized.

The volume at which the vapor phase is saturated is in agreement with Figure 26, however, the peak area counts at which the vapor phase becomes saturated is 650,000, which is 240,000 more than in the first trial. At volumes greater than 15 μL, it is unclear to the naked eye whether the sample in the vial is completely in the vapor phase, or partially in the vapor phase and partially in the liquid phase. The points from the non-pressurized system are taken only to the limit of 10 μL because of the more unsteady nature of the trend. For the non-pressurized data, the trend is linear up to 5 μL with a smaller slope than the pressure-balanced data, but after 5 μL, the points of peak area increase greater and faster than the pressure-balanced data.

Avg Raw Peak Area of Toluene vs. Vol. Toluene

$y = 41170x$

$R^2 = 0.9184$

Volume of Toluene (uL)   ◆ PB   ■ NP —— Linear (PB)
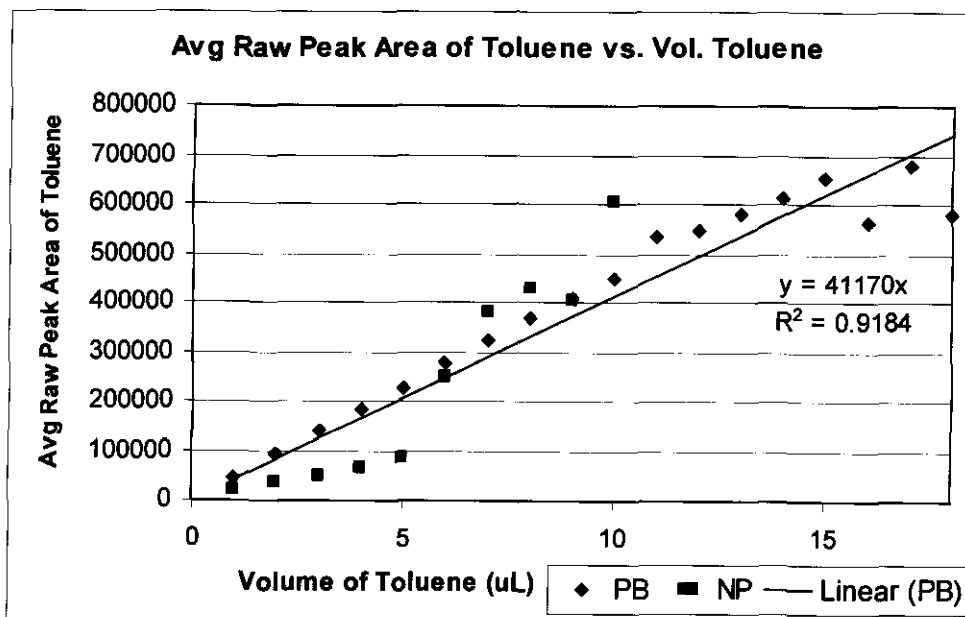
Figure 28 – A plot of average peak areas vs. volume of toluene in the vial, run on the pressure-balanced and non-pressurized system at 75°C. The equation of the trendline and the R^2 value from the pressure-balanced system are displayed on the graph.

4.2.2 Internal Standard of Benzene

Figure 29 is an internal standard of benzene, similar to the graphs of toluene.

This was performed at 55°C, 65 °C, and 75 °C on the pressure-balanced system and 75 °C

on the non-pressurized system. It shows that in the pressure-balanced system, the

samples of up to .02 mL at all 3 temperatures are completely vaporized. Also, the slope

of the data from non-pressurized system is smaller than the slopes of the pressure-

balanced data, which follows the trend of the toluene data from both headspace-gas

chromatograph systems.

Figure 30 is from the same data set as in Figure 28 except that the x-axis (volume)

range is extended out to .1 mL. This shows that after a volume of .02 mL, the trends of

the lines begin to curve until they plateau, having a slope of near zero, showing that the

vapor phase is saturated and that the samples are not completely vaporized. The slope of

the data shows a sharp increase after .2 mL, as in the toluene graphs, except that in the

toluene graphs, the peak areas from the non-pressurized system rise distinctly above the

data at 75 °C from the pressure-balanced system by about 750,000 peak area counts,

whereas on the benzene graph, the peak areas from the non-pressurized system rise to

about the same amount of peak area counts as the pressure-balanced at 75 °C. This is still

a reflection of the nature of the non-pressurized system, independent of the chemical

injected in the vial, in the respect that in lower volumes, the peak area response increases

slowly but as it approaches the vapor saturation point, the slope shows a sharp increase.
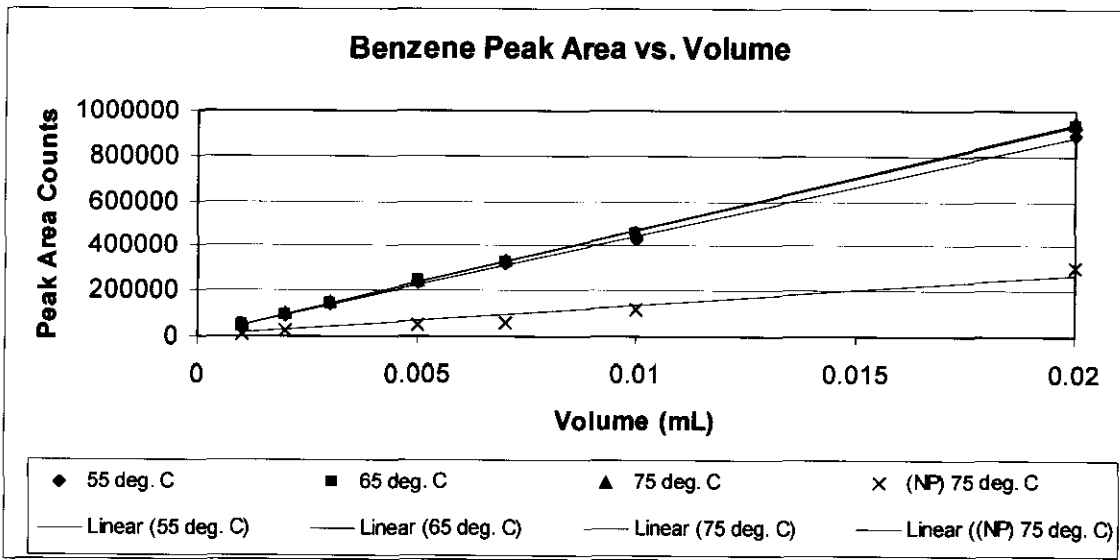
Figure 29 – A plot of peak area vs. volume of benzene over a range from 0.0 to 0.02 mL, analyzed at 75°C.

Benzene Peak Area vs. Volume
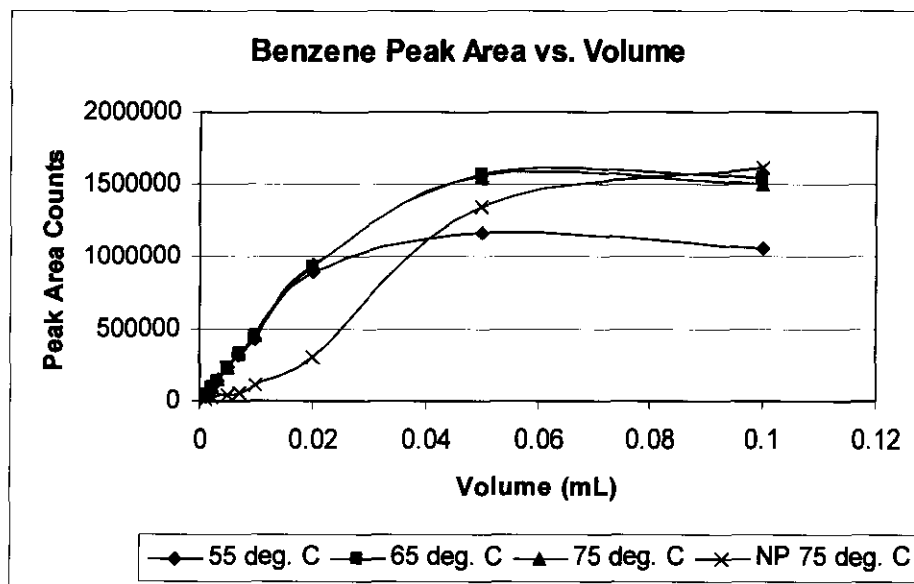
Figure 30 – A plot of peak area vs. volume of benzene in the vial, over a range from 0.0 to 0.1mL. The plots are overlapped of data from the pressurized system at 55°C, 65°C, 75°C, and 75°C from the non-pressurized system.

4.2.3 Internal Standard of Methyl Ethyl Ketone

Figure 31 is a graph of the raw peak areas of MEK vs. the respective volumes of pure MEK. In this study, the peak areas were analyzed on the non-pressurized system at 75 °C and at 3 different temperatures on the pressure-balanced system: 55 °C, 65 °C, and 75°C. It shows that the lines from the pressure-balanced system data appear close to linear and overlap, proving that MEK is completely vaporized at 55 °C to 75 °C up to at least 10 μL. As in the graph of the raw peak area of toluene, the trend of data for the non-pressurized data is similar in that the volumes up to 5 μL appear to be linear but the behavior of the data points change after that. According to the data at 75°C from both systems, it can be seen that the response factors of the two systems are distinctly different.

The internal standard studies are relevant to the overall physicochemical studies. They are relevant to the partition coefficients because for the VPC method, half of the data comes from internal standards that have to be completely vaporized. They are useful for the activity coefficients because there are pure peak areas needed to complete studies in which the mole fractions of benzene and toluene range from 0 and 1. Finally, they are useful for the temperature study because an aliquot needs to be small enough to be both economical and to ensure fast equilibration, yet above the volume in which the sample is completely vaporized.
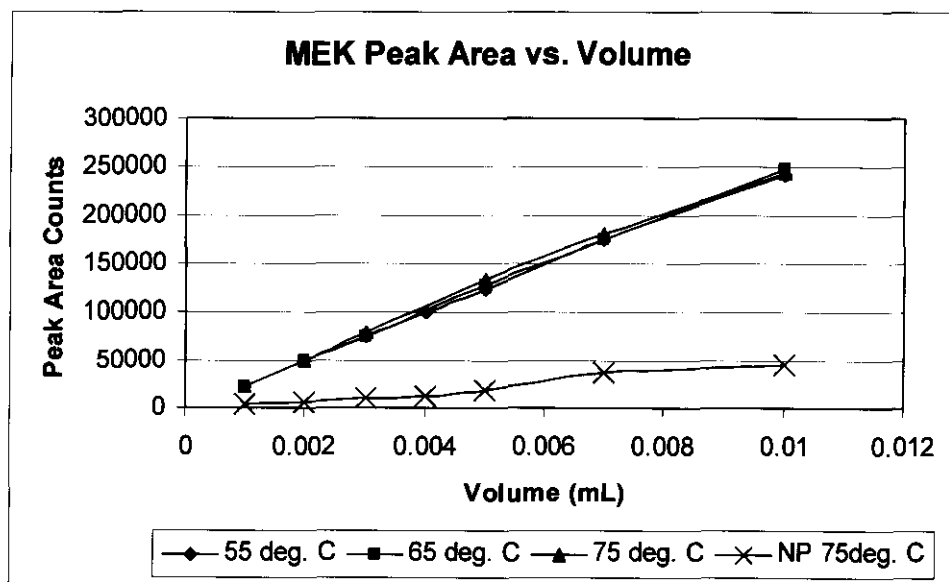
Figure 31 – A plot of the peak area of methyl ethyl ketone vs. volume in the vial. The plots are overlapped of data from the pressurized system at 55°C, 65°C, 75°C, and 75°C from the non-pressurized system.

4.2.4 Internal Standard of Toluene/Benzene

Figure 32 is a graph of the average peak area ratio of a 1:1 (v/v) toluene/benzene mix vs. volume in the vial. This data was used to study the behavior of the toluene-benzene mix in relation to the temperature study and to compare to the graphical trend of pure toluene. It is clear that this graph reflects similar behavior to the graph of pure toluene at 75 °C. For instance, the points from the pressure-balanced system have a steady linear positive slope up to and including 15 µL. Also, the slope of the non-pressurized data is a steady positive linear positive slope up to and including 5 µL, as in the pure toluene graph in Figure 28.

There is one distinguishable difference however, which is that the points of the pressure-balanced and the non-pressurized systems overlap almost exactly in Figure 32 up to and including 5 µL, and they do not overlap in the pure toluene graph in Figure 28. The points do not overlap in Figure 28 probably due to the presence of one analyte and the different response factors of the two instruments. The data points (up to and including 5 µL) overlap in Figure 32 because the respective response factors cancel out since the peak responses of the two analytes (completely vaporized at equilibrium at 75 °C) are relative and expressed as ratios. In those ratios (which make up the y-values in Figure 32), the peak response of toluene is divided by the peak response of the benzene.

One key similarity of Figures 28 and 32 is that the chromatographic response of the non-pressurized system from samples greater than 5 µL is inconsistent with the data points from lower sample volumes. This is evident because the data points (of volumes greater than 5 µL) do not follow the linear extrapolation trend the way they do from the
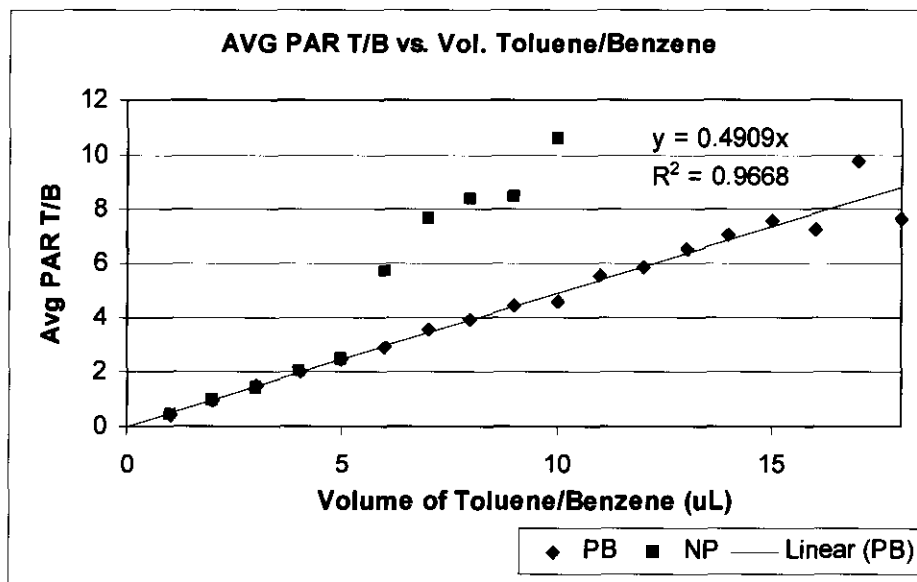
Figure 32 – A plot of peak areas of a 1:1 v/v benzene-toluene mix vs. volume in the vial at 75°C. The squares are the data points for the non-pressurized system and the diamonds are data from the pressure-balanced system, with equation of the line and correlation coefficient included in the upper right corner.

117

pressure-balanced system. In fact, at volumes greater than 5 μL, the points are unsystematically scattered. This reveals a major difference between the reliability of each system, particularly that the non-pressurized system is much less reliable.

4.3 Partition Coefficients

The partition coefficients of MEK in water, cyclohexane in water, and benzene in water were determined at 70°C using the vapor phase calibration (VPC) and phase ratio variation (PRV) methods in both the pressure-balanced and non-pressurized systems [166, 176]. At 75°C, the partition coefficients for benzene in water and toluene in water were determined using the VPC and PRV methods in both the pressure-balanced and non-pressurized systems. The reason these chemicals were selected to be studied is that, according to literature values, they represented a range of partition coefficients ranging 4 orders of magnitude from 47.7 to 1.71 to .03 [166, 176]. Toluene and MEK were selected also because there are previous data for these found by both the VPC and PRV methods, so there are multiple points of reference to compare new data to.

In the previous VPC study of MEK by Kolb, the method called for using 3 mL of water as the liquid sample phase. However, in the same paper, partition coefficients of other compounds are determined using 5 mL of water instead of the previous 3 mL, and there is no explanation given as to why. According to theory, the volume of the sample should not matter because a partition coefficient is constant and is not dependent on volume. This being true, changing the volume in the vial does change the phase ratio significantly.

In addition, the determined partition coefficients from the literature were not compared to any previous literature values. Although accuracy was calculated, this assures that the method will produce values close in relation to each other, however it is more a reflection of precision because precision indicates reproducibility and closeness of results. Accuracy is a measure of closeness to the true value and must be proven by comparing to other values measured that are accepted as true, and this must be done by comparing to other methods and other instruments. Prior to the paper by Kolb, there were no published K values for these compounds at the respective temperatures [166].

One method performed that is slightly different than the VPC method is the PRV method. In the paper in which the PRV method was introduced to determine K values, the K values were compared to some of the same values as determined in the first VPC paper [176, 166]. But in the first VPC paper, the partition coefficient for benzene in water was not determined and in the following PRV paper, the partition coefficient for cyclohexane in water was not found either. In this study, the partition coefficient for benzene in water was determined by the VPC method, the partition coefficient for cyclohexane in water was determined by the PRV method, and these values are compared with previous data. Also, few uncertainty values were reported previously in the literature. Table 5 displays all of the gas-liquid partition coefficients for MEK in water, cyclohexane in water, toluene in water, and benzene in water.

In previous studies, the partition coefficient for MEK in water at 70°C was found to be 47.7 ±0.334 by VPC [166] and 51.1 by PRV [176]. The K values of 65.2 ±2.8 from the VPC method on the pressure-balanced system and 60.0 ±26.8 from the PRV method on the non-pressurized system are higher than the values from literature. The K value of

Compound in Water	Pressure-balanced				Non-pressurized				Literature (Pressure-balanced)			
	VPC	S_K	PRV	S_K	VPC	S_K	PRV	S_K	VPC	S_K	PRV	S_K
MEK (70°C)	65.2	±2.8	50.0	±34.1	31.0	±7.3	60.0	±26.8	47.7	±.334	51.1	not given
Cyclohexane (70°C)	0.86	±0.17	0.068	±0.36	1.87	±.20	0.33	±.700	0.03	*not given*	none found	
Benzene (70°C)	1.48	±.03	1.54	±.18	1.44	±.34	1.29	±4.66	none found		1.71	not given
Benzene 75°C	.89	±.015	1.31	±.35	4.80	±1.6	0.16	±1.23	none found		(1.71)	none found
Toluene 75°C	1.10	±.015	1.01	±.14	3.57	±1.08	6.31	±2.3	(1.35)	none found	(1.37)	none found

Table 5 – Experimental Gas-Liquid (Air-Water) Partition Coefficients

31.0 ±7.3 from the VPC method on the non-pressurized system is lower than values from literature. The only K value of MEK that falls within the range of previous literature values is 59.7 ±11.6, found by PRV in the pressure-balanced system.

Every K value calculated for benzene in water at 70°C is less than the literature value of 1.71, which was determined by the PRV method [176]. On the pressure-balanced system, the K value of 1.54 ±0.18 found by PRV is greater than the K value of 1.48 ±.0.3 found by VPC, but the opposite is the case when found on the non-pressurized system. Both values found on the pressure-balanced system are greater than the K values of 1.44 ±0.34 from VPC and 1.29 ±4.66 from PRV found on the non-pressurized system. The value of 1.54 ±0.18, found by PRV on the pressure-balanced system is closest to the literature value. The value from the original PRV paper falls within the range all determined values including experimental error in this paper except for 1.48 ±.03 found by VPC on the pressure-balanced system.

The only previous value from literature of cyclohexane in water is 0.03 from the VPC method [166]. All values determined in this paper are at least one order of magnitude greater than 0.03 except for 0.068 ±.36 which was determined by PRV on the pressure-balanced system. Figure 33 is a sample graph of the reciprocal of the average peak area plotted vs. the phase ratio and is used to determine the partition coefficient of cyclohexane by the PRV method from the pressure-balanced instrument. The graph is constructed of 3 points, from 3 sets of vials of varying phase ratio. The slope of the line is 8.53×10^{-7}, the y-intercept is 5.77×10^{-8}, and the R^2 value is 1. Since, by the PRV method, the K value is deteremined by dividing the y-intercept by the slope, according to Equations 30 and 31, $(5.77 \times 10^{-8})/(8.53 \times 10^{-7})$ equals .068, which is the K value

**1/Avg PA of Cyclohexane vs. Phase Ratio
(Pressure-balanced)**

$y = 8.53E\text{-}07x + 5.77E\text{-}08$

$R^2 = 1.00E\text{+}00$

1/Avg Peak Area
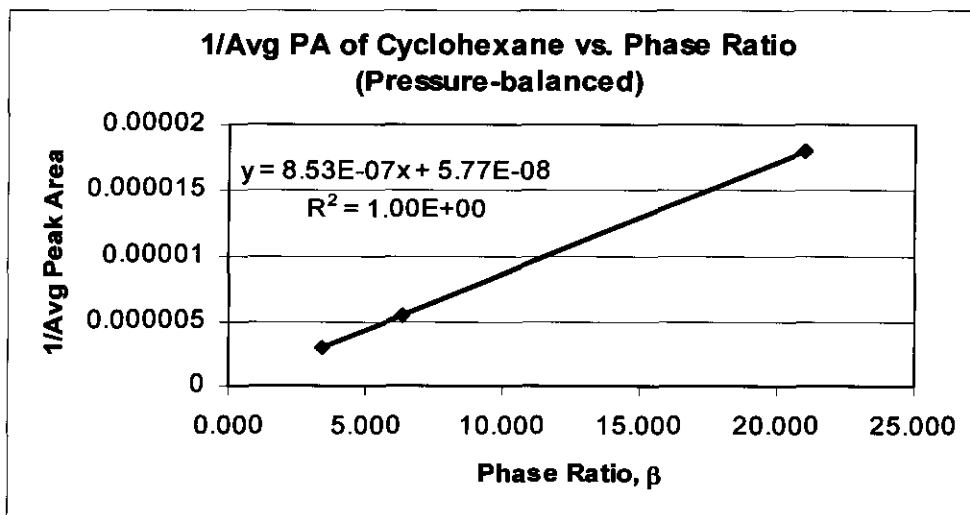
Phase Ratio, β

Figure 33 – A plot of 1/peak area vs. the corresponding phase ratio, used to solve for the partition coefficient by PRV.

determined for cyclohexane from the pressure-balanced system. The PRV method from the pressure-balanced system yielded values closest to all those previously reported in literature, for all 3 components in water. Also, the VPC method from the pressure-balanced system showed lower uncertainties in general than other systems.

In the previous papers by Kolb and Ettre et al., the K values determined by the VPC [166] and PRV [176] methods were performed on a Perkin-Elmer Model HS-101 Automatic Headspace Sampler (which is a pressure-balanced system) connected to a Perkin-Elmer Model 8700 GC with FID. Since the publication date of these papers, a newer model of the Perkin-Elmer HS-GC has been released and used in this study. The fact that there have been few measurements of partition coefficients of these chemical systems before shows that it is still in an early stage of development, and that there is still a venue for further investigation.

There are two main underlying questions that this study brings to the surface: how significantly do the two methods contribute differently to the accuracy of the partition coefficient, and how significantly do the two systems contribute differently to the determination of the partition coefficient? These questions and answers are relevant, not only for partition coefficient measurements, but also for other quantitative and physicochemical calculations, because the factors that affect the partition coefficient might also affect other determinations such as in temperature studies.

It is clear in the results that the values determined by the two methods and two instruments yield values that are close, albeit still too different to make any confident conclusions as to which are most accurate. Examing previous data, there is not enough evidence to conclude that the reported values are completely accurate. Because of this

and from comparing recent values with previous values from literature, it is possible that the recently determined values should be considered no less accurate than the previously reported values. This case is strong for benzene and cyclohexane since they have only been tested using one method each, and their uncertainties are not reported.

The data for MEK in water shows uncertainties of ±11.6 from the pressure-balanced system and ±10.8 from the non-pressurized system for the PRV method. This data was from a second trial of this method because in the first study, the partition coefficient was determined to be 63.0 ±42.93 on the pressure-balanced system and 53.2 ±23.7 on the non-pressurized system. A second trial was done because the high uncertainties are unacceptable. The results from the second trial showed lower uncertainties from the first trial, but the uncertainties were still large in comparison to the K values. Even though the uncertainties from the first trial were large, it did allow for the determined partition coefficients to be within the range of the two values previously reported in literature. The error for this chemical system from both trials shows MEK to have a higher uncertainty overall than the cyclohexane, benzene, and toluene. This does not necessarily suggest that the other values found are inaccurate though because the value 51.1 found first by PRV also does not fall in the range of uncertainty of 47.7 ±.334. Also, there is no uncertainty reported for the PRV values of any of the four components from this study.

The partition coefficients for benzene and toluene separately in water were also determined by both VPC and PRV methods on both instruments at 75°C. There were no literature values published at this exact temperature. However, air-water K values for

benzene and toluene were estimated at 75°C from the data in Figure 34. Figure 34 is a graph in which previously determined air-water K values from various sources were plotted vs. temperature, which ranged from 10 °C to 80 °C. In the PRV paper [176], K values were found at 45 °C, 60 °C, 70 °C, and 80 °C for benzene and toluene, and in the VPC paper [166], K values were found for toluene (but not benzene) at 40 °C, 60 °C, 70 °C, and 80 °C. The K values in the temperature range of 10-30°C came from a different source [90].

According to the regression curve, the partition coefficients for benzene in water and toluene in water decrease as temperature increases. More specifically, these values can be plotted in a logarithmic regression curve to calculate for the theoretical values at 75°C. The K value for benzene by PRV at 75 °C is 1.71 found by Equation 62

$$y = -2.303 \bullet \ln(x) + 11.653 \qquad (62)$$

The K value for toluene by PRV is 1.37 found by Equation 63.

$$y = -2.0051 \bullet \ln(x) + 10.027 \qquad (63)$$

The K value for toluene by VPC is 1.35 found by the Equation 64.

$$y = -2.2735 \bullet \ln(x) + 11.167 \qquad (64)$$

The partition coefficient for benzene at 75°C was found to be $0.89 \pm .015$ by VPC and 1.31 ± 0.35 by PRV on the pressure-balanced system, and 4.80 ± 1.6 by VPC and 0.16 ± 1.23 by PRV on the non-pressurized system. The partition coefficient for toluene at 75°C was found to be $1.10 \pm .015$ by VPC and 1.01 ± 0.14 by PRV on the pressure-balanced instrument, and 3.57 ± 1.08 by VPC and 6.31 ± 2.3 by PRV on the non-pressurized system.
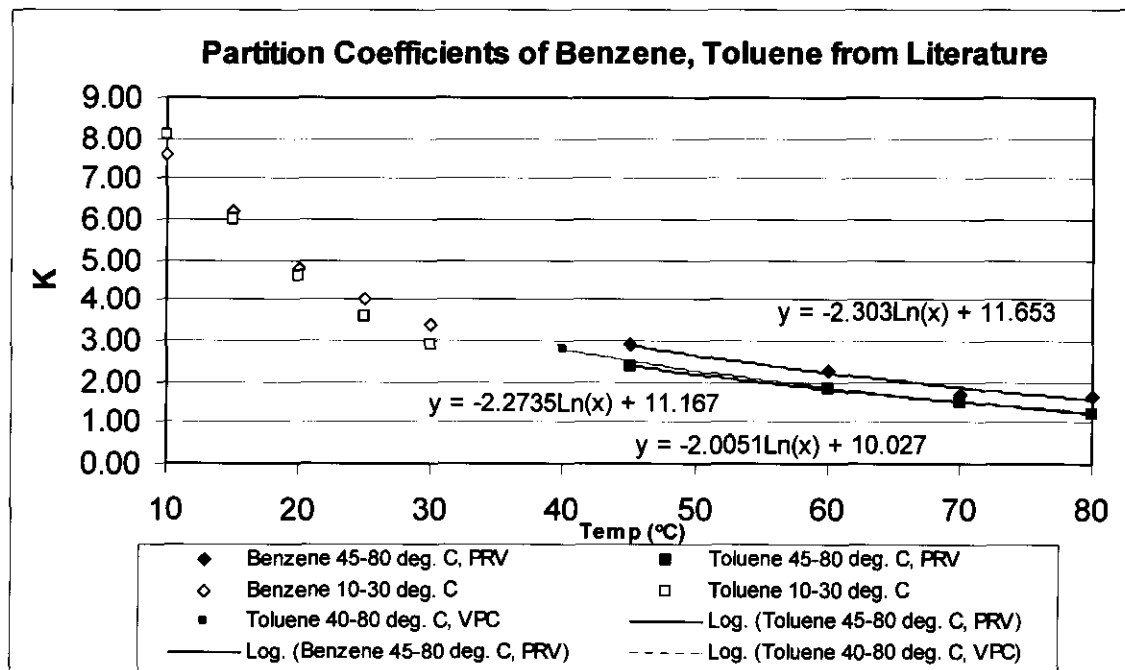
Figure 34 – A plot of previously published K values over a temperature range of 10°C to 80°C. The equation of the line is included for the data of higher temperatures from 40 °C to 80 °C.

By having the extra K values determined for benzene at a slightly higher temperature of 75°C, this can inspire more discussion on the variability between instruments. For instance, since the partition coefficient is expected to decrease as temperature increases, it can immediately be noticed that the value of 4.80 found by VPC is extremely out of range of what would be an expected value because it is more than 3 whole numbers larger than the value found by the same method but from the non-pressurized system. The estimated K value is 1.71, according to previous data (in Figure 32). Even though the other 3 values are all lower than the values of the respective method and instrument found at 70°C, again, the value of .16 falls into the opposite extreme, of being much lower than 1.71; the uncertainty of 1.23, however, compensates for this. The pressure-balanced system revealed data that followed the expected trend much more expectedly, since 0.89 ± 0.015 and 1.31 ± 0.35 are slightly less than a difference of 1 of their respective value at 70°C.

Being that there were two previous sources of K values for toluene, there are more values for new data to be compared to. Since there are no actual values previously found for toluene in water at 75°C (but rather at 70°C and 80 °C), it can first be analyzed whether the calculated values are less than the values reported at 70°C and greater than the values reported at 80°C. Although both values determined at 75°C on the pressure-balanced system were less than the K values at 70°C (1.49 by VPC and 1.52 by PRV on the pressure-balanced system), they also are less than the values found previously at 80°C (1.27 by VPC and 1.21 by PRV on the pressure-balanced system). This also indicates that the values of 3.57 ±0.108 by VPC and 6.31 ±2.3 by PRV appear to be large in comparison to other newer and previous values, even when the uncertainties are

considered. These values reflect the high combined uncertainty of the non-pressurized system with the sensitive nature of a measurement such as the partition coefficient.

The range of values and uncertainties determined for all 3 components in water by each method and instrument shows that determining physicochemical properties such as partition coefficients is possible, but may be more difficult than originally anticipated. That being said, one of the true difficulties in making such calculations is the fact that it is nearly impossible to calculate the concentrations of the vapor phase and/or the liquid phase without disrupting the true concentrations because once an aliquot is taken, the equilibrium is automatically disrupted. This is an example of a thermodynamic-related reason, but reasons of error related to uncertainties are not limited to this. Mechanical related reasons may increase uncertainty values.

For example, the higher uncertainty and standard deviation of data from the non-pressurized system can be associated with the screw-on caps for the vials and/or the heated sampling syringe (because, for this study, all screw-on caps were used with the non-pressurized system and all crimp-style caps were used with the pressure-balanced system. Screw-on caps do not have the same reputation for remaining as tightly sealed as the crimped caps do. Crimped caps can be tested by trying to twist them by hand; if the caps do not move as they are being twisted, this indicates that the caps are crimped tightly enough to remain air-tight during pressurization. Screw caps can not be tested in this way; they can only be screwed on by hand as tightly as possible. The reason this can give rise to error is because a cap that is not completely sealed can allow vapor to escape the vial. If this occurs during heating, the volatile analytes will be lost to the atmosphere, and thus will yield an inaccurate peak area at the time of sampling. Also, either during or

before heating, if there is a leak and volatile analyte is escaping, the vial will constantly be re-equilibrating, which can cause the peak area of the analyte to be lower than it should.

The possible problem with the heated syringe on the non-pressurized headspace auto-sampler is that there is no guarantee that it draws up the same volume of vaporous aliquot each time. Furthermore, since the sample is in the vapor form, there can either be a loss of sample due to thermal expansion of the gas. Condensation of the sample may also occur in the syringe if the vapor comes in contact with a cooler spot.

The pressure-balanced system also has a heated syringe, but most likely does not lose sample due to thermal expansion because there is a transfer line connected directly from the needle to the GC inlet, although this does not rule out the possibility of sample condensation in the needle or transfer line. Condensation seems unlikely in the needle or transfer line though, because the temperature of each is set at a temperature higher than the equilibration temperature of the sample vial. Loss of sample due to a non-air-tight cap, thermal expansion of the vapor sample, and condensation of analyte would result in a lower peak response of the respective sample, thus deviating from the true partition coefficient, causing it to be too high. If condensation were to occur, carryover could also occur, causing a deviation in peak responses from previous samples, causing partition coefficients to be too low.

Since the contents of the vial are pressurized (for 2.0 minutes) before sampling, the question is raised of how the equilibrium in the vial changes due to increased pressure, and then eventually an increase of volume once pressurization is complete and the needle opens to the transfer line. Furthermore, the carrier gas coming in to pressurize

the vial (usually helium) is most likely at a lower temperature than the temperature set to equilibrate the vial. The affect of the change in peak area due to the pressurization process can be judged by graphing peak area vs. pressurization time. Once the points level out to a slope of zero, which is usually at and after 2 minutes, it can be assumed that equilibrium is achieved, however it is not necessarily the same to assume that post-pressurized equilibrium is the same as pre-pressurized equilibrium. This matters because partition coefficient is mathematically related to temperature, as evident in Figure 33.

Lastly, there can be error associated to calculations with assumptions made about measurements. In Equation 27 for the VPC method, the variable V_S stands for the volume of the sample in the vapor phase, and V_G is the volume of the headspace. V_S is measured and V_G is found by the difference of the volume of the vial and the measured V_S added to the vial. Because partition coefficients and vapor pressures are temperature dependent, the true values of the volumes of the liquid and headspace change slightly from the time of sample preparation to the time of heated equilibrium. When calculations are carried out, differences in the volumes can change the numerator and denominator because V_S should be slightly less than when added to the vial, and likewise, V_G should be slightly higher. In the case of VPC, the differences can change the value of the calculated partition coefficient, and in the case of PRV, the x-value, which is the phase ratio may be slightly different than what is graphed, and the resulting calculation may be slightly different as well.

In general, the pressure-balanced system shows to be more reliable, in terms of precision because of overall lower uncertainties than from the non-pressurized system. The accuracy of each determined result is still inconclusive, which is why it is beneficial

to utilize both methods and instruments as confirmation for the same partition coefficient system. Partition coefficients appear be very sensitive to the method of measurement, and future work includes compensating for and controlling the potential errors that exploit these sensitivities.

4.4 Activity Coefficients

The activity coefficient, γ, of benzene-toluene solutions was determined using the resulting peak areas of varied concentrations (mole fractions) of the mixtures, ranging from mole fractions of benzene of zero to 1, and substituted into Equation 43. This study was performed with a range of volumes in the vial in order to compare results from each volume of sample. The results were also to be compared with the activity coefficient of 1, found from one literature source [100]. The results are shown in Table 6, which presents the mole fraction of benzene in the left column and the volume of sample of benzene/toluene mixture in the vial in the top row; the left half includes results from the pressure-balanced system and the right half includes results from the non-pressurized system. All the results (with the exception of 2) are within 1 order of magnitude of the literature value.

Since the activity coefficient study was taken up to supplement the temperature inside the vial study, the question of how it relates remains to be further discussed. As the activity between molecules in liquid increase, the reflected concentration (as mole ratio) changes accordingly. According to Equation 34, the mole fraction can affect the activity between molecules in liquid. Likewise as activity changes relative to changes in

	γcalculated, pressure-balanced			γcalculated, non-pressurized		
x_{Ben}	.01 mL	.02 mL	.05 mL	.01 mL	.02 mL	.05 mL
0.01	0.84	1.49	0.89	124.61	0.05	89.15
0.07	0.87	1.46	0.78	0.34	0.003	0.22
0.35	1.88	3.00	0.66	0.39	0.13	0.27
0.52	0.94	1.38	0.51	1.46	1.64	1.52
0.94	1.05	1.56	0.89	1.94	6.50	1.79
0.99	1.06	1.25	1.01	0.62	9.31	1.35

Table 6 – Calculated activity coefficients at varied mole fractions of benzene and toluene, at various volumes.

pressure, the concentration reflected as peak area in Equation 17 will change as well. If activity is high, the reflected concentration will be lower than it should reflect. Attempting to find a mixture with an activity coefficient of 1 at all concentrations completely eliminates that factor of uncertainty among the scheme of inter-related variables pertaining to the concentration of the headspace reflected as peak area, and the temperature.

The results proved to be favorable to use for the temperature inside the vial study because at varied concentrations and volumes, the activity coefficient was found to be within an order of magnitude of 1 (with the exception of 1 calculated value). Calculated activity coefficients remain the same as different volumes of the same concentration are analyzed, as it should. The γ values also remain the same as the mole-fraction of benzene is varied, which it should.

There is a clear difference between the calculated values from the pressure-balanced system in contrast to the non-pressurized system. The values from the pressure-balanced system show little deviation from any one value to another. Although most values from the non-pressurized system are within 1 order of magnitude from unity, the values vary more by difference from any one value compared to another than on the pressure-balanced system. For example, for vials containing .02 mL of the benzene/toluene mixture, some γ values from the lower mole fraction mixture differ with γ values from higher mole fractions by up to 9 whole numbers whereas the most any γ value differs from the pressure-balanced system is no greater than 3.

Some values calculated from the non-pressurized system deviate by 2 orders of magnitude, which appear to be instrument related errors, and not due to a trend related to

variation of mole fraction or volume. The possible instrument related errors include the thermodynamic change in the vial after pressurization and during injection in the pressure-balanced system, errors associated to the temperature of the syringe and thermodynamic expansion of the headspace aliquot on the non-pressurized system, and loss of sample due to splitting in both GC systems.

4.5 Determining Temperature by Internal Standard and Partition Coefficient

In addition to the peak area and temperature relationship-chromatographic method using Equation 17, two other chromatographic methods show relationships between temperature and chromatographic data. These methods are from the internal standard study and the partition coefficient study. From the internal standard study, the amount of vaporization of a chemical can be tracked by the relationship between temperature and volume in the vial. For example, according to Figures 26 and 27, it can be determined that the temperature inside the vial is $55^{\circ}C$ when the headspace is saturated from 20 µL of toluene having a peak area of 410397. In other words, samples of higher volumes will saturate the headspace at higher temperatures and samples of smaller volumes will saturate the headspace at lower temperatures. Additionally, partition coefficients are related to temperature through a logarithmic relationship as in Figure 34. Thus, if a partition coefficient profile is created over a range of temperatures, the partition coefficient can accurately reflect the temperature of the system, according to the equation of the line in the graph. For example, when the partition coefficient for toluene is calculated to be 1.86 by the PRV method, it can be deduced that the temperature is $60^{\circ}C$.

4.6 Relation of Physicochemical Variables

As the original study began with investigating a method to determine the temperature inside a headspace sample vial, other studies of partition coefficients and activity coefficients were spun-off to supplement the temperature study. In the scheme of the main temperature study, each study served to supplement the bases of each other study because they are all mathematically linked through a series of equations as shown in Figure 35. Equations 9, 17, 44, and 52 show that temperature, peak area, concentrations of liquid sample and headspace, phase ratio (volumes of liquid sample and headspace), headspace sensitivity, partition coefficient, and activity coefficient are all mathematically inter-related and connected like a web.

For instance, it is already established in Equation 17 that the natural log of the peak area ratio of 2 components is inversely proportional to temperature, but according to Equation 9, which is a sensitivity expression shows that peak area is directly proportional to the concentration of the headspace, which is inversely proportional to the sum of K and β, proving that K and β affect the determination of the temperature through the common variable of peak area. The variables of the sensitivity expression are also linked to the variables in Equation 52, which shows that K is inversely proportional to γ, through the common variable of K. Through this link, it not only proves that γ is mathematically related to the b, C_o, C_G, and peak area, but the temperature as well. Equation 44, which shows the relationship between γ, peak area, and mole fraction, supports the link between g and temperature because it also has a direct link with Equation 17 through the common

Figure 35 – Diagram of the cycle of investigation as well as relationship of equations with common variables pertaining to peak areas, temperature, partition coefficient, phase ratio, concentration, and activity coefficient. The study began with the temperature study which led to studying the partition coefficient and the activity coefficient of the chemicals involved.

variable of peak area, due to the inversely proportional relationship with the mole fraction, which is an expression of concentration.

It is from these relationships and the respective studies of K and γ that prove how uncertainties from variables not even contained in Equation 17 can amplify the errors involved in determining the temperature inside a vial with acceptable reproducibility. To be specific, if temperature is related to K, and partitioning is inconsistent or theoretical K values are inaccurate due to high activity between solute and solvent or inaccurate γ values, then inaccuracies from the γ will contaminate the results of the calculated temperature inside a vial.

This is supported by Figure 36 which is a graph of the activity coefficients at infinite dilution of benzene in water vs. temperature. This graph contains activity coefficients at infinite dilution obtained by a variety of methods from a variety of sources [147]. It can be seen in this graph that there is a frequent amount of variability of γ^{∞}. For instance, at 25°C, there are 9 different γ^{∞} values ranging from 1700 to 2530. Also, at 25 °C, 40 °C, and 60°C, it can be seen that the γ^{∞} values are virtually the same at about 1700. There is an apparent trend that activity coefficients like these have large uncertainties and are sensitive and difficult to measure by nature. The information displayed in Figure 36 along with Equation 52 not only explains why there is high variation among the values of air-water partition coefficients found by VPC and PRV, but also supports the claim that values previously found should be considered subjectively accurate.
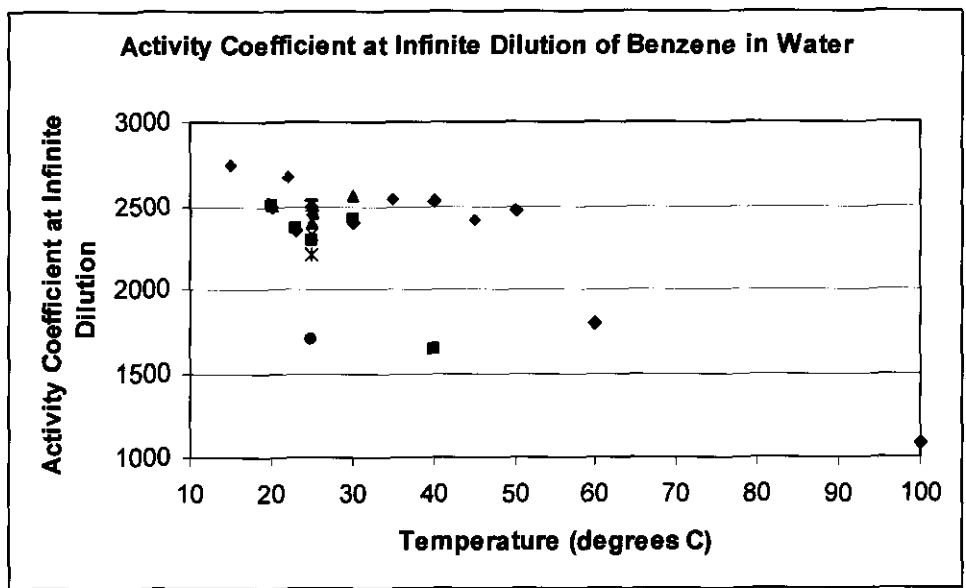
Figure 36 – A graph of the activity coefficients at infinite dilution of benzene in water vs. temperature.

5. CONCLUSIONS

The results from these studies lead to 6 major conclusive points:

1. It is possible to chromatographically determine the temperature inside a sample headspace vial with the controlled use of a 2-component system and the minimization of controllable variables.

2. There are two other studies which chromatographically support the temperature study: the internal standard study on a pure component at low sample volumes and the study of air-water partition coefficients.

3. A series of equations show that temperature, peak area, concentrations of liquid sample and headspace, phase ratio (volumes of liquid sample and headspace), headspace sensitivity, partition coefficient, and activity coefficient are all mathematically inter-related like a web.

4. The accuracy of certain partition coefficients found in literature is somewhat subjective.

5. Built on the last two conclusions, the accuracy of the results of the temperature and physicochemical studies appears to be in jeopardy due to certain instrumental causes of uncertainty along with the sensitivity of values from a small chemical scale.

6. Of the two methods, the phase ratio variation (PRV) method is more suitable than the vapor phase calibration (VPC) method for determining air-water partition coefficients, showing overall lower uncertainty and better precision.

The internal standards show the profile of the ranges of volumes of samples that are completely volatilized and partially volatilized in regards to samples used in the

partition coefficient and activity coefficient studies. The partition coefficients can be determined by the VPC and PRV on the pressure-balanced system and the non-pressurized system. The PRV method proved to be the best method based on the lowest overall uncertainties relative to other methods reported in the literature. The values determined by the pressure-balanced system had greater precision than values determined by the non-pressurized system. The activity coefficients for benzene-toluene were determined to be 1, in agreement with the claim in literature [100]. There were higher (and in some cases, extremely higher) uncertainties for activity coefficients found by the non-pressurized system.

Based on 4 separate, albeit related, studies, the uncertainties for the non-pressurized system are unanimously higher than the pressure-balanced system. This is associated with the differences of the instrument, as for example, mechanical reasons. For studies in which precision of a measurement is important, the pressure-balanced system is more reliable than the non-pressurized system. Due to the experimental uncertainties and the mathematical relationships linking temperature, partition coefficient, and activity coefficient, experimental error of physicochemical properties can magnify the experimental error in determining the temperature inside a vial.

In regards to the original study, the information learned from all the studies changes the question of "What is the temperature inside the vial?" to "What is the best way to most accurately determine the temperature inside the vial?" This new question addresses the inevitability of a precarious amount of uncertainty due to mechanical and activity coefficient related reasons, but leaves room for improvement in other controllable areas. To be specific, the best way to determine the temperature inside a headspace vial

is to use a 2-phase only, 2-component mixture having an activity coefficient of 1 at all

mole fractions, such as benzene/toluene, with Equation 17, on an up-to-date pressure-

balanced headspace system with optimized conditions.

6. REFERENCES

1. Ketola, R. A.; Virkki, V. T.; Ojala, M.; Komppa, V.; Kotiaho, T.; *Talanta*, **1997**, *44*, 373-382.

2. Ettre, L. S.; *LCGC North America*. **2002**, *20*, 1120-1129.

3. Harger, R. N.; Bridwell, E. G.; Raney, B. B; *Proc. Am. Soc. Biol. Chem., J. Biol. Chem.* **1939**, *128*, xxxviii-xxxix.

4. Harger, R. N.; Bridwell, E. G.; Raney, B. B; Kitchel, M. F.; *J. Biol. Chem.* **1950**, *183*, 197-213.

5. Foote, H. W.; Scholes, S. R.; *J. Am. Chem. Soc.* **1911**, *33*, 1309.

6. Thomas, R.; *J. Soc. Chem. Ind.* **1922**, *41*, 34.

7. Dobson, J. E.; *J. Chem. Soc.* **1925**, *127*, 2866.

8. Wrewsky, M.; *Z. Physik. Chem.* **1912**, *81*, 1.

9. Liljestrand, G.; Linde, P.; *Skand. Arch. Physiol.* **1934**, *52*, 150.

10. Haggard, H. W.; Greenberg, L. A.; *J. Pharmacol. and Exp. Therap.* **1934**, *52*, 150.

11. Haggard, H. W.; Greenberg, L. A.; Miller, D. P.; Carroll, R. P.; *J. Lab. and Clin. Med.* **1941**, *26*, 1527.

12. Landolt-Bornstein; *Physikalisch-chemische* Tabellen, 5th ed.; Berlin, 1923, pp. 762.

13. Harger, R. N. *J. Lab. and Clin. Med.* **1935**, *20*, 746.

14. Schulek, E.; Pungor, E.; Trompler, J.; *Mikrochim. Acta.* **1956**, 1005-1022.

15. Schulek, E.; Pungor, E.; *Mikrochim. Acta.* **1956**, 1120-1135.

16. Schulek, E.; Pungor, E.; Trompler, J.; *Mikrochim. Acta.* **1957**, 85-95.

17. Schulek, E.; Pungor, E.; Trompler, J.; *Mikrochim. Acta.* **1958**, 53-59.

18. Schulek, E.; Trompler, J.; Pungor, E.; *Mikrochim. Acta.* **1959**, 18-21.

19. Schulek, E.; Trompler, J.; Konkoly-Thege, L. I.; Pungor, E.; *Mikrochim. Acta.* **1959**, 22-25.

20. Schulek, E.; Pungor, E.; Trompler, J.; Konkoly-Thege, L. I.; *Mikrochim. Acta.* **1959**, 706-711.

21. Schulek, E.; Pungor, E.; Trompler, J.; Konkoly-Thege, L. I.; *Mikrochim. Acta.* **1960**, 406-408.

22. Bovijn, L.; Pirotte, J.; Berger, A.; *Gas Chromatography 1958 (Amsterdam Symposium).* Desty, D. H., Ed.; Butterworths: London, 1958, pp. 310-320.

23. Stahl, W. H.; Voelker, W. A.; Sullivan, J. H.; *Food Technol.* **1960**, *14*, 14-16.

24. "Beckman Laboratory Oxygen Sensor, bulletin number 7013," Beckman Scientific and Process Instruments Division (Fullerton, California, October 1962).

25. "Beckman Headspace Sampler, bulletin number 7012," Beckman Scientific and Process Instruments Division (Fullerton, California, September 1962).

26. http://www.cfsan.fda.gov/~ebam/bam-22a.html

27. Nundy, D. C.; http://www.hc-sc.gc.ca/fn-an/res-rech/analy-meth/microbio/volume2/mfhpb04-01-eng.php

28. McWilliam, G.; *Chromatographia.* **1983**, *17*, 241-243.

29. Weurman, C.; *Food Technol.* **1961**, *15*, 531-536.

30. Weurman, C.; *J. Food Sci.* **1961**, *26*, 670-672.

31. Mackay, D. A. M.; Lang, D. A.; Berdick, M.; *Anal. Chem.* **1961**, *33*, 1369-1374.

32. Buttery, R. G.; Teranishi, R.; *Anal. Chem.* **1961**, *27*, 1439-1441.

33. Bailey, S. D.; Mitchell, D. M.; Bazinet, N. L.; Weurman, C.; *J. Food Sci.* **1962**, *27*, 165-170.

34. Dorrscheidt, W.; Friedrich, K.; *J. Chromatogr.* **1962**, *7*, 13-18.

35. Bassette, R.; Ozeris, S.; Whitnah, C.; *Anal. Chem.* **1962**, *34*, 1540-1543.

36. Curry, A. S.; Hurst, G.; Kent, N. R.; Powell, H.; *Nature.* **1962**, *195*, 603-604.

37. Machata, G.; *Mikrochimica Acta.* **1964**, *2/4*, 262-71.

38. Kolb, B.; Ettre, L. S.; *Static Headspace-Gas Chromatography, 2nd ed.;* Wiley: Hoboken, NJ, 2006, pp. 72.

39. Amoni, M.; *Federal Registrar.* **2006**, *71*, 37159-37162.

40. Ainsworth, M. C.; *American Journal of Police Science.* **1932**, *3*, 169-182.

41. Lucas, D. M.; *Forensic Science Review.* **2000**, *12*, #1/2, 1-21.

42. Labianca, D. A.; *Journal of Chemical Education.* 1990, *67*, 259-261.

43. http://www.breathalyzer.net/alcohawk-precision.html

44. Alcohawk Precision Owner's Manual, Q3 Innovations, LLC, **2005.**

45. Jentzsch, D.; Kruger, H.; Lebrecht, G.; *Applied Gas Chromatography.* **1967**, *No. 10E.*

46. Jentzsch, D.; Kruger, H.; Lebrecht, G.; Dencks, G.; Gut, J.; *Z. Anal. Chem.* **1968**, *236*, 96-118.

47. Hauch, G.; Terfloth, H. P.; *Chromatographia,* **1969**, *2*, 309-314.

48. Machata, G.; *Blutalkohol,* **1967**, *4(5)*, 3-11.

49. Machata, G.; *Blutalkohol,* **1970**, *7(5)*, 345-348.

50. Widmark, E. M. R.; *Biochem. J.* **1919**, *13*, 432-445.

51. Widmark, E. M. R.; *Biochem. Z.* **1922**, *131*, 473-484.

52. Bonichsen, R. K.; Theorell, H.; *Scand. J. Clin. Lab. Invest.* **1951**, *3*, 58-62.

53. Ioffe, B.V.; Vitenberg, A.G.; *Head-Space Analysis and Related Methods in Gas Chromatography*; Wiley: New York, NY, 1984; pp. 16-21.

54. Kebbekus, B. B.; Mitra, S.; *Environmental Chemical Analysis*; Blackie Academic & Professional: New York, NY, 1998; pp. 269-270.

55. Grob, K.; *J. Chromatogr.* **1973**, *84*, 255.

56. Curvers, J.; Noy, T.; Cramers, C.; Rijks, J.; *J. Chromatogr.* **1984**, *289*, 171-182.

57. Osemwengie, L. I.; Steinberg, S.; *J. Chromatogr.* **2003**, *993*, 1-15.

58. Kroupa, A.; Dewulf, J.; Van Langenhove, H.; Viden, I.; *J. Chromatogr.* **2004**, *1038*, 215-223.

59. Burger, B. V.; Munro, Z., *J. Chromatogr.* **1987**, *402*, 95-103.

60. Clausen, P. A.; Wolkoff, P.; *Atmos. Environ.* **1997**, *31*, 715.

61. Lakatos, M.; *Journal of Pharmaceutical and Biomedical Analysis.* **2008**, *47*, 954-957.

62. Lee, R. M.; Lee, J. S.; Hsiang, W. S.; Chen, C. M.; *J. Chromatogr. A.* **1997**, *775*, 226.

63. Wasik, A.; Janicki, W.; Wardencki, W.; Namiesnik, J.; *Analysis.* **1997**, *25*, 59.

64. Dewulf, J.; Langenhove, H. W.; *J. Chromatogr. A.* **1999**, *843*, 163.

65. Wang, J. L., Chen, S. W.; Chew, C. *J. Chromatogr. A.* **2000**, *863*, 31.

66. Adlard, E. R.; Davenport, J. N.; *Chromatographia.* **1983**, *17*, 421-425.

67. Dreisch, F. A.; Munson, T. O.; *J. Chromatogr. Sci.* **1983**, *21*, 111-118.

68. Nouri, B.; Fouillet, B.; Toussaint, G.; Chambon, R.; Chambon, P.; *J. Chromatogr. A.* **1996**, *726*, 153-159.

69. McAullife, C. *Chem. Tech.* **1971**, Jan, 46-51.

70. Suzuki, M.; Tsuge, S.; Takeuchi, T.; *Anal. Chem.* **1970**, *42*, 1705-1708.

71. Novak, J.; *Quantitative Analysis by Gas Chromatography*; Marcel Dekker, Inc., New York, NY, 1975; pp. 107-156.

72. Ioffe, B.V.; Vitenberg, A.G.; *Chromatographia.* **1978**, *11*, 282-186.

73. Drozd, J.; Novak, J.; *J. Chromatogr.* **1984**, *285*, 478-483.

74. Kolb, B.; *Chromatographia.* **1982**, *15*, 587-594.

75. Vitenberg, A. G.; Reznik, T. L.; *J. Chromatogr.* **1984**, *287*, 15-27.

76. Kolb, B.; Ettre, L. S.; *Chromatographia.* **1991**, *32*, 505-513.

77. Kolb, B.; Auer, M.; Pospisil, P.; *Gewasserschutz, Wasser, Abwasser.* **1982**, *57*, 101-125.

78. Chai, X. S.; Schork, F. J.; DeCinque, A.; *J. Chromatogr. A.* **2005**, *1070*, 225-229.

79. Pawlinszyn, J.; *Solid Phase Microextraction: Theroy and Practice*; Wiley-VCH, New York, NY, 1997

80. Hawthorne, S. B.; Miller, D. J.; Pawliszn, J.; Arthur, C. L.; *J. Chromatogr.* **1992**, *603 (1-2)*, 185-191.

81. Potter, D. W.; Pawliszn, J.; *J. Chromatogr.* **1992**, *625 (2)*, 247-255.

82. Pawlinszyn, J.; *Applications of Solid Phase Microextraction*; RSC Chromatography Monographs, Royal Society of Chemistry, London, 1999.

83. Pawlinszyn, J.; *Theory of Solid Phase Microextraction, J. Chromatogr. Sci.* **2000**, *38*, 270-278.

84. Supelco Bulletin, 929, 595 North Harrison Rd. Bellefonte, PA.

85. Matisova, E.; Medvedova, M.; Vraniakova, J.; Simon, P.; *J. Chromatogr. A.* **2002**, *960*, 159-164.

86. *EPA Method 107A*: Determination of Vinyl Chloride Content of Solvents, Resin-Solvent Solution, Poly(Vinyl Chloride) Resin, Resin Slurry, Wet Resin and Latex Samples. *September,* **1982**.

87. *ASTM F-151-86(91):* Standard Test Method for Residual Solvents in Flexible Barrier Materials.

88. Robbins, G. A.; Wang, S.; Stuart, J. A.; *Anal. Chem.* **1993**, *65*, 3113-3118.

89. Grob, R. L., Ed.; Barry, E. F., Ed.; *Modern Practice of Gas Chromatography*, 4th ed.; Wiley-Interscience: Hoboken, NJ, 2004; pp. 85-86.

90. Tsibulskii, V.V.; Tsibulskaya, I.A.; Yahlitskaya, N.N. *Zh. Analit. Khim.* 1979, *34*.

91. Rohrschneider, L. In *Advances in Chromatography*; Zlatkis, A., Ed.; 1973; pp 179.

92. Tsibulskaya, I.A.; *doctoral dissertation*. Leningrad University, 1979.

93. Vitenberg, A. G.; Kostkina, M. I.; *Zh. Analit. Khim.* **1979**, *34*, 1800.

94. Vitenberg, A. G.; Kostkina, M. I.; *Vestn. Leningr. Univ.* **1980**, *4*, 10.

95. Smirnova, S. A.; Novye, V.; *Kand. Diss.* Leningrad University, **1978**.

96. Tsibulskii, V.V.; Vitenberg, A. G.; Khripun, I. A.; *Zh. Analit. Khim.* **1978**, *33*, 1184.

97. Atlan, S.; Trelea, C. I.; Saint-Eve, A.; Souchon, I.; Latrille E.; *J. Chromatography A,* **2006**, *1110*, 146-155.

98. Maaßen, S.; Knapp, H.; Arlt, W; *Fluid Phase Equilibria,* **1996**, *116*, 354-360.

99. Hildebrand, J. H.; Scott, R. L.; *The Solubility of Nonelectrolytes*; Dover, New York, 1964; pp. 468-472.

100. Hachenberg, H.; Schmidt, A. P.; *Gas Chromatographic Headspace Analysis*; London, 1977; pp. 3-4.

101. Kojima, K.; Zhang, S.; Hiaki T.; *Fluid Phase Equilibria,* **1997,** *131,* 145-179.

102. Vrbka, P.; Rozbroj, D.; Dohnal, V.; *Fluid Phase Equilibria.* **2003,** *209,* 265-280.

103. McMillan, W. G.; Mayer, J. E.; *J. Chem. Phys.* **1945,** *13,* 276.

104. Alessi, P.; Fermeglia, M.; Kikic, I.; *Fluid Phase Equilibria.* **1986,** *29,* 249.

105. Shing, K. S.; *Chem. Phys. Lett.* **1985,** *119,* 149.

106. Tiegs, D.; Gmehling, J.; Medina, A.; Soares, M.; Bastos, J.; Alessi, P.; Kikic, I.; *DECHEMA: Frankfurt/Main.* **1986,** *IX,* Pts 1 and 2.

107. Carlson, H. C.; Colburn, A. P.; *ind. Eng. Chem.* **1942,** *34,* 581.

108. Redlich, O.; Kister, A. T.; *Ind. Eng. Chem.* **1948,** *40,* 341.

109. Nord, M.; *Chem. Eng. Progr. Sym. Series.* **1952,** *48 (3),* 55.

110. Ibi, N. V.; Dodge, B. F.; *Chem. Eng. Sci.* **1953,** *2,* 120.

111. Gautreaux, M. F.; Coates, J.; *AIChE J.* **1955,** *1,* 496.

112. Hala, E. J.; Pick, J.; Fried, V.; Vilini, O.; *Vapor-Liquid Equilibrium;* Peramon Press, London, 1967.

113. Kojima, K., Toehigi, K.; Seki, H.; Watase, K.; *Kagaku Kogaku.* **1968,** *32 (2),* 149.

114. Kojima, K.; Kato, M.; *Kagaku Kogaku.* **1969,** *33,* 769.

115. Tochigi, K.; Kojima, K.; *J. Chem. Eng. Japan.* **1976,** *9 (4),* 267.

116. Tochigi, K.; Kojima, K.; *J. Chem. Eng. Japan.* **1977,** *10,* 343.

117. Ellis, S. R. M.; Jonah, D. A.; *Chem. Eng. Sci.* **1962,** *17,* 971.

118. Martin, A. J. P.; *Biochem.* **1956,** *81,* 52.

119. Kobayashi, R.; Deans, H. A.; Chappelear, P. S.; *Ind. Eng. Chem.* **1967,** *59,* 63.

120. Belfer, A. I.; *Neftekhimiya.* **1972**, *12(3)*, 435.

121. Anand, S. C.; Grolier, J. P. E.; Klyohara, S.; Halpin, C. J.; Benson, G. C.; *J. Chem. Eng. Data.* **1975**, *20*, 184.

122. Leroi, J. C.; Masson, J. C.; Renon, H.; Fabrics, J. F.; Sannier, H.; *Ind, Eng. Chem., Process Des, Dev.* **1977**, *16(1)*, 139.

123. Hradetzky, G.; Wobst, M.; Vopel, H.; Bittrich, H. J.; *Fluid Phase Equilib.* **1990**, *54*, 133.

124. Richon, D.; Antoine, P.; Renon, H.; *Ind, Eng. Chem., Process Des, Dev.* **1980**, *19*, 144.

125. Li, JJ.; Carr, P. W.; *Anal. Chem.* **1992**, *65*, 1443.

126. Gautreaux, M. F.; Coates, J.; *AIChE J.* **1955**, *1*, 496.

127. Eckert, C. A.; Newman, C. A.; Nicolaides, G. I.; Long, T. C.; *AIChE J.* **1981**, *27(1)*, 33.

128. Tramp, D. M.; Eckert, C. A.; *J. Chem. Eng. Data.* **1990**, *35*, 156.

129. Belfer, A. J.; Locke, D. C.; *Anal. Chem.* **1984**, *56*, 2485.

130. Barr, R. S.; Newsham, D. M. T.; *Fluid Phase Equilib.* **1987**, *35*, 435.

131. Itsuki, H.; Terasawa, S.; Yamana, N.; Ohotaka, S.; *Anal. Chem,* **1987**, *59*, 2918.

132. Park, J. H.; *Ph.D Thesis*, 1988, University of Minnesota, Minneapolis, MN.

133. Belfer, A. J.; Locke, D. C.; Landau, I.; *Anal. Chem.* **1990**, *62*, 347.

134. Cheong, W. J.; Carr, P. W.; *J. Chromatogr.* **1990**, *500*, 215.

135. Djerki, R. A.; Laub, R. J.; *J. Liquid Chromatogr.* **1988**, *11*, 585.

136. Schantz, M. M.; Barman, B. N.; Martire, D. E.; *J. Res. Natl. Bur. Stand,* **1988**, *93 (2)*, 161.

137. Dohnal, V.; Horakova, I.; *Fluid Phase Equilib.* **1991**, *68*, 173.

138. Wobst, M.; Hradetzky, G.; Bittrich, H. J.; *Fluid Phase Equilib.* **1992**, *77*, 297.

139. Li, J. J.; Dallas, A. J.; Eikens, I. I.; Carr, P. W.; Bergmann, D. L.; Halt, M. J.; Eckert, C. A.; *Anal. Chem.*; **1993**, *65*, 3212.

140. Tramp, D. M.; Eckert, C. A.; *AIChE J.* **1993**, *39 (6)*, 1045.

141. Orbey, H.; Sandler, S. I.; *Ind. Eng. Chem. Res.* **1991**, *30*, 2006.

142. Tse, G.; Sandler, S. I.; *Environ. Sci. Technol.* **1994**, *39*, 354.

143. Baccouri, O.; Bendini, A.; Cerretani, L.; Guefel, M.; Baccouri, B.; Lercker, G.; Zarrouk, M.; Miled, D. D. B.; *Food Chemistry.* **2008**, *111*, 322-328.

144. Burbank, H.; Qian, M. C.; *International Dairy Journal.* **2008**, *18*, 811-818.

145. Soto, E.; Hoz, L.; Ordonez, J. A.; Hierro, E.; Herranz, B.; Lopez-Bote, C.; Camero, M. I..; *Meat Science*, **2008**, *79*, 666-676.

146. Paraschivescu, M. C.; Alley, E. G.; French, W. T.; Hernandez, R.; Armbrust, K.; *Biosource Technology*, **2008**, *99*, 5901-5905.

147. *EPA Method 107A*: Determination of Vinyl Chloride Content of Solvents, Resin-Solvent Solution, Poly(Vinyl Chloride) Resin, Resin Slurry, Wet Resin and Latex Samples. *September,* **1982**.

148. *EPA Method 107*: Determination of In-Process Wastewater Samples and Vinyl Chloride Content of Solvents, Resin-Solvent Solution, Poly(Vinyl Chloride) Resin, Slurry, Wet Cake and Latex Samples. *September,* **1982**.

149. *EPA Method D-1-VOA-Q*: Quick Turnaround Method for Contract Laboratory Practice (CLP): Static Headspace Method for Volatile Organic Analytes (VOA) in Soil/Sediments, Employing an Automatic Headspace Sampler. *November,* **1989**.

150. *EPA Method 3810:* Headspace Screening. **1996.**

151. *EPA Method 5021A:* Volatile Organic Compounds in Various Sample Matrices Using Equilibrium Headspace Analysis. **2003.**

152. Diachenko, G. W.; Breder, C. V; Brown, Me. E.; Dennison, J. L.; *J. Assoc. Off. Anal. Chem.* **1978,** *61,* 570.

153. Pace, B. D.; O'Grody, R.; *J. Assoc. Off. Anal. Chem.* **1977,** *60,* 576.

154. Dennison, J. L.; Breder, C. V.; McNeal, T.; Snyder, R. C.; Roach, J. A.; Sphon, J. A.; *J. Assoc. Off. Anal. Chem.* **1978,** *61,* 813.

155. *U.S. Pharmacopeia XXIII.* Organic Volatile Impurities (467). Method IV, 1995, pp. 1746-1747.

156. *ASTM F-151-86(91):* Standard Test Method for Residual Solvents in Flexible Barrier Materials.

157. *ASTM D-4526-85:* Standard Practice for Determination of Volatiles in Polymers by Headspace Gas Chromatography.

158. *ASTM D-3749-95(2002):* Standard Test Method for Residual Vinyl Chloride Monomer in Poly-(Vinyl Chloride) Resins by Gas Chromatographic Headspace Analysis.

159. *ASTM D-4443-84(89):* Standard Test Method of Analysis for Determining the Residual Vinyl Chloride Monomer Content in ppb Range in Vinyl Chloride Homo and Copolymers by Headspace Gas Chromatography.

160. *ISO 6401-1985:* Determination of Residual Vinyl Chloride Monomer in Homopolymers and Copolymers by Gas Chromatography.

161. *ASTM D-4322-96(2001)e1*: Standard Test Method for Residual Acrylonitrile Monomer in Styrene-Acrylonitrile Copolymers and Nitrile Rubber by Headspace-Gas Chromatography.

162. *ASTM D-5508-94a(2001)e1*: Standard Test Method for Determination of Residual Acrylonitrile Monomer in Styrene-Acrylonitriole Copolymer Resisns and Nitrile-Butadiene Rubber by Headspace-Capillary Gas Chromatography (HS-CGC).

163. *ASTM E-1413-00*: Standard Practice for Separation and Concentration of Ignitable Liquid Residues from Fire Debris Samples by Dynamic Headspace Concentration.

164. *ASTM E-2154-01*: Standard Practice for Separation and Concentration of Ignitable Liquid Residues from Fire Debris Samples by Passive Headspace Concentration with Solid Phase Microextraction (SPME).

165. Camarasu, C. C.; Mezei-Szuts, M.; Varga, G. B.; *Journal of Pharmaceutical and Biomedical Analysis.* **1998**, *18*, 623-638.

166. Kolb, B.; Welter, C.; Bichler, C.; *Chromatographia*, **1992**, *34*, 235-240.

167. Rohrschneider, L. Fresenius' Z. Anal. Chem. 1965, 211, 18, 18-31.

168. Rohrschneider, L.; *Anal. Chem.* **1973**, *45*, 1241-1247.

169. Reichardt, C.; *Fortschr. Chem. Fortsch.* **1968**, *11*, 1.

170. Snyder, L. R.; *Principles of Adsorption Chromatography*; New York, NY, 1968.

171. Friel, E. N.; Linforth, R. S. T.; Taylor, A. J.; *Food Chemistry.* **2000**, *71*, 309-317.

172. Jouquand, C.; Ducruet, V.; Giampaoli, P. *Food Chem.* **2003**, *85*, 467-474.

173. Jouquand, C.; Aguni, Y.; Malhiac, C.; Grisel, M.; *Food Hydroclloids*, **2008**, 22, 1097-1104.

174. Sandler, S. L.; *Fluid Phase Equilibr.* **1996**, *116*, 343.

175. Fredenslund, F. C.; *Environmenal Exposure Analysis of Chemicals,* NERI

Technical Report. **1993**, *69,* 9-43.

176. Ettre, L. S.; Welter, C.; Kolb, B.; *Chromatographia.* **1993,** *35,* 73-84.

177. Ott, J. B.; Boerio-Goates, J.; *Chemical Thermodynamics: Principles and Applications*; Elsevier Academic Press, San Diego, CA, 2000; pp. 280.

178. Williamham, C.B.; Taylor, W.J.; Pignocco, J.M.; Rossini, F.D.; *J. Res. Natl. Bur. Stand. (U.S.),* 1945, *35,* 219-24.